8-2014

Design and Fabrication of a Low-Cost Turbine Engine Component Testbed (TECT)

Joshua A. Hartman
University of Tennessee - Knoxville, jhartma6@vols.utk.edu

To the Graduate Council:

I am submitting herewith a thesis written by Joshua A. Hartman entitled "Design and Fabrication of a Low-Cost Turbine Engine Component Testbed (TECT)." I have examined the final electronic copy of this thesis for form and content and recommend that it be accepted in partial fulfillment of the requirements for the degree of Master of Science, with a major in Mechanical Engineering.

Trevor Moeller, Major Professor

We have read this thesis and recommend its acceptance:

Milton Davis, James Simonton

Accepted for the Council:
Carolyn R. Hodges

Vice Provost and Dean of the Graduate School

(Original signatures are on file with official student records.)

Design and Fabrication of a Low-Cost Turbine Engine Component Testbed (TECT)

A Thesis Presented for the
Master of Science
Degree
The University of Tennessee, Knoxville

Joshua A. Hartman
August 2014

DEDICATION

I dedicate this work to my family and friends who have supported me throughout this extensive effort. I particularly would like to thank my wife, Shayne, who witnessed all aspects of this work from the 8 years since its original inception, and encouraged me at every opportunity along the way.

I dedicate my work to you.

ACKNOWLEDGEMENTS

I would like to thank the following individuals for their contributions to this project. Without their support, none of this would have been possible. I would like to thank a few individuals for making this work a success. Aaron Marshall worked with me early in the project when this work started at Wright State University and without his knowledge of CAD and his skills for fabrication it would not have been possible. I would also like to thank Jonathan Kolwyck from University of Tennessee for all of the help with setting up the lab. He was invaluable for help with the LabView programming and various engine subsystems. I would also like to recognize Steve Arnold for all of his assistance with setting up the high speed data system as well as being a champion for a portion of the funding required to make the TECT a reality.

I am deeply indebted to all below.

Dr. Trevor Moeller	Advisor
Dr. Milton Davis	Advisor
Dr. James Simonton	Advisor
Jonathan Kolwyck	University of Tennessee Space Institute
Andrew Davis	University of Tennessee Space Institute
Joel Davenport	University of Tennessee Space Institute
Dr. Rory Roberts:	Wright State University
Aaron Marshall	Wright State University
Steve Arnold	Aerospace Testing Alliance
David Patko	Aero-Composites
Frank Beafore, Eric Wise	Select-Tech

ABSTRACT

With gas turbine engine testing becoming very expensive because of the increasing complexity involved with the engine, engine subsystems, and test support systems, a low-cost Turbine Engine Component Testbed (TECT) is proposed. This engine build is given the designation J1-H-02. In the present study, a small augmented gas turbine engine (GTE) is constructed. The TECT engine is built with modularity as a key design consideration to allow for flame-tube patterns and augmentor sections to be changed quickly for combustion experiments that have gained impetus due to combustion anomalies/instabilities inherent with future military engine augmentors. This testbed allows for an effective way to test new sensors or analytical techniques before full scale testing by allowing an intermediate Technology Readiness Level (TRL) at low-cost and quick schedule turnaround. The TECT was completed using a minor financial investment when matched to comparable capabilities. A data acquisition and control system was developed and tested that allows for real-time engine feedback and control schemes. The components were analyzed for the proper failure modes and performance was predicted using a combination of hand calculations and engine performance prediction software. The compressor performance was predicted using turbomachinery relationships and geometry, then compared with experimental data. The TECT engine was tested across its intended operational envelope at sea-level static (SLS) conditions, with the baseline performance data documented. The applied data reduction approaches were developed and presented.

TABLE OF CONTENTS

LIST OF TABLES

LIST OF FIGURES

Nomenclature

A	= area; constant
a	= speed of sound
C	= joint constant
c_p	= specific heat at constant pressure
c_v	= specific heat at constant volume
d	= diameter
E	= energy; modulus of elasticity
e	= internal energy per unit mass; polytropic efficiency
F	= uninstalled thrust, force
f	= fuel/air ratio; function; friction coefficient
g	= acceleration of gravity
g_c	= Newton's constant
h	= enthalpy per unit mass; height
h_{PR}	= low heating value of fuel
k_a	= surface condition modification factor
k_b	= size modification factor
k_c	= load modification factor
k_d	= temperature modification factor
k_e	= reliability factor
k_f	= miscellaneous-effects modification factor
K	= kinetic energy, stiffness
L	= length
ln	= natural logarithm
Ma	= Mach number
m	= mass
$\dot{m}$	= mass flow rate
N	= core speed, revolutions per minute
n	= factor of safety

P = pressure, performance analysis

p = pressure, stress analysis

P_t = total pressure

r = radius

R = universal gas constant

S_y = rotary-beam endurance limit

S_y = yield strength

S_{sy} = shear yield strength ($0.577S_y$)

S_{su} = torsional fatigue strength

S_{ut} = tensile strength

T = temperature

T_t = total temperature

t = time, wall thickness

u = velocity

W = weight; width

α = bypass ratio, angle

γ = ratio of specific heats

Δ = change, deflection

δ = dimensionless pressure

θ = dimensionless temperature

ε = slip factor

e_c = polytropic efficiency

η = efficiency

π = total pressure ratio

ρ = density

τ = total temperature ratio, shear stress

ω = angular speed

σ = stress

β = angle

Subscripts

0 = freestream condition
1 = compressor inlet
2 = compressor discharge/combustor inlet
3 = combustor exit/turbine inlet
4 = turbine discharge/EGT
8 = nozzle exit
av = average
max = maximum condition
b = burner or combustor, bolt
c = compressor; corrected; centrifugal
i = initial, inside diameter, pre-load
ref = reference condition
T = Tresca
‘ = Von Mises
f = Goodman
t = total
m = mean
$throat$ = weld throat area

Acronyms

AB	Afterburner
AIAA	American Institute of Aeronautics and Astronautics
APU	Auxiliary Power Unit
CAD	Computer Aided Design
CMD	Command
CNC	Computer Numerical Control
COTS	Commercial Off-The-Shelf
CPR	Compressor Pressure Ratio
DAQ	Data Acquisition
DIO	Digital Input/Output
DoD	Department of Defense
ECU	Engine Control Unit
EGT	Exhaust Gas Temperature
EOP	Elements of Propulsion
FEA	Finite Element Analysis
FOD	Foreign Object Damage
GTAW	Gas Tungsten Arc Welding
GTE	Gas Turbine Engine
GUI	Graphical User Interface
J1-H-01	Gas Turbine Engine Build-01
J1-H-02	Gas Turbine Engine Build-02
NI	National Instruments
PARA	Parametric Cycle Analysis
PERF	Performance Cycle Analysis
PLA	Power Lever Angle
PWM	Pulse Width Modulation
RPM	Revolutions per Minute
RTD	Resistance Temperature Detector

SL	Sea-Level
SLS	Sea-Level Static
SS	Stainless Steel
SSDP	Steady State Data Point
SSR	Solid State Relay
TECT	Turbine Engine Component Testbed
TIG	Tungsten Inert Gas
TiT	Turbine Inlet Temperature
TRL	Technology Readiness Level
TSFC	Thrust Specific Fuel Consumption
TTL	Transistor-Transistor Logic
USAF	United States Air Force
USB	Universal Serial Bus
VAC	Volts Alternating Current
VDC	Volts Direct Current

CHAPTER I
BACKGROUND AND PROJECT GOALS

INTRODUCTION

This work started while a student at Wright State University located in Dayton, Ohio. Although the goals have changed significantly from the original concept, the basic framework was established. Without the foundation of this early work, the TECT would not have been possible. The project has been significantly upgraded and developed using techniques gained from graduate studies while a student at the University of Tennessee Space Institute located in Tullahoma, Tennessee, while pursuing a Master of Science degree in Mechanical Engineering. A historical timeline for work on the engine is shown in Figure 1 for reference.

This project involves building a ground based gas turbine engine (GTE) for use as a technology demonstrator that has been given the title, Turbine Engine Component Testbed (TECT). This particular GTE will be in the ≈60 lbf thrust class with afterburning/augmented capability. Although engine thrust is not a primary function or measurement goal, the engine augmentor acts as a relevant high enthalpy environment for technology demonstration. The augmentor assembly is easily removed if not required for the test objectives. The TECT is designed with modularity as a key design consideration for all components. The TECT is fully instrumented with basic performance measurements, as well as engine health and safety parameters required for safe operation. The data acquisition system allows real-time data acquisition and control with programmable automated engine sequences for start-up, shutdown, and abort functions. The TECT is configured for single user control, although depending on the test objectives multiple users may be required for additional data systems or control of secondary systems if required.

The TECT was built using many off-the-shelf (OtS) parts and can be run and modified for only a fraction of the cost of a larger production engine or development engine. The TECT gives a relevant environment for advanced technology programs

that may require testing at a lower technology readiness level (TRL) before moving up to a full scale system to reduce the inherent technical risk of these types of projects.

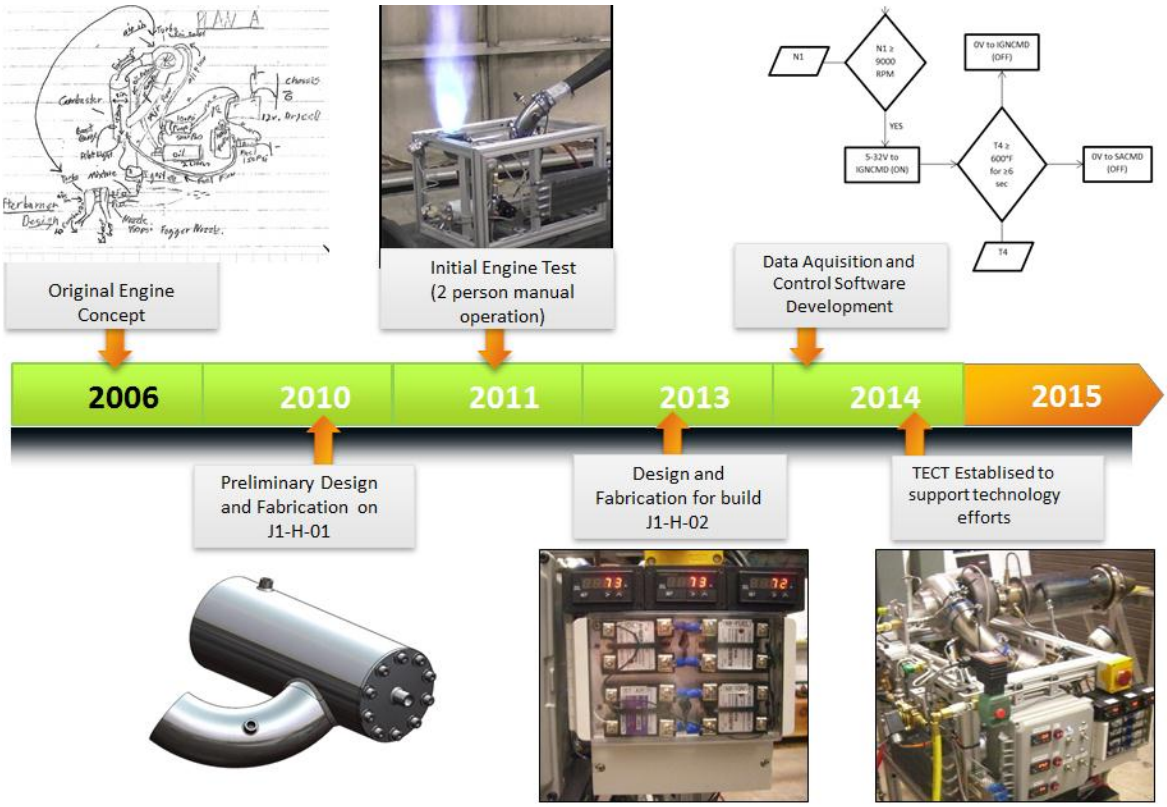

Figure 1. Engine development history

Background

Basic Gas Turbine Review

All air breathing gas turbine engines have four major components in common: the compressor, combustor, turbine, and nozzle. A typical non-augmented turbojet engine cross-section is shown in Figure 2 with the main components (Cumpsty 2006). The compressor takes the free-stream ambient flow and compresses it to a higher enthalpy state to prepare it for combustion in the combustor where the air and fuel are mixed together and ignited to form hot high

pressure gas. The gas is next expanded across turbine blades that extracts a portion of the energy from the flow to drive the compressor through the engine shaft. Downstream of the turbine, the flow is accelerated by the nozzle and according to Newton's 3rd law creates thrust. If the engine is augmented (afterburning), as within the current testbeds capability, there is another region for combustion, after additional fuel has been added, downstream of the last turbine stage to increase the temperature and therefore the enthalpy of the fluid flow before being accelerated through the nozzle. The augmentor is a way to add power output for a given compressor pressure ratio. The gas turbine engine operates using the Brayton cycle for thermodynamics. The T-s diagram for a 'real' (with component efficiency losses) afterburning turbojet engine is shown in Figure 3. Note that the 'AB Operation' region increases the useful work (Thrust, *F)* of the engine. This increase in useful work comes at a large increase in fuel consumption (typically 3-5x). It is assumed that the reader has some background with thermodynamics and turbo-machinery as well as basic understanding of engineering design. The reader is referred to Huenecke 2005 for a more in-depth review. For a full review on the basics of gas turbine engine propulsion see Cumpsty, 2006 or Mattingly, 2006.

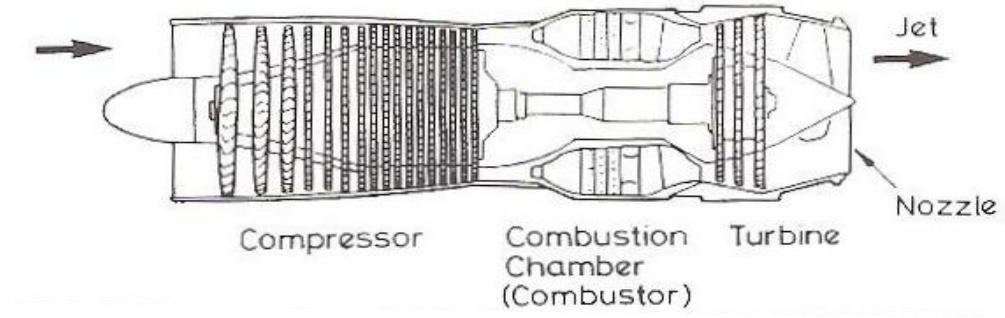

Figure 2. Typical turbojet engine showing four main components [7]

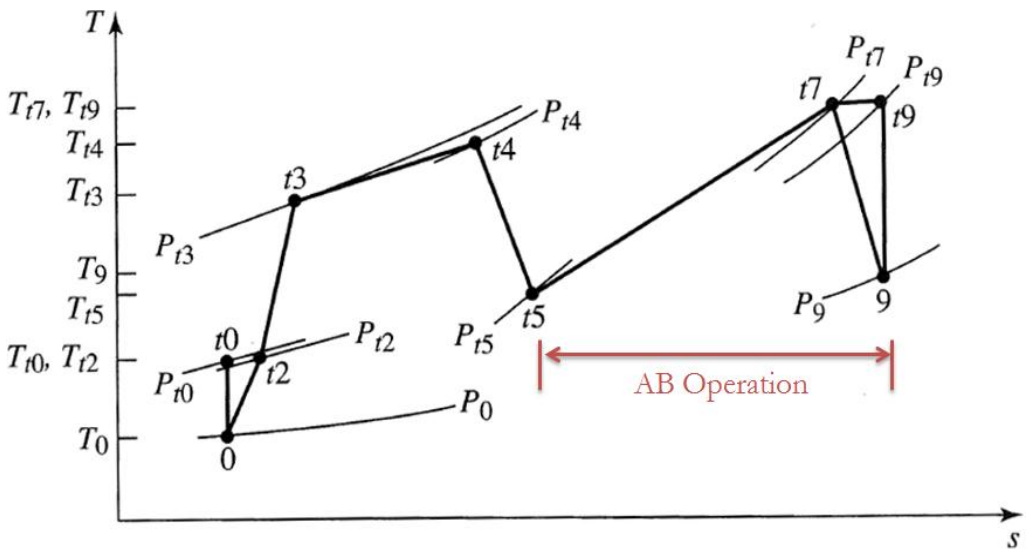

Figure 3. T-s diagram for real afterburning turbojet engine [19]

Project Goals

The goals of the TECT engine have evolved from build 1 to build 2 (J1-H-01 to J1-H-02). The second engine builds project goals are as follows:

1. Design and fabricate the engine using off-the-shelf (OtS) parts where appropriate
2. **Keep modularity as the top consideration when designing the major components***
3. Obtain data real-time from engine i.e. pressure, temperature, shaft speed, etc
4. Easily adaptable data acquisition and control software
5. Ability to shutdown engine when predetermined operating conditions are met
6. Ability to perform extended runs >10 mins without overheating
7. Run on hydrocarbon fuels
8. Compressed air starting capability
9. Model engine with a 3D computer aided design (CAD) software
10. Test at ground non-ram, Sea-Level (SL) conditions

11. Run support systems on 12VDC for remote location operating capability
12. Deliver accurate data upon project completion for analysis

*Highest Priority

Challenges

- Many interdisciplinary aspects: design, fabrication, and analysis (requires self-education for less proficient areas)
- Parts for the intended use are very expensive and have long lead times (need to be innovative to be successful)
- Large number of custom components requires fabrication techniques that lead to higher costs and longer schedule
- Control system must be robust enough to handle unexpected occurrences while still shutting down the engine safely
- High rotational speeds are a concern for safety along with the use of hydrocarbon fuels
- Keeping the system ‘mobile’ requires subsystems to be on-board the engine test stand
- Modularity requirement requires that all components be easily changed and replaced with newly ‘modified’ components

Potential Work

Future turbine engine development programs (particularly military) have identified a need for advanced engine diagnostics and test techniques. These techniques can require unrestricted access to flow field environments that are normally unavailable for technology efforts that are still in the early stages of development. Often the costs and schedule associated with attempting to develop

one of these programs is enough to stop the effort altogether. Potential work for the TECT includes:

- Combustion instability characterization and analytical techniques
- Augmentor screech and rumble onset prediction
- Non-intrusive instrumentation diagnostic techniques
- Combustion imaging/Light off detection
- Combustion products/species measurement
- Advanced optical/laser techniques
- New COTS measurement risk reduction
- New controls techniques risk reduction
- Advanced augmentor combustion/stability techniques

The TECT can be run and modified for only a fraction of the cost of a larger production or development engine but gives a relevant environment for advanced technology programs that may require some testing at a lower technology readiness level (TRL) before moving up to a full scale system. The TRL system is a metric that is commonly employed by various government agencies as well as some industry to assess the maturity of a component, technology, system before it is fielded or released for purchase. Depending upon the maturity of the technology under consideration the project can start anywhere within the TRL's. The TECT engine will allow a relevant test environment for TRL's 3-5 when approached from a Department of Defense (DoD) definition. Table 1 shows the DoD TRL levels with their respective definitions. The TECT engine targeted TRL levels are highlighted and will change depending on the technology project being tested. For a more complete background on TRL see the *DoD 5000.2-R.*

Table 1. List of Technology Readiness Levels with their descriptions

Technology Readiness Level	Description
1. Basic principles observed and reported.	Lowest level of technology readiness. Scientific research begins to be translated into applied research and development. Examples might include paper studies of a technology's basic properties.
2. Technology concept and/or application formulated.	Invention begins. Once basic principles are observed, practical applications can be invented. Applications are speculative and there may be no proof or detailed analysis to support the assumptions. Examples are limited to analytic studies.
3. Analytical and experimental critical function and/or characteristic proof of concept.	Active research and development is initiated. This includes analytical studies and laboratory studies to physically validate analytical predictions of separate elements of the technology. Examples include components that are not yet integrated or representative.
4. Component and/or breadboard validation in laboratory environment.	Basic technological components are integrated to establish that they will work together. This is relatively "low fidelity" compared to the eventual system. Examples include integration of "ad hoc" hardware in the laboratory.
5. Component and/or breadboard validation in relevant environment.	Fidelity of breadboard technology increases significantly. The basic technological components are integrated with reasonably realistic supporting elements so it can be tested in a simulated environment. Examples include "high fidelity" laboratory integration of components.
6. System/subsystem model or prototype demonstration in a relevant environment.	Representative model or prototype system, which is well beyond that of TRL 5, is tested in a relevant environment. Represents a major step up in a technology's demonstrated readiness. Examples include testing a prototype in a high-fidelity laboratory environment or in simulated operational environment.
7. System prototype demonstration in an operational environment.	Prototype near, or at, planned operational system. Represents a major step up from TRL 6, requiring demonstration of an actual system prototype in an operational environment such as an aircraft, vehicle, or space. Examples include testing the prototype in a test bed aircraft.
8. Actual system completed and qualified through test and demonstration.	Technology has been proven to work in its final form and under expected conditions. In almost all cases, this TRL represents the end of true system development. Examples include developmental test and evaluation of the system in its intended weapon system to determine if it meets design specifications.
9. Actual system proven through successful mission operations.	Actual application of the technology in its final form and under mission conditions, such as those encountered in operational test and evaluation. Examples include using the system under operational mission conditions.

DoD 5000.2-R, April 5, 2002

CHAPTER II
THEORETICAL ANALYSIS

The engine was analyzed for both “On-Design” and “Off-Design” performance using gas turbine engine cycle analysis theory. The engine performance was predicted using Dr. Jack Mattingly’s EOP software package. Dr. Mattingly is an expert in the field of gas turbine engine cycle analysis.

Parametric Cycle Analysis

The parametric cycle analysis was applied to determine “design point” performance. This allows considerations to be made for engineering trade-space between components. Because the engine is limited by off-the-shelf components as a key project goal consideration, the engine design is limited by many variables such as compressor pressure ratio and EGT. Parametric cycle analysis has the following characteristics:

- *Useful for determining variations in engine performance with design parameters*
- *Determines engine performance at a single ‘design-point’ given design choices such as compressor pressure ratio and Turbine inlet temperature, etc.*
- *Characterized by property changes not geometry, therefore when plotting performance parameters each point is a different engine (rubber engine)*
- *Primary purpose is to relate engine performance parameters (Thrust, F and Thrust Specific Fuel Consumption, TSFC) to design choices and limitations (Compressor Pressure Ratio, Turbine Inlet Temperature, TiT, etc.)*
- *This can help to limit design space and will allow engine type to be determined*

The PARA software program calculates the variation in performance with design parameters (on-design analysis) of gas turbine engines (ideal and real cycles). This software is complementary to the text, Elements of Propulsion: Gas Turbines and Rockets (2006) published by AIAA. This program was written in the VisualBASIC programming environment. A screenshot of the basic setup page for the PARA software is shown in Figure 4. The raw data output from the PARA program is shown in Table 2, note that the program is iterating for compressor pressure ratios from 1.2-3. The specific thrust and TSFC vs. the compressor pressure ratio and combustor exit total temperature is shown in Figure 5-Figure 6. Note that the specific thrust and thermal efficiencies increase, while the TSFC decreases for increasing compressor pressure ratio and total temperature leaving the combustor. This behavior is the driving factor for gas turbine engines to push both of these parameters to their materials limits.

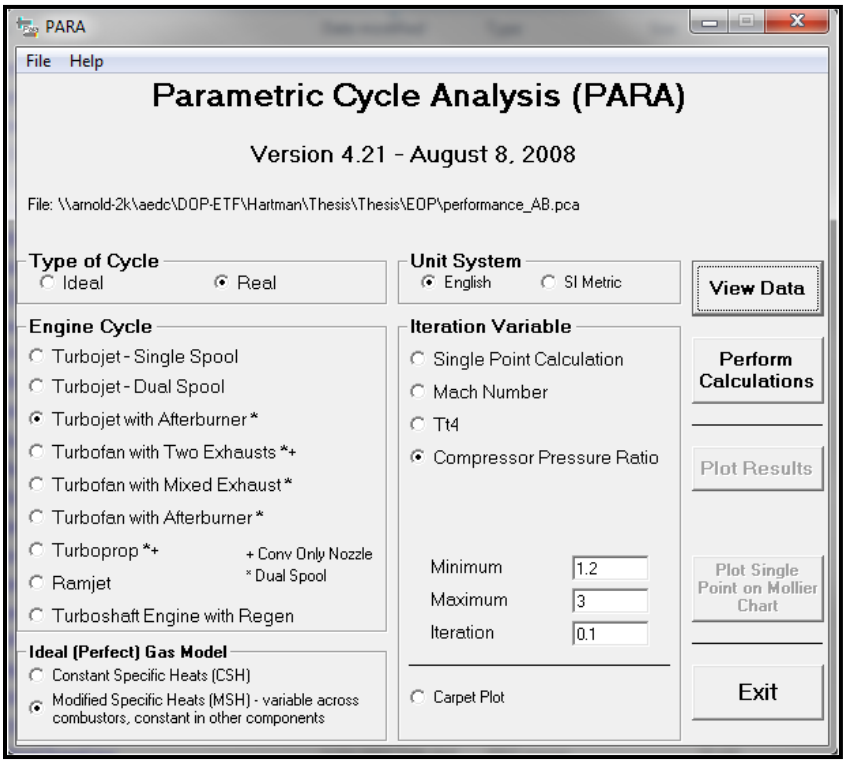

Figure 4. Screenshot of the PARA analysis software

Results

Table 2. Input and Output data for Parametric Analysis

```
                Real Turbojet Engine with Afterburning
    with Variable Specific Heats across Combustors - Curve Fit
**********************      Input Data      **********************
      Mach No    =  0.000
      Alt (ft)   =      0               Pi cL         =  1.000
      T0 (R)     = 518.69               Pi d (max)    =  0.999
      P0 (psia)  = 14.300               Pi b          =  0.950
      Density    = .0023125             Pi n          =  0.980
       (Slug/ft^3)                     Efficiency
      Cp c       = 0.2400 Btu/lbm-R     Burner        =  0.995
      Cp t       = 0.2950 Btu/lbm-R     Mech Hi Pr    =  0.995
      Gamma c    = 1.4000               Mech Lo Pr    =  0.995
      Gamma t    = 1.3000               LP Comp       =  0.890 (ecL)
      Tt4 max    = 1660.0 R             HP Comp       =  0.750 (ecH)
      h - fuel   =  18400 Btu/lbm       HP Turbine    =  0.800 (etH)
      P0/P9      = 1.0000               LP Turbine    =  0.800 (etL)
           ** Afterburner **
      Tt7 max    = 3500.0 R             Pi AB         =  0.950
      Cp AB      = 0.2950 Btu/lbm-R     Eta A/B       =  0.950
      Gamma AB   = 1.3000
*************************    RESULTS    *************************
      Tau r      =  1.000               a0 (ft/sec)  = 1116.5
      Pi r       =  1.000               V0 (ft/sec)  =   11.2
      Tau L      =  3.934
  Pi c F/mdot    S    Tau t Pt9/P9  V9/a0  T Eff  P Eff
  1.20  V9^2 is negative. This case is meaningless.
  1.30  V9^2 is negative. This case is meaningless.
  1.40  16.7710.8535 0.9656  1.02346.9606  0.620  4.174
  1.50  24.59 7.4029 0.9580  1.05068.3917  1.315  2.884
  1.60  29.82 6.1023 0.9506  1.07582.7475  1.925  2.390
  1.70  33.77 5.3877 0.9436  1.09793.5775  2.463  2.116
  1.80  36.90 4.9288 0.9368  1.117102.179  2.937  1.939
  1.90  39.47 4.6077 0.9302  1.135109.209  3.356  1.816
  2.00  41.60 4.3706 0.9239  1.151115.059  3.726  1.724
  2.10  43.39 4.1889 0.9177  1.165119.982  4.052  1.654
  2.20  44.91 4.0461 0.9117  1.178124.157  4.340  1.599
  2.30  46.21 3.9317 0.9059  1.190127.711  4.593  1.554
  2.40  47.31 3.8390 0.9002  1.200130.743  4.815  1.519
  2.50  48.26 3.7633 0.8947  1.209133.327  5.008  1.489
  2.60  49.06 3.7010 0.8893  1.217135.523  5.176  1.465
  2.70  49.73 3.6499 0.8840  1.224137.378  5.320  1.446
  2.80  50.30 3.6080 0.8789  1.229138.930  5.442  1.430
  2.90  50.76 3.5740 0.8738  1.234140.213  5.544  1.417
  3.00  51.14 3.5467 0.8689  1.238141.253  5.628  1.406
```

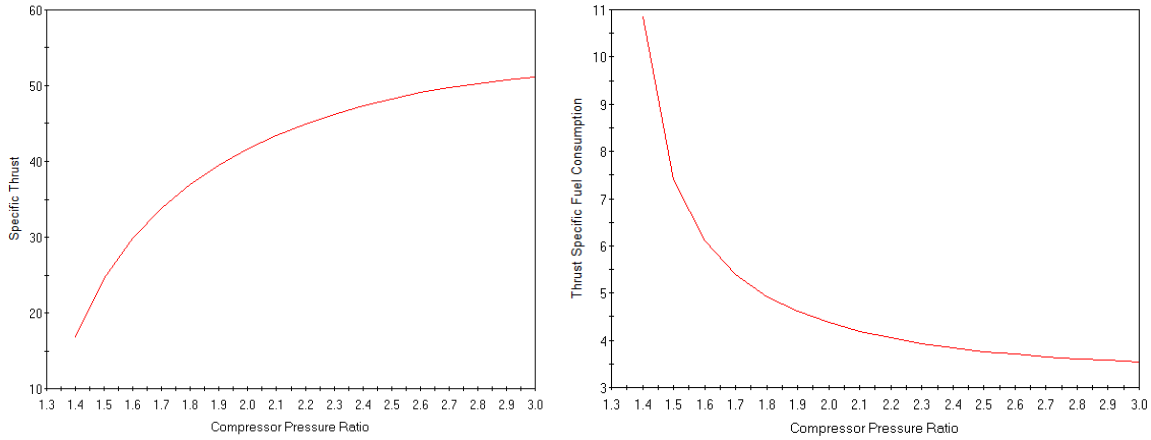

Figure 5. Specific Thrust and TSFC vs. CPR at sea-level

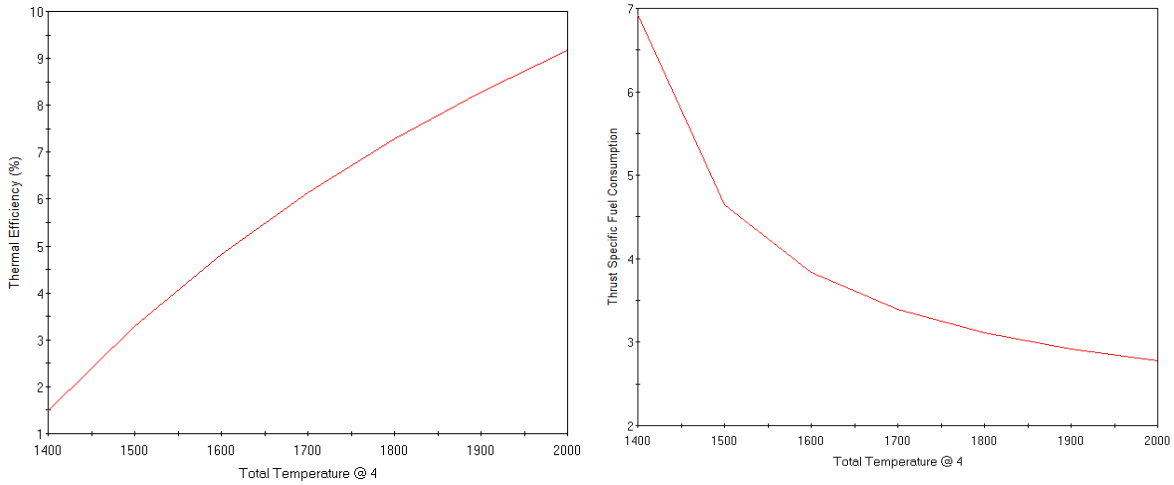

Figure 6. Thermal Efficiency and TSFC vs. TiT

Performance Cycle Analysis

Once the engine design has been selected from the engineering trade-space with the help of the parametric cycle analysis, performance cycle analysis is performed to estimate both the on-design and off-design performance. Performance cycle analysis has the following characteristics:

- Allows for the prediction of engine performance with flight condition and throttle setting of a single engine design

- Very useful for prediction ‘off-design’ performance and will allow for a good estimate for preliminary design
- Allows for performance prediction when new technology is available for components

The PERF software calculates the variation in an engine's performance with changes in flight condition and throttle setting (without any driven engine accessories). The performance analysis is based on the application of mass, energy, momentum, and entropy of a one-dimensional flow for a perfect gas at steady state operation only. For the current configuration being a ground based test stand, the variation in engine performance from different flight conditions is not applicable as all testing is performed at Sea-Level Static (SLS) conditions. If the testbed were to be inserted into a RAM air environment to simulate Mach number, the software should be ran to estimate the performance impact. The PERF analysis was run for both augmented and non-augmented performance.

Results

The TECT was analyzed at the maximum expected operating conditions provided with the compressor performance map. The largest contributors to performance are the compressor pressure ratio and the turbine inlet temperature. The performance analysis was run using a compressor pressure ratio, PiC of 3:1 and a maximum turbine inlet temperature of 1,200 ºF (1660ºR). The 1,200 ºF turbine inlet temperature was selected, as this is the maximum inlet temperature that the turbine would experience in an automotive installation. The results of the performance analysis are shown in Figure 7 for the non-augmented case and Figure 8 for the augmented case. Note that there is an increase in the predicted thrust of ~50% while in augmented operation. This increase in thrust comes at a much larger increase in thrust specific fuel consumption ~180%. The station numbering for the TECT engine begins at station 1 at the engine inlet face for the remainder of the analysis.

Uninstalled Engine Performance at Reference Point

Thrust		**45**	**lbf**	**Turbomachinery Efficiency (%):**	Compressor	75.00
Thrust Specific Fuel Consumption		**1.3455**	**lbm/(hr-lbf)**			
Thermal Efficiency (%)		10.40			Turbine	81.38
Propulsive Efficiency (%)		2.01				

Station:	2	3	4	5	8	9
Tt (R)	518.68	788.24	1660.00	1442.39	1442.39	1442.39
Pt (psia)	14.29	42.86	40.72	19.02	19.02	18.45
Mach			1.00		0.64	0.6354

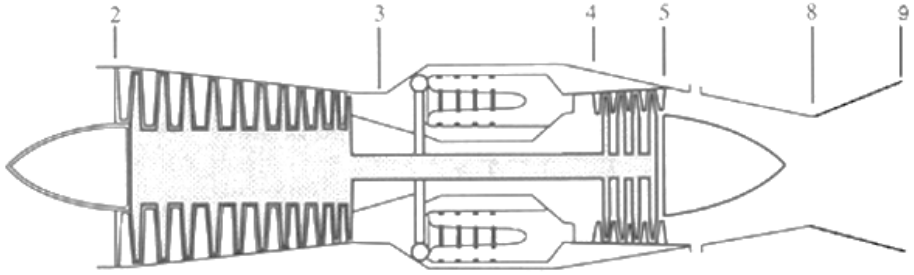

Figure 7. Performance station results for non-augmented engine operation

Uninstalled Engine Performance at Reference Point

Thrust		**66**	**lbf**	**Turbomachinery Efficiency (%):**	LP Compressor	70.95
Thrust Specific Fuel Consumption		**3.7356**	**lbm/(hr-lbf)**		HP Compressor	75.00
					Fan	70.95
Thermal Efficiency (%)		5.29			HP Turbine	80.00
Propulsive Efficiency (%)		1.42			LP Turbine	81.38

Station:	2	2.5	3	4	4.5	5	8	9
Tt (R)	518.68	788.24	788.24	1660.00	1660.00	1442.39	3600.00	3600.00
Pt (psia)	14.59	43.76	43.76	41.57	41.57	19.42	18.45	17.89
Mach				1.00	1.00		0.57	0.5662

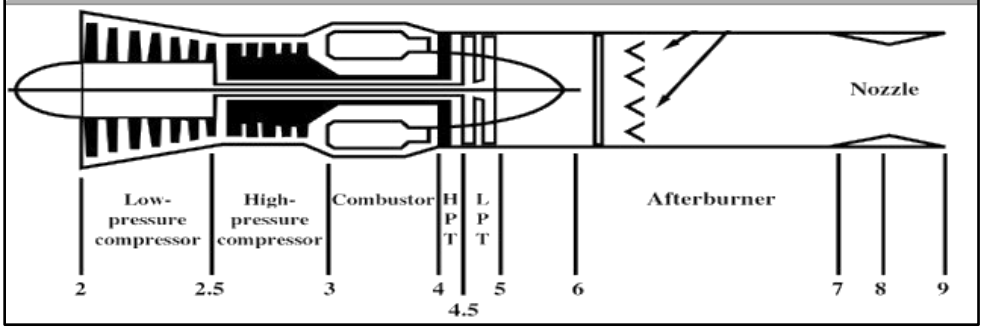

Figure 8. Performance station results for augmented engine operation

Note that this analysis does include properties for fuel and gas properties, total pressure losses across the components, as well as polytropic efficiencies. These values were either known for the different components or assumed by similarity to known components for the technology level. The properties for the TECT performance analysis are shown in Table 4. Note that the total pressure lost across the diffuser is very low because the engine does not have a diffuser installed. A diffuser is not required for the TECT, as the engine will only be tested at sea-level static conditions, therefore a diffuser is not required to slow down the entry flow before entering the compressor. A good reference for component efficiency figures of merit are provided for reference in Table 3.

Table 3. Component efficiencies figures of merit [19]

			Level of technology[b]			
Component	Figure of merit	Type[a]	1	2	3	4
Diffuser	$\pi_{d\,max}$	A	0.90	0.95	0.98	0.995
		B	0.88	0.93	0.96	0.98
		C	0.85	0.90	0.94	0.96
Compressor	e_c		0.80	0.84	0.88	0.90
Fan	e_f		0.78	0.82	0.86	0.89
Burner	π_b		0.90	0.92	0.94	0.95
	η_b		0.88	0.94	0.99	0.999
Turbine	e_t	Uncooled	0.80	0.85	0.89	0.90
		Cooled		0.83	0.87	0.89
Afterburner	π_{AB}		0.90	0.92	0.94	0.95
	η_{AB}		0.85	0.91	0.96	0.99
Nozzle		D	0.95	0.97	0.98	0.995
	π_n	E	0.93	0.96	0.97	0.98
		F	0.90	0.93	0.95	0.97
Mechanical shaft	η_m	Shaft only	0.95	0.97	0.99	0.995
		With power takeoff	0.90	0.92	0.95	0.97
Maximum T_{t4}		(K)	1110	1390	1780	2000
		(R)	2000	2500	3200	3600
Maximum T_{t7}		(K)	1390	1670	2000	2220
		(R)	2500	3000	3600	4000

[a]A = subsonic aircraft with engines in nacelles D = fixed-area convergent nozzle
B = subsonic aircraft with engine(s) in airframe E = variable-area convergent nozzle
C = supersonic aircraft with engine(s) in airframe F = variable-area convergent-divergent nozzle
[b]Notes: Stealth may reduce π_{dmax}, π_{AB}, and π_n. The levels of technology can be thought of as representing the technical capability for 20-yr increments in time beginning in 1945. Thus level 3 of technology presents typical component design values for the time period 1985–2005.

Table 4. Properties for performance analysis

Fuel and Gas Properties

Fuel Heating Value (Btu/lbm)	18400
Cp c {Btu/(lbm-R)}	0.24
Gamma c	1.4
Cp t {Btu/(lbm-R)}	0.295
Gamma t	1.3

Component Efficiencies

Burner	0.999
Mechanical Shaft	0.995

Component Total Pressure Ratios

Pi Diffuser Max (Pt2/Pt1)	0.999
Pi Burner (Pt4/Pt3)	0.95
Pi Nozzle (Pt9/Pt7)	0.97

Polytropic Efficiencies

Compressor	0.75
Turbine	0.8

Exhaust Nozzle

P0/P9	1

CHAPTER III
DESIGN AND FABRICATION

The TECT program involves multi-disciplinary aspects: mechanical design, materials engineering, and electrical design. Proper design analysis was exercised prior to fabrication using modern engineering tools to ensure component life and durability. The engine design is analyzed using Computer Aided Design (CAD), Finite Element Analysis (FEA), and hand calculations to aid in the design of the engine as well as form, fit, and function of components. The engine was then fabricated using a mixture of design features obtained from the analysis and trial and error where appropriate. The methods are described in the following sections. It should be noted that this work is not intended to serve as an 'engine design' guide but rather to present some of the approaches used to create a laboratory style gas turbine that is not built for flight, ground based power generation, regenerative cycles, or many other gas turbine applications. The sole purpose is described in the Background section above.

Theory of Operation

The current TECT engine configuration is shown in Figure 9 below. Note the same gas turbine operating principles are applied, as the more familiar axial flow style engine that all modern aircraft use. The TECT engine operates using the equivalent thermodynamic Brayton cycle. While a typical turbojet/turbofan engine may have anywhere from 5-12 compressor stages and 1-5 turbine stages, the experimental TECT engine consists of a single stage centrifugal compressor and radial inflow turbine. The single stage centrifugal compressor gives a maximum pressure ratio of ≈3:1. The decision to use a centrifugal compressor has many advantages for a ground based testbed, namely for simplicity, these advantages will be discussed in detail in the compressor and centrifugal compressor analysis sections. The compressor is performance matched to the radial inflow turbine for automotive 'turbo-charging' applications, and although it's current application is

different than its intended use it still provides enough energy to the compressor to continue the Brayton cycle for a gas turbine application and withstands the temperature environment well. The main combustor is a single canned style design with a circular cross-section and removable flame-tube. The main combustor operates on gaseous propane fuel because of its easy combustion characteristics and does not require the use of a fuel pump because the gas is pressurized at ~120 psig, which is much higher than the compressor discharge pressure, and therefore is easily injected into the main combustor. The TECT engine augmentor runs on liquid hydrocarbon fuels such as kerosene through a series of augmentor spray nozzles. The engine employs a modular fixed area convergent nozzle. The details associated with this design are covered in the following sections.

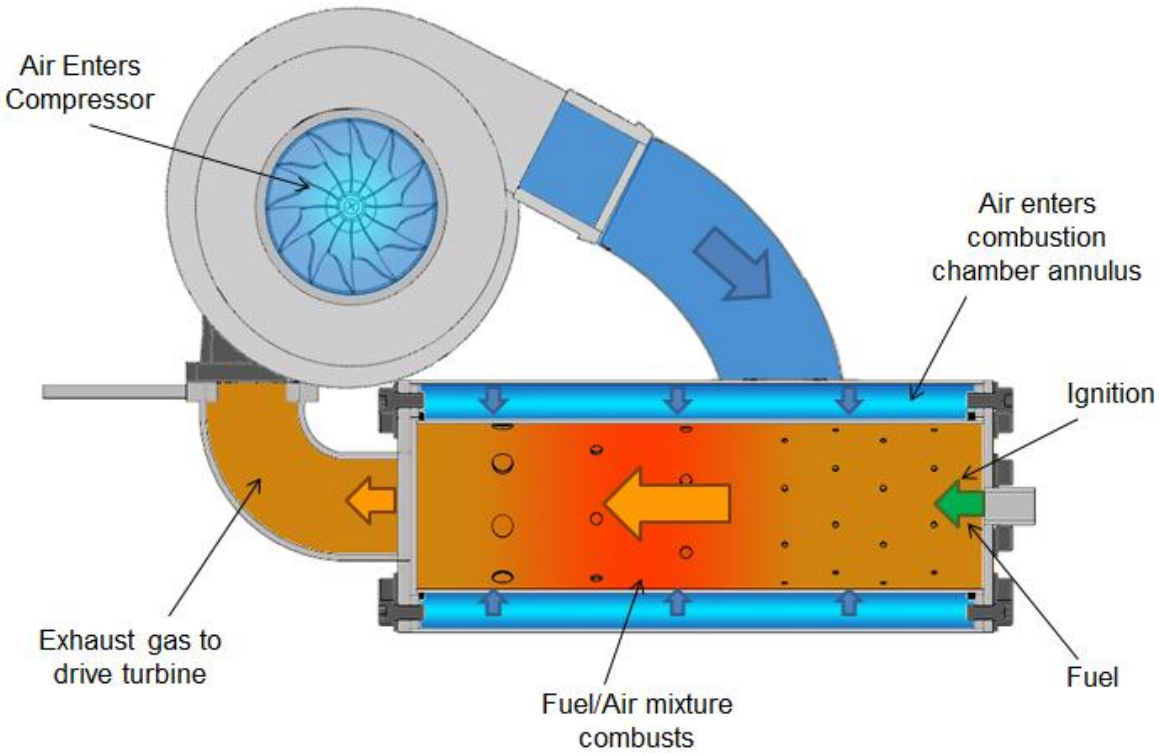

Figure 9. TECT Engine Cross-Section

CAD Modeling

In the early stages of the project, the CAD model was used to assist with component placement and fabrication of the engine, see Figure 10. Having the components modeled allowed for easier fabrication of components, as the engineering drawings were readily available to the machinist. The CAD model also assisted with creating parts lists for budgeting and mocking up future components to ensure proper fit within the confined space of the test stand. The combustor was modeled and then used for additional analysis, see Figure 11. Space within the engine test stand was very critical and component placement needed to be planned before installation to ensure that none of the components would interfere with one another. The final model is not a full representation of the completed engine, but an accurate model of most of the fabricated components and is a good starting point for adding future components that may be required for the TECT, see Figure 12. The CAD model was used to generate engine component cross-sections and assembly drawings to assist with the project documentation. Temperature critical components, such as the electronics needed to be kept away from heat sources such as the combustor. ANSYS FEA software was used with the CAD model to perform heat transfer

Figure 10. CAD assembly of basic components

Figure 11. CAD model of canned combustor

analysis on the electronics package to ensure that the temperatures would not exceed the specifications. If heat soaking occurred where the instrumentation signal conditioning is being handled, then measurement uncertainty could be affected by thermal drift, see Appendix E.

Figure 12. CAD assembly of critical components

Fabrication Techniques

The fabrication and assembly of this engine requires off-the-shelf, modified, and fabricated components. Off-the-shelf parts were used where applicable and being a project goal to use as many off-the-shelf parts as possible, all attempts were made to find parts that would work even if they were not originally designed for the exact intended function. Without the use of parts from the aerospace, automotive, and petrochemical industry to reduce design and fabrication time, the project would not have become a reality without heavy financing and contracted support. However, as

a result of the ‘one of a kind’ aspects and unique design of the project, many components were required to be custom made using techniques that were new to the designer and in many cases had to be studied and practiced to continue with progress. This approach was taken to keep overall project costs down. The building and assembly of the engine required the use of almost all machinery commonly found in a modern machine shop, see Figure 13. The majority of the fabrication work was performed in house, but some of the more intricate machining needed to be performed by a trained professional/technician. This included any work that required the use of a CNC machine or GTAW/TIG welder. Most of the major system components required some modification for use on the TECT or in most cases completely custom parts from raw materials were required to be built see Figure 14. A list of some of the major required equipment used is as follows:

- Metal Lathes
- Vertical End Mill with multi-axis
- CNC
- GTAW/TIG Welder
- Sheet metal brake/shear
- Vertical Band-Saw
- Horizontal Band-Saw
- Drill Press
- Sandblaster
- Belt sander/grinder
- Various taps and dies

Figure 13. Fabrication of components

Figure 14. Various parts after machining and TIG welding

Compressor

The type of compressor present on the current engine is a single-stage centrifugal compressor, also commonly referred to as a radial compressor. These types of compressors have been around for over 100 years. The original applications were first used in air blowers and then into turbo-superchargers for early aircraft. This would allow piston engine aircraft to fly higher and faster at increasing altitudes. At these upper altitudes the air density is lower and by providing greater than atmospheric pressure, and therefore density from the turbo-supercharger into the cylinders, this yields more horsepower from the engine to

drive the prop. The waste energy from the exhaust is used to drive the compressor or in some cases the compressor is driven from a pulley attached to the engines crankshaft. This proved to be a weight saving and fuel efficient option for adding power to piston engine aircraft when compared to adding more cylinders or increasing displacement. The centrifugal compressor was first used in jet engines independently by both Frank Whittle and Hans Von Ohain in the late 1930's. Both Whittle and Von Ohain are credited with independently inventing the jet engine. Whittle performed his work in Great Britain, while Von Ohain was in Germany.

A typical centrifugal compressor cross-section is shown in Figure 15. Centrifugal compressors usually consist of two main parts: a *rotor* or *impeller* and a static *diffuser* section as shown in Figure 15**.** The impeller imparts energy to the flow from the turbine. The flow through the impeller increases both velocity and pressure as it is turned 90^0 into the diffuser section where the air is collected and manifolded for preparation to go to the combustor. The flow leaving the centrifugal compressor is perpendicular to the axis of rotation.

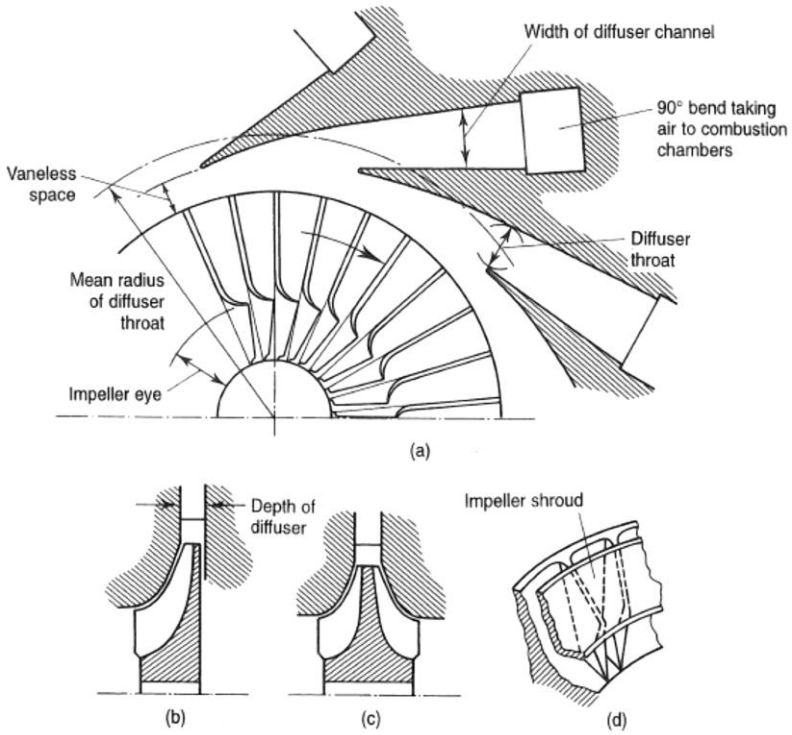

Figure 15. Sketches of centrifugal compressors [2]

Because no work is imparted on the flow in the diffuser, the energy state of the flow will be determined by the conditions at the inlet and outlet of the impeller. The flow goes from a high kinetic energy state from the impeller to a conversion into increased static pressure in the diffuser. The polytropic efficiency, e_c is taken from the compressor performance map and for the TECT has a maximum efficiency of 75%. The compressor efficiency decreases from a series of losses in the rotor and diffuser assembly. A plot of typical losses through the compressor stage is shown in Figure 17, (Boyce, 2002). According to Church (1972), he describes the centrifugal compressor as: “consisting essentially of one or more impellers equipped with vanes, mounted on a rotating shaft and enclosed by a casing. Fluid enters the impeller axially near the shaft and has energy, kinetic and potential, imparted to it by the vanes. As the fluid leaves the impeller at a relatively high velocity, it is collected in a volute or series of diffusing passages which transforms the kinetic energy into pressure. This is, of course, accompanied by a decrease in velocity.” In most cases, the pressure rise occurs approximately half in the impeller and half in the diffuser section as shown on the right in Figure 16**.**

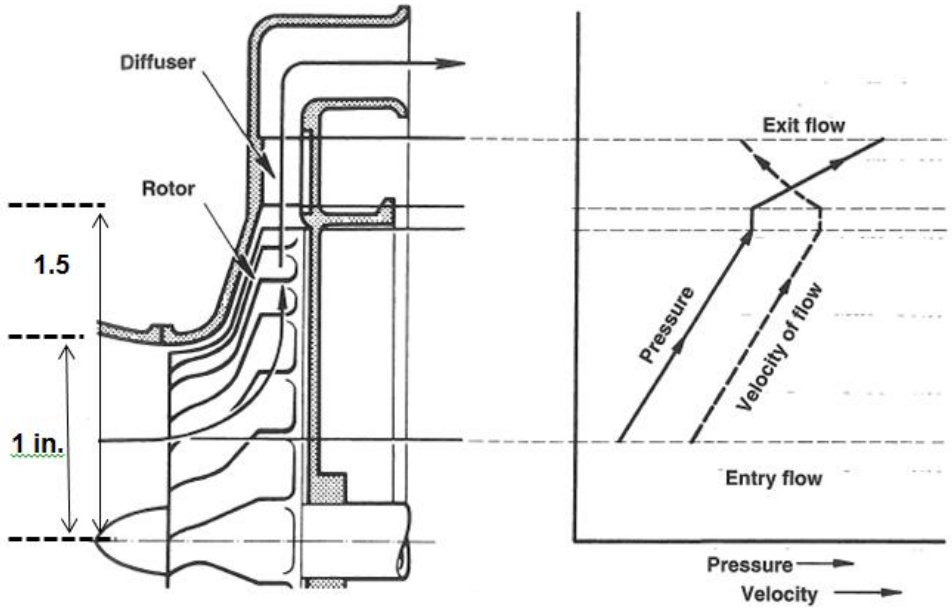

Figure 16. Pressure and velocity profile in a centrifugal compressor [12]

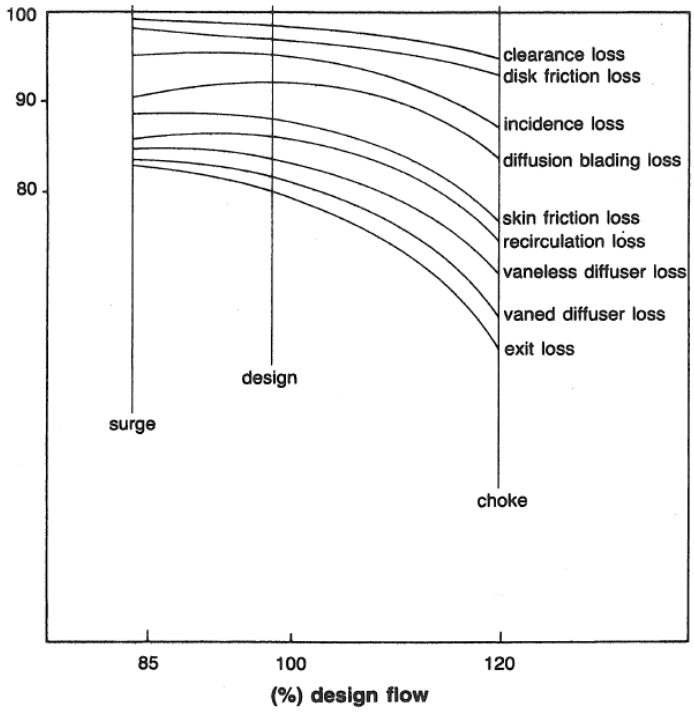

Figure 17. Losses in a centrifugal compressor [2]

The centrifugal compressor has some large benefits when compared to its axial counterpart. The largest advantage, being single-stage pressure rises can be as high as 4:1-8:1, depending on the materials, blade design, inlet conditions, and loses. These higher stage compressor pressure ratios can significantly shortens the overall length of the compressor section when compared to the equivalent pressure rise of its axial counterpart, if high mass flow rates are not required (<15 lbm/sec). Another major advantage is, they are less prone to compressor stall when compared to the axial compressor and are less susceptible to foreign object damage (FOD), as well as less susceptible to building up deposits on the blades causing preformation deterioration over long periods of operation. Centrifugal compressors are also relatively cheap to manufacture because they can be cast and then machine finished, see Table 5. Some of the major disadvantages of the centrifugal compressors are: they have a large frontal area, which for aircraft cause large drag at increasing flight velocities. They cannot move as much air (mass flow) per cross-sectional area as their axial counterparts, therefore putting a limit on

overall engine thrust for a given aircraft engine bay integration goal. This is a direct outcome of the standard equation for thrust. There are two ways to increase thrust, either increase the amount of air through the engine (mass flow) or increase the air's exit velocity through the engine nozzle. Modern day axial compressors achieve both objectives more efficiently than their centrifugal counterparts. Centrifugal compressors are still used today, mostly in small engines and aircraft APU's (auxiliary power units), as well as for ground based support equipment, such as gas turbine engine start carts and flight line generators.

Table 5. Advantages of centrifugal compressor

Advantages of Centrifugal Compressor:
• Single-stage pressure rises can be as high as 4:1-8:1 • Less susceptible to foreign object damage (FOD) • Less susceptible to building up deposits on the blades causing performance deteration • **Relatively cheap to manufacture because they can be cast and then machined finished/balanced*** • Less prone to compressor stall when compared to the axial compressor • Shorter overall length when compared to the axial compressor for an equivalent pressure rise *Highest Priority

The centrifugal compressor was chosen for the current application because of its relatively simple and economical design and large single-stage pressure rise (approx 3:1). Because the current engine is to be used as a technology demonstrator at static conditions, the larger frontal area is not of any concern with regard to aerodynamic drag, which is a concern for fixed-wing aircraft. The compressor discharge is also easily adaptable to the chosen canned combustor arrangement. For the current application, the centrifugal compressor was taken

from the automotive application of a car turbocharger. This allowed for a large cost savings and eliminated design complexities associated with design and fabrication of a one-off part. This also allowed for a simplified combustor design when compared to the axial compressor because of the single outlet of the volute diffuser section.

The turbine is a single-stage radial inflow turbine. The compressor and the turbine are connected through the center housing. The center housing holds the bearings and the rotating assembly consisting of the compressor, shaft, and turbine. It does not include the compressor volute/diffuser or the turbine casing/scroll. The centrifugal compressor is shown in Figure 18**.** Note that the blades are curved at the impeller inlet eye so that the flow can pass smoothly into the device axially. The blades are also slightly backward swept.

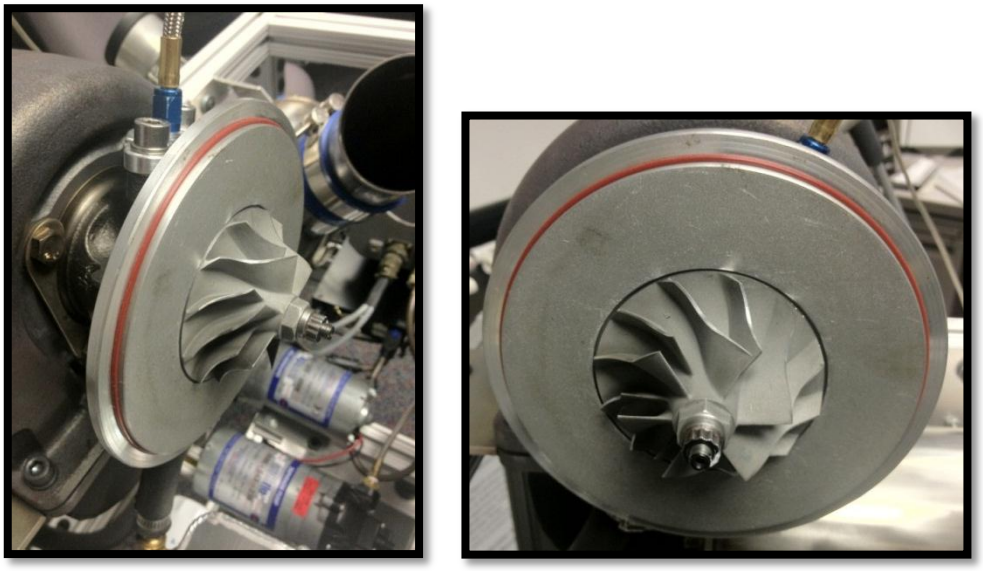

Figure 18. Views of the current engines centrifugal compressor

The oil feed line to the center housing is shown at the top of Figure 18. This oil feed keeps the two brass journal bearings and the one thrust bearing lubricated and cooled, as shown in Figure 19. The center-housings steady state temperatures are quite a bit higher for the gas turbine application when compared to its intended

automotive application. This is mainly caused by the internal combustion engines transient operation and subsequent combustion process. The turbine engine undergoes typically a less transient operation and requires a constant combustion process to operate, increasing the steady state turbine inlet temperatures. For the current application, the oil flow requirement is driven by cooling rather than lubrication because of the considerations mentioned above. To increase the oil flow rate and therefore increase the cooling to the center housing, the oil inlet orifice diameter was increased from 1/32 in. to 3/16 in. This allows more oil to flow for a given pressure through the center housing keeping it cooler and extending life, this also reduces the risk of oil coking in the center housing; a real concern for extended operation. If the turbo is water jacketed the orifice can be left unmodified.

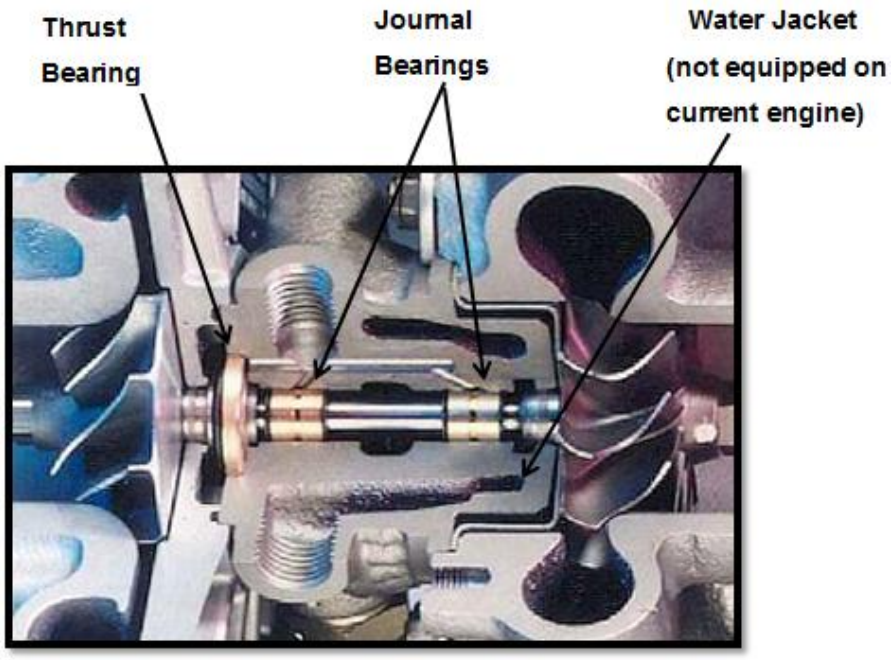

Figure 19. Cross-section showing the journal and thrust bearings

There are many types of diffusers that can be used with the centrifugal compressor but the three main types according to Church (1972), are “the annular diffuser, which is a ring shaped space; the volute diffuser, which is a spiral-shaped passage having increasing cross-sectional area as it approaches the discharge, and

the diffusing vane diffuser, consisting of a number of relatively short expanding passages". The latter two can be seen in Figure 20. The current engine design employs the volute diffuser which is shown in Figure 20. This diffuser gives the pressure rise in the expanding cross-sectional area before it is introduced into the combustor. The diffusers primary purpose is to converts the flows kinetic energy into pressure energy. This diffuser was used because it is coupled with the centrifugal compressor from the automotive type car turbocharger. The volute diffuser section also does not incorporate any vanes; therefore, it is commonly referred to as the vaneless diffuser type.

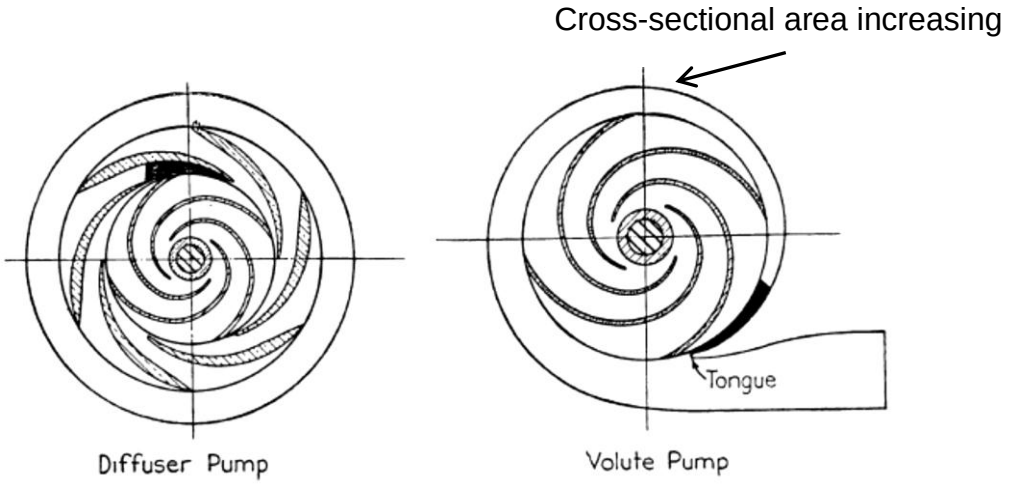

Figure 20. Sections through diffuser and volute

Figure 21. Photo of current engines volute diffuser section

Combustion Chamber

The system component on the TECT that requires the most fabrication work and design time is the engines combustion chamber or combustor, as it is often referred to. Therefore, a detailed mechanical design analysis must be undertaken to ensure that the combustor will operate safely across the intended use and environment. The combustor is under the highest pressures and temperatures during operation, thus is one of the most critical components on the engine. There are many types of designs and configurations that can be used for gas turbine engine combustors. The type of combustor chosen is commonly referred to as the 'canned' style combustor. The canned combustor has many advantages for the TECT demonstrator. Some of the advantages listed in order of their relative importance to the design choice of selecting a canned combustor are shown in Table 6.

Table 6. Advantages of canned combustor

Advantages of Canned Combustor:

1. **Circular cross-section allows for easily interchangeable flame-tubes for combustion experiments**
2. Easier to fabricate because of common pipe diameters available in SS off-the-shelf
3. Well understood because of many years of use in aerospace and power generation
4. Adaptable to current compressor and turbine configuration without heavy modification of the center housing (longer spool shaft required)
5. More compact arrangement within the engine test stand
6. Because the engine is ground based, there is not a large change in inlet conditions and therefore, the stoichiometric ratio for stable combustion does not need as much margin that an annular combustor can provide

The combustor is primarily a pressure vessel with temperatures on the lining reaching ≈ 400 °F during steady state operation and temperatures within the flame-tube region exceeding 3,000 °F. Two canned combustor designs are analyzed to determine the effect on the Factors of Safety (FoS). They are referred to as a 5 bolt and 10 bolt design. Both designs are nearly identical except for the combustor end caps joining with either a 5 bolt or 10 bolt arrangement. The CAD model of the 10 bolt design combustor is shown in Figure 22.

The fabrication techniques and materials used for the combustor were based on the following analysis. The combustor was analyzed for the proper design considerations in the intended environment. This includes stresses due to the pressure and temperature on the casing, welds, and bolts, for both static and fatigue failure criterion.

Figure 22. CAD isometric view of combustor

The maximum operating pressure in the combustor can be obtained through the compressor map for our system presented in the Centrifugal Compressor Analysis section. For a maximum speed of 105,800 rpm the max pressure in the combustor can be backed out through the relationship:

$$P_2 = P_1 * P_{ratio}$$

It is assumed that P_1 is the standard atmospheric pressure of 14.69 psia at Sea-Level which yields a maximum operating pressure of ~ 65 psia. This will be the pressure used for design analysis as a worst case scenario. Naturally there is a pressure drop from the compressor discharge piping as well as a required pressure drop in the combustor to allow for a low pressure region to sustain combustion. The combustor is analyzed for three main areas of failure. Stresses caused by the pressure in the lining are approximated using thin wall pressure vessel theory;

stresses developed in the weldment are calculated with their respective factors of safety; stresses in the bolts are analyzed for the axial loading on the end caps due to the internal pressure. All design analyses are considered for both static and fatigue failure with a mean repeated stress using *Budynas and Nisbett, (2008)*.

The first analysis considered was looking at the component as a pressure vessel. Since the thickness of the pressure vessel is less than one twentieth of the diameter, approximations for thin-walled pressure vessels were considered appropriate. The values for hoop stress and longitudinal stress were calculated using:

Hoop Stress $$(\sigma_t)_{av} = \frac{pd_i}{2t}$$

Longitudinal stress $$(\sigma_t)_{av} = \frac{pd_i}{4t}$$

The maximum of these two values can be used to determine a Tresca factor of safety using:

Tresca Factor of Safety $$n_T = \frac{S_y}{\sigma_1}$$

Likewise, both stresses can be taken as the principle stresses because no shear is present and used to find an equivalent Von Mises stress using:

Von Mises Stress $$\sigma' = \frac{1}{\sqrt{2}}[(\sigma_1 - \sigma_2)^2 + (\sigma_2 - \sigma_3)^2 + (\sigma_3 - \sigma_1)^2]^{\frac{1}{2}}$$

This stress can then be used to find a factor of safety based on Von Mises criteria using the relationship:

Mises Factor of Safety $$n_M = \frac{S_y}{\sigma'}$$

The second analysis done was on the weld around the top rim of the vessel. The shear stress acting in the weld can be found:

Shear stress in weld $$\tau' = \frac{V}{A_{throat}}$$

Where *V* is the force on the weld based on effective sealing diameter and A_{throat} is the weld throat area. The factor of safety for static loading can then be found from using:

Static Load Factor of Safety $$n = \frac{S_{sy}}{\tau'}$$

However, the weld is more likely to fail under fatigue loading. Therefore, fatigue analysis was done with a repeated pressure varying from 0 to P_{max} psia. The endurance limit for infinite life can be found using the Marin equation:

Marin Equation $$S_{se} = k_a k_b k_c k_d k_e k_f S'_e$$

Since the minimum pressure is 0 psia, the amplitude and median applied stress are the same and can be calculated as:

Median/Amplitude of Stress $$\tau_m, \tau_a = \frac{\tau_{max}}{2}$$

These values can then be used to find the factor of safety using a Goodman's criteria using:

Goodman Factor of Safety $$n_f = \frac{1}{\frac{\tau_a}{S_{se}} + \frac{\tau_m}{S_{su}}}$$

where S_{su} is the torsional fatigue strength. The third property analyzed was failure in the bolts. The first step in the bolt analysis is to calculate the total load experienced by each bolt by:

$$P = \frac{Pressure\ A_{seal}}{n_b}$$

Where A_{seal} is the area from the effective diameter of the end plate. The next few steps are calculations of parameters for all of the equations used. To calculate the bolt stiffness, K_b, values were obtained from the schematic of the fasteners used shown in Figure 23. The fasteners used are 18-8 stainless steel alloy with a standard metric M8-1.25 size. The properties of the material were selected from the *Designer Handbook*.

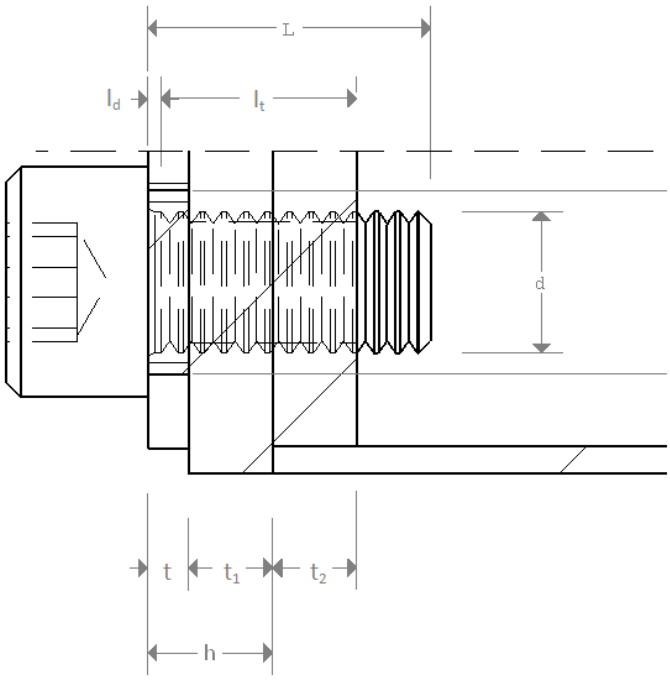

Figure 23. Schematic of bolt in member for combustor analysis

Because t_2 is less than the diameter of the bolt, the effective grip can be defined by:

Effective Grip

$$l' = h + {}^{t_2}/_{2}$$

The second step in analyzing the bolts under fatigue is calculating the joint constant C. This is the fractional amount of the load that is carried by the bolt. First however, k_b and k_m must be calculated using the relationships:

Bolt Stiffness

$$k_b = \frac{A_d A_t E}{A_d l_t + A_t l_d}$$

Member Stiffness

$$k_m = \frac{0.5774\pi E d}{2\ln\left(5\,\frac{0.5774l + 0.5d}{0.5774l + 2.5d}\right)}$$

To simplify the problem an approximation for k_m is taken assuming the diameter of the bolt head was 1.5 times larger than the diameter of the bolt. Once k_b and k_m have been calculated, the joint constant can be calculated from:

Joint Constant

$$C = \frac{k_b}{k_b + k_m}$$

Another assumption that was made for this problem is that the bolts would be fastened in a non-permanent manor, as per the intended design. This would cause the pre-load F_i to be:

Nonpermanent Pre-load

$$F_i = 0.75\, A_t\, S_p$$

With all the factors calculated the load factor for failure in the bolt and separation in the joint can be calculated for static failure.

Load Factor

$$n = \frac{S_p A_t - F_i}{CP}$$

Joint Separation Factor of Safety

$$n_0 = \frac{F_i}{P(1-C)}$$

After calculating all of the values for the bolt fatigue and separation of the members, the factors of safety for each can be calculated using the equations below. Initially, the factor of safety was much higher for the bolts than the factor of safety for the welds and for the thin-walled pressure vessel. For this application, it is important that the joints do not become separated because the purpose of the plate is to contain the pressure from the combustor. If the members become separated the load on the bolts is increased, and the effective sealing performance will be lower driving down the mass flow rate through the engine.

The Goodman equations, Budynas and Nisbett, (2008) were chosen because the factor of safety will be more conservative than the factor of safety of the Gerber equations. Therefore, the factors of safety can be calculated using:

Fatigue Factor of safety

$$n_f = \frac{2S_e(S_{ut}A_t - F_i)}{CP(S_{ut} + S_e)}$$

Joint Separation Factor of Safety

$$n_{f0} = \frac{2S_e S_{ut} A_t}{P(S_{ut} + S_e)}$$

After the 10 bolt design was analyzed, in accordance to the equations listed above the results are shown in Table 7 below. A redesign was proposed after the analysis. It was decided that the FoS for the pressure vessel and welds were conservative but cannot be altered easily because there is a restriction in the weld throat area A_{throat}. It was found that the thickness of the pressure vessel liner limits the weld throat thickness to its current value of 1/16 in. without using advanced fabrication techniques that would most likely give up combustor modularity. The welds and liner materials were decided to be sufficient in the current configuration

and a more advanced joining technique is not required for the current project goals. The bolt analysis proved to be highly overdesigned with FoS > 50. A new redesign was proposed with the number of bolts reduced by half from 10 to 5. The new design is shown in Figure 24. The redesign was analyzed using the same method above but with the number of bolts reduced to five. To reduce computational effort, Matlab code was used to program all of the equations and run for both the original and redesigned configurations. The Matlab code and the respective outputs for the FoS can be seen in Appendix B. For the redesign, the only change in the Matlab file is the number of bolts is reduced to 5.

Table 7. Results of combustor analysis showing all FoS

Factors of Safety							
	Pressure Vessel		Weldments		Bolts		
	Tresca	Mises	Static	Fatigue	Load Factor	Joint Separation	Fatigue Preload/ NoPreload
10 bolt	9.8	8.5	7.2	5.2	53.7	60.9	53.2/28.4
5 bolt	9.8	8.5	7.2	5.2	26.9	30.45	26.57/14.2

Economic consequences of the redesign involve lower machining and material costs. As the original 10 bolt design analysis proved to be very safe and the users are confident that the combustor will not fail. The 10 bolt design has another advantage for working as a better effective seal against the high pressure and temperature gases when compared to the 5 bolt design. This is mainly because, due to the intense heat, there is not sealing material on the end of the combustor between the end caps. The seal is made by the tight machine tolerances between the end caps and the combustor. Another advantage of the 10 bolt design

is the ability to clock or rotate the end cap in smaller increments depending on the arrangement of the final engine layout.

Two designs were analyzed for primary points of failure. A recommendation was made to reduce the number of bolts on the combustor head from 10 to 5. The redesign seems to represent a more sound engineering approach to the combustor. The redesign attempt was successful by allowing where changes could be made to the 10 bolt design to obtain more reasonable FoS. Insight was found in the weld throat constraint, where the throat thickness has a limitation from the lining wall thickness. The combustor is singular and exhibited very conservative factors of safety. The decision was made to use a 10 bolt design because of the other advantages associated with the sealing and end cap rotation.

Figure 24. Proposed combustor redesign with number of bolts reduced from 10 to 5

The combustion chamber is built using type 304 stainless steel (304SS). The selection of this material is mainly due to its high melting temperature and very corrosive resistant properties needed for the harsh environment caused by hot combustible gases. The 304SS also is economical, readily available in common pipe diameters, easily machinable, and has good welding properties. The combustor is welded together using the GTAW/TIG welding process as this technique provides the welder with the most control, as well as very precise heat affective areas. This keeps distortion down to a minimum. The flame-tube that sits on the inner portion of the combustor sits on two concentric rings, one on each side of the combustor. This allows the flame-tube to ‘float’ inside. A 1/64 in. gap was allowed for thermal expansion inside of the combustor. The fuel is injected through the main combustor primary fuel nozzle at the end cap and ignited using a custom fabricated 250 kV ignition system. The flame-tube introduces air radially through

three zones of combustion. The respective flow amounts for each zone were determined using common percentages of air for each zone intended for the canned style combustor. The hole diameters for the three zones of combustion on the flame-tube are area weighted to the mass flow rate through the engine determined by the compressor map. The hole diameters for the three zones are: $^{1}/_{8}$, $^{1}/_{4}$, and $^{7}/_{16}$ in. for the Primary, Secondary, and Dilution zones respectively. A general rule for canned combustor design is to keep the primary holes in the flame-tube to less than 10% of the flame-tube diameter (Boyce, 2002). For the TECT this equates to ≤ ~$^{11}/_{32}$ in. Within the primary combustion zone, the fuel and air are mixed and ignited; this starts the combustion process and is the most fuel rich region in the combustor. The secondary zone introduces additional air to complete the combustion process. The dilution zone introduces the largest amount of air; this cools the very hot combustion gases prior to entering the turbine. The combustion process is completed before entering the dilution zone. If these zones are not appropriately balanced, the combustion process will be unstable, causing blowouts or turbine inlet temperatures that exceed the turbines material limits. A cross-section of the flame-tube sitting inside the combustion liner is shown in Figure 25 and the exploded view of the combustor after completing design and fabrication is shown in Figure 26 and the engineering drawing shown in Figure 27.

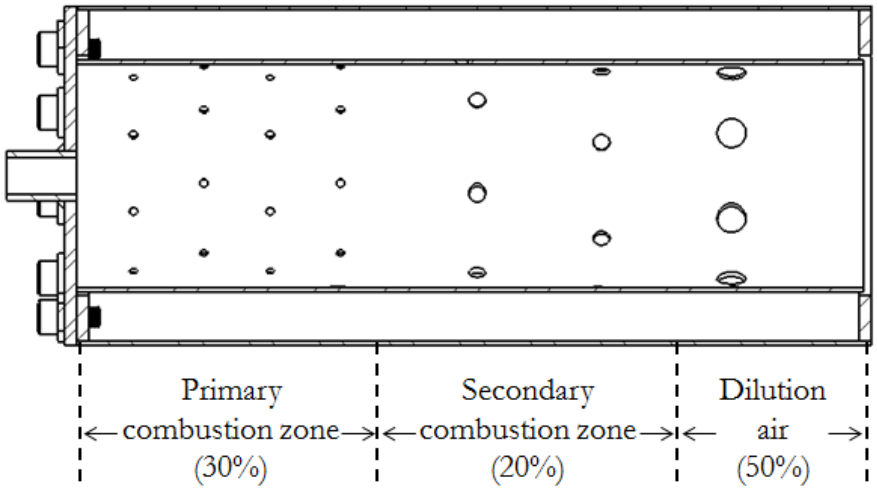

Figure 25. Main Engine Combustion Chamber Cross-Section

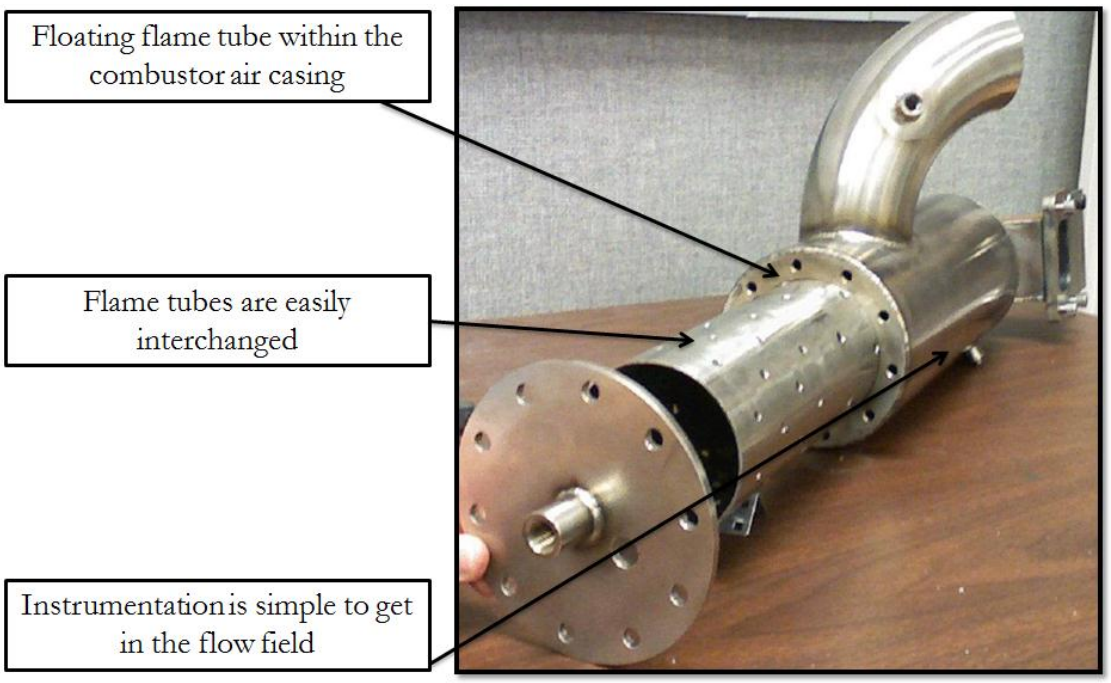

Figure 26. Combustor exploded view removed from engine

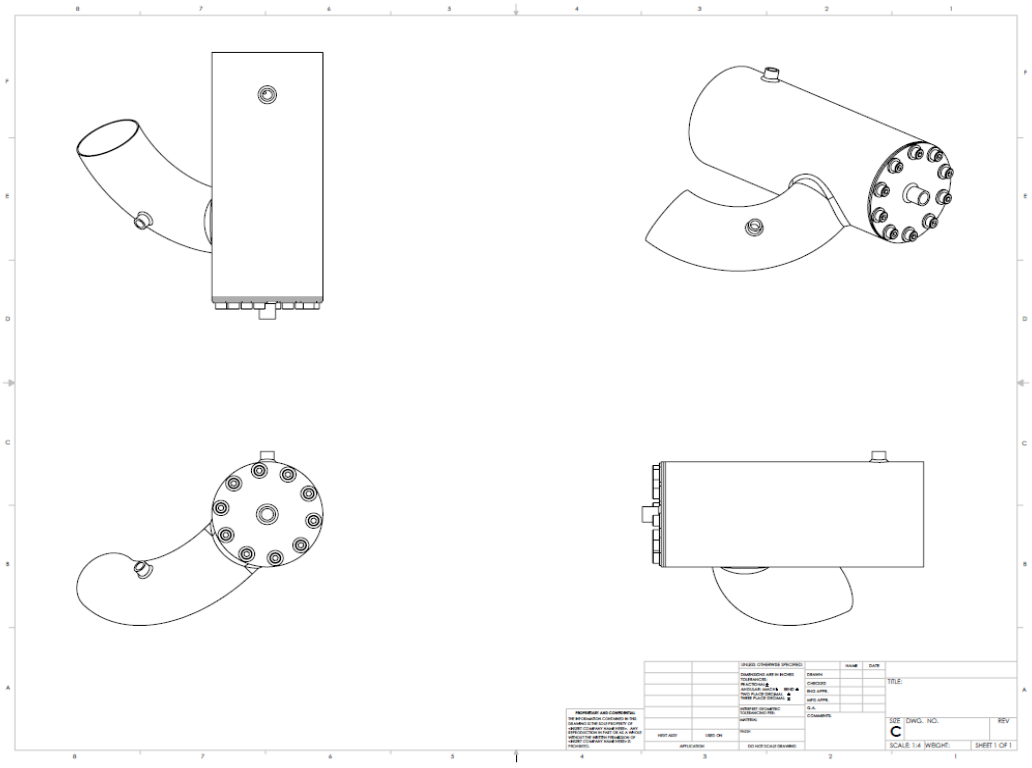

Figure 27. Engineering drawing of canned combustor

Turbine

The turbine on the TECT is a single-stage radial inflow type that is performance matched to the compressor during the original design of the turbocharger for its intended automotive use. It takes the high enthalpy gas after combustion and expands it to create shaft horsepower to drive the centrifugal compressor. The steady state temperatures that the turbine will see are ~10-15% higher than its intended application. It is for this reason that the max rotational speed of the TECT is set at 85,000 RPM vs. its maximum rated speed of ~100,000 RPM. This lower speed will give a longer life, as the stresses in the turbine are decreased back to within its intended range from the lower rotational speed. This type of turbine takes the gas in radially through turbine nozzle that is cast internally within the cast iron turbine housing and then turns the gases 90 degrees to exit in the axial direction. The turbine is a reaction type, where part of the flow expansion occurs in turbine nozzle as well as the rotating blade assembly, this is typical for gas turbine engines. The temperature drop across the turbine for the TECT engine ranges from 60-200 °F across the operational envelope. The turbine viewed from downstream (aft looking forward) with the augmentor hardware removed is shown as the left image in Figure 28. The image on the right is the turbine with the turbine housing removed

The turbine is connected through the main power shaft, which is supported through journal bearing in the turbocharger center housing. The center housing for most automotive turbochargers, including the current, is cast from grey cast iron. The grey cast iron is easy to cast oil and cooling passages for low cost. It also exhibits good temperature resistance for the high temperature application induced by the combustor gases. For this reason, the turbine housing is made from grey cast iron as well. For an aircraft application, this would not be used as the weight of cast iron is extremely high when compared to other suitable aerospace materials. The turbine is coupled through the power shaft to the compressor and performance matched. This again, significantly reduces design and fabrication effort for the engine as the turbine is difficult to manufacture because of the high stresses

induced from the thermal environment. The turbine housing is modified with a 4-bolt v-band flange. This allows for easy installation and removal of the augmentor assembly.

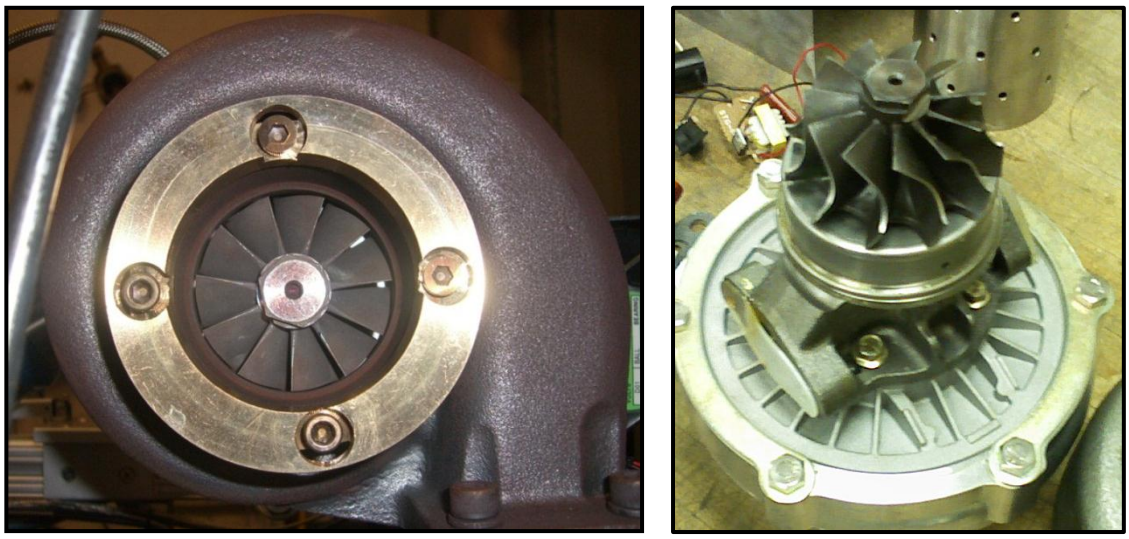

Figure 28. View of turbine, aft looking forward

Augmentor

The engines augmentor (afterburner or reheat, as it is commonly referred), is a way to increase work output for a given compressor pressure ratio. The augmentor takes the gases after being expanded across the radial inflow turbine and injects additional fuel into the flow for combustion. This increases the temperature, and therefore the energy of the flow, before being accelerated through the nozzle to make higher exit velocities and therefore thrust. The flow, although already having been through combustion in the main combustor, has plenty of oxygen remaining to promote combustion a second time in the augmentor after the augmentor fuel manifold injects more fuel through the augmentor fuel nozzles. This is possible as the combustion process in the main combustor is very air rich and typically burns less than 50% of the available oxygen.

There are three necessary features of the augmentor: the fuel injection system, recirculation zone, and augmentor duct. The fuel is injected directly after

the turbine radially (normal to the flow) through three fine atomizing spray nozzles. The recirculation zone acts as a flame holder by forming a low pressure, low velocity region where the flame can be held and combustion can occur without blowing out from the high flow velocities. This low pressure region for the flame holder is accomplished by a step up in diameter from the turbine discharge pipe exit to the augmentor duct creating the recirculation zone. This step is ¾ in. around the pipe radius and has an igniter (250kV) for ignition in this region. A sketch of the cross-section of the augmentor is shown in Figure 29. The augmentor duct and nozzle is made from the same 304 SS as the main engine combustor because of its inherent material properties. The nozzle exit area is nearly the same size as the turbine exit area, therefore there is a minimal increase in velocity while the engine is running under normal non-augmented operating conditions.

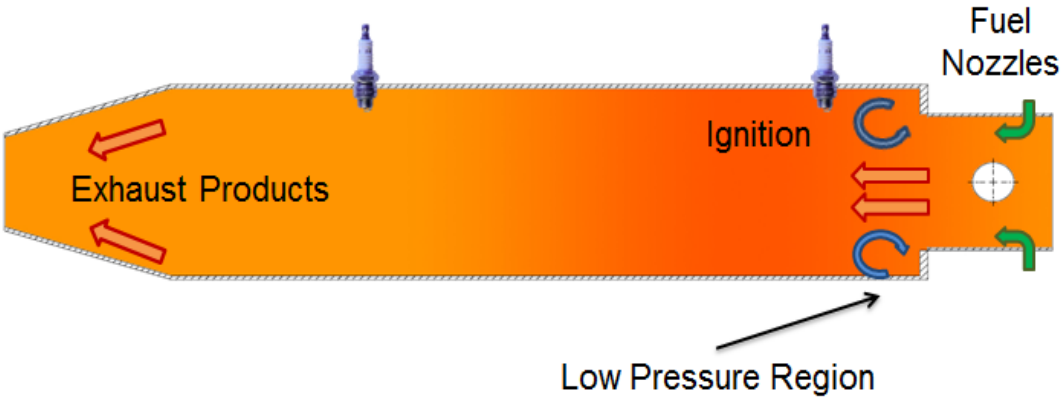

Figure 29. Cross-Section of Augmentor

The nozzle exit area is oversized for ‘dry’ (non-augmented) operation because the nozzle has a fixed exit area. The nozzle is a convergent only nozzle, as the flow field is subsonic and operates under sub-critical expansion. Therefore, the nozzle exit is sized for operation while under augmented power. If the nozzle exit area were sized for dry operation only, than when lighting the augmentor a backpressure would result and a compressor stall is likely to occur. Because the TECT is not specifically designed for thrust output but rather technology demonstration, this is an acceptable design and keeps the overall engine design simpler vs building a variable area nozzle that can change the nozzle exit area

depending on where the engine is operating. When the augmentor is activated, the nozzle will become near choked resulting in a higher thrust output and much higher exhaust exit temperatures. With the engine at max power, the exhaust temperatures are in excess of 3,000 °F.

The augmentor is designed into segments with easily removable nozzle and spool pieces to change the overall characteristic length of the augmentor section. The augmentor was designed to have an easily changeable duct length by adding in segments. This modularity was added because the combustion stability is affected by this length as well as fuel/air ratio. Therefore the TECT can be used for augmentor combustion experiments for methods such as screech/combustion instability on-set prediction using different augmentor geometries. The nozzles can also easily be interchanged for different styles or exit areas. This could be a benefit for an experiment to find which nozzle geometries produce less jet noise as one example. The augmentor and nozzle is attached using a v-band clamp quick disconnect assembly. The completed augmentor assembly is shown in Figure 30.

Figure 30. Various views of the augmentor assembly

Table 8. Advantages of modular augmentor

Advantages of Modular Augmentor:
• Nozzles are interchangeable
• Characteristic length can easily be changed by adding or removing segments
• Test sections can be added into the flow field easily for high enthalpy environment testing
• AB nozzles are easily replaced if higher/lower flow rates are required
• Augmentor can be easily removed if not required and the engine run in a ‘dry’ configuration

To deliver the fuel to the augmentor, a secondary augmentor fuel system was required to be designed and fabricated. This system is separate from the main fuel system for the main engine combustor. The schematic of the fuel system is shown in Figure 31. The bypass style fuel system is designed to run the augmentor fuel pump at a constant speed by allowing the bypass/return line to return fuel back to augmentor fuel tank that is not sent into the augmentor fuel manifold. The augmentor fuel pump is a 12VDC diaphragm pump with Buna-N seals rated for liquid hydrocarbon fuels, such as kerosene. It is important to note, none of the engine support systems, such as the pumps are not driven from the engine, but rather a separate power source. The augmentor fuel pump is controlled via the engine ECU (Engine Control Unit). The augmentor fuel system has an emergency shut off fuel solenoid before the fuel manifold to stop cock the fuel flow in case of an emergency. This solenoid can be both manually triggered and triggered from the ECU. All the lines downstream of the bypass valve are rigid steel and rated for the heat and pressure around the environment of the hot section of the engine.

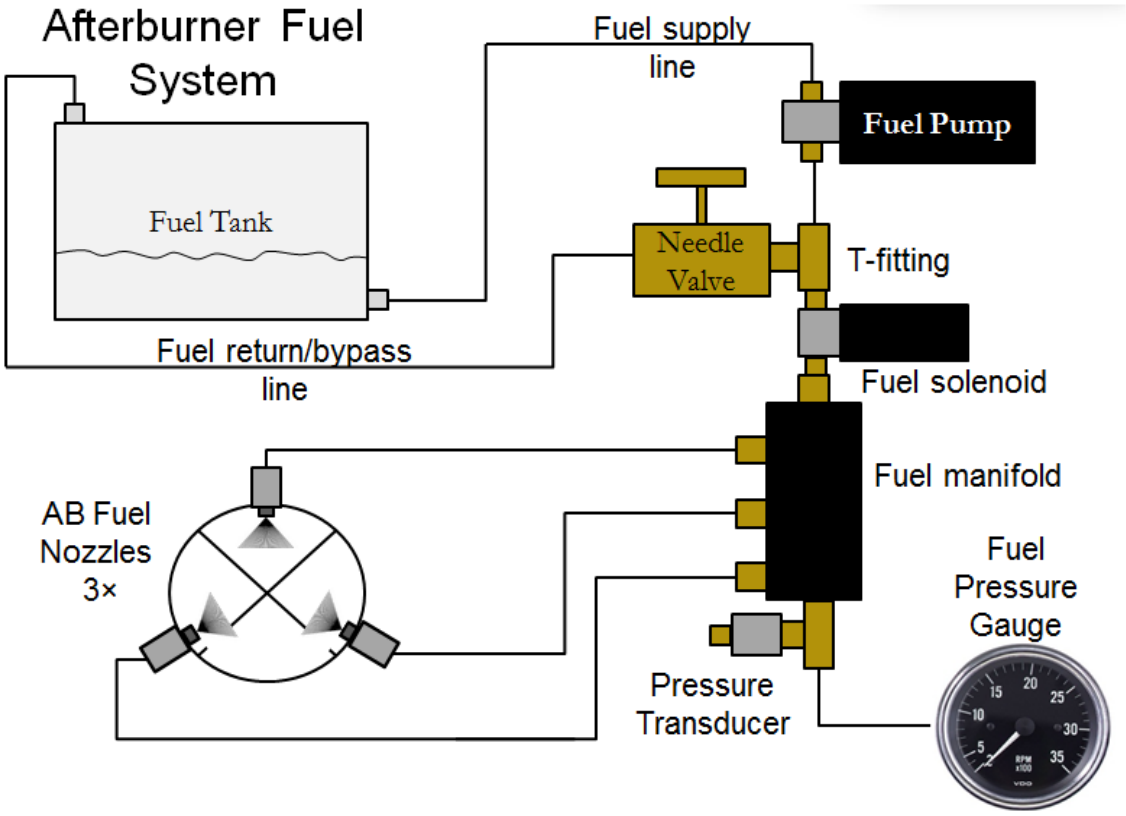

Figure 31. Augmentor fuel system schematic

The augmentor runs on a separate fuel than the main combustor. The augmentor runs on a liquid fuel rather than the gaseous propane because it is easier to ignite the liquid fuel after it has been exposed to the 800 -1,000 °F flow from downstream of the turbine. The augmentor can run on a variety of liquid fuels for this reason, but kerosene or a jet fuel such as JP-8 or Jet-A work well. The augmentor fuel system is activated and allowed to prime before injecting fuel through the augmentor fuel nozzles. The system is primed by being directed through a bypass valve which is adjusted to the proper pressure prior to the engine run. This fuel tuning allows the augmentor to run fuel rich or lean depending on the test objectives. If there is a requirement to test combustion instabilities in the augmentor from a technology program, it is crucial to have this adjustment. This manifold pressure is necessary because it determines the fuel flow rate through the

augmentor nozzles. Once ready to engage the afterburner, a safety switch is released allowing the ECU to have control of the augmentor system. Because of safety concerns the augmentor can only be controlled remotely from the control room. The fuel primes the manifold and is injected through nozzles. The fuel injection is comprised of three fine atomizing spray nozzles. The nozzles create a 30-45 micron droplet at an 80 degree spray angle. The fuel is sprayed as a full cone pattern radial to flow direction. A sketch of the augmentor spray nozzles is shown in Figure 33. An upstream view of the three spray nozzles and the low pressure recirculation zone is shown in Figure 32.

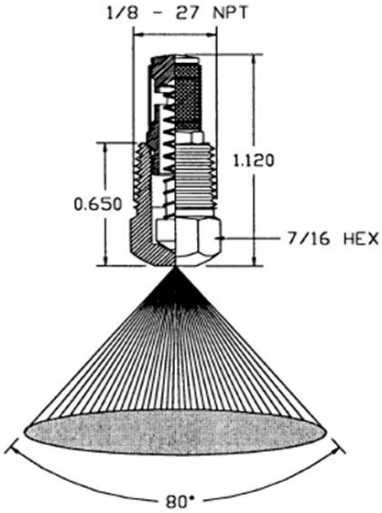

Figure 33. Augmentor spray nozzle sketch

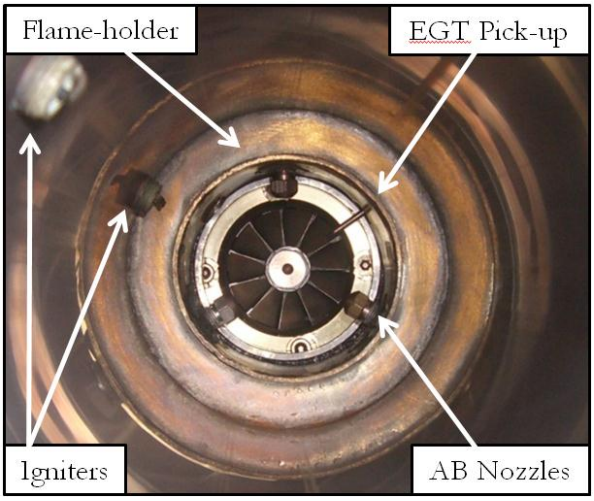

Figure 32. Upstream view of augmentor

The augmentor fuel pressure can be adjusted from 20-100 psig depending on the bypass valve opening percentage. At 100% open on the bypass valve the pressure in the augmentor fuel manifold is at 20 psig, while 10% open results in ~100 psig. The fuel flow rate into the augmentor is measured by using the nozzle flow curves. The data from the flow calibration is shown in Figure 34. The max flow rate in the augmentor at 100 psig is ~100 lbm/hr or 15 gallons per hour. This flow curve is for all three augmentor nozzles combined to get the total fuel flow into the augmentor. The detailed flow data and technical data sheets for the augmentor nozzles, is provided in Appendix E.

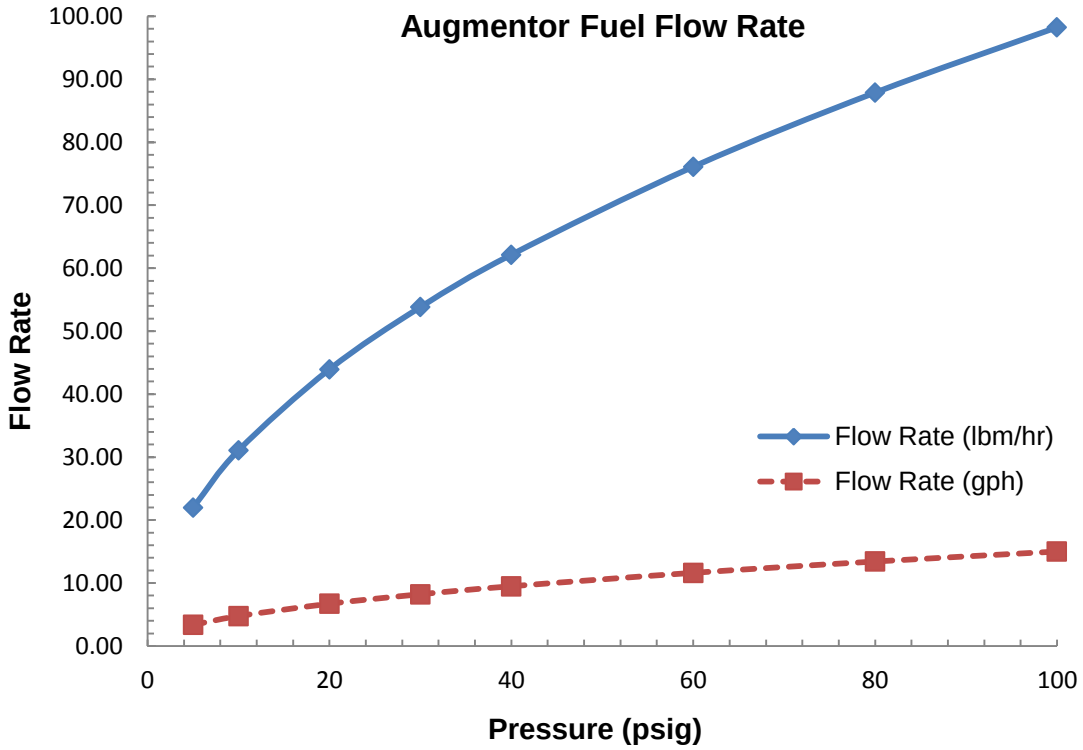

Figure 34. Augmentor fuel flow rate vs. supply pressure

Engine Control

Engine Control Unit

The engine has many electronic devices such as data acquisition cards, signal conditioning equipment, multimeters, switches, power devices, and solid state relays. In order to consolidate the electronic equipment in one area and protect this sensitive equipment from exposure from the heat, vibration, and fuels produced from the TECT environment, a project enclosure was fabricated using a temperature and chemical resistant thermoplastic to serve as the main engine control center. The engine control unit (ECU) displays the engine temperatures in real-time, as well as serves as location to turn on support equipment. There are 4 switches on the front of the main ECU panel that allow for both manual and computer controlled operation depending on their orientation. These switches turn

on the main power supply, oil cooler fan, oil pump, and the afterburner fuel pump. There are separate remote devices for ignition and afterburner solenoid activation that allow for both manual and computer control. If the switches are oriented in the UP position, the engine is in the manual control configuration and this will allow the operator to override the computer control at the ECU. If the switches are in the in the neutral switch position on center, all devices are OFF. When the switches are oriented in the DOWN position, the engine is under computer control, see Figure 35.

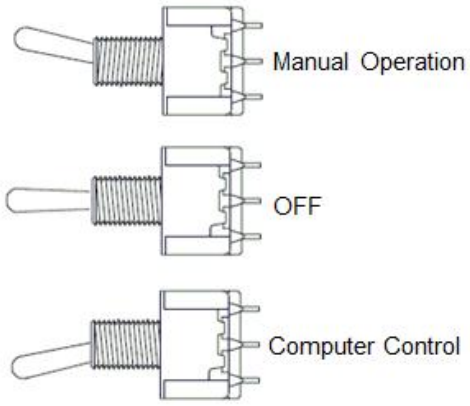

Figure 35. ECU control states

While the TECT is under the computer control mode, the engine can be controlled remotely from the control room. When the engines hardware is switched to the computer control mode the secondary control enclosure is activated where the computer will have complete control of the engine through a series of solid state relays (SSR's), see Figure 36. The SSR's are digitally switched using the 5VDC digital input/output (DIO) lines from the NI 6008-USB controller using pull-up resistors. The pull-up resistors are required to set the required high logic level to trigger the SSR's. An ANSYS finite element analysis was performed on the ECU enclosure to model the heat transfer from the combustion chamber, as the enclosure is within close proximity to the combustion chamber and may overheat the sensitive electronic equipment. The results from this study are presented in Appendix D.

Inside of the main ECU there is a patch panel for the instrumentation and control interconnects. This allows for the DAQ cards or the instrumentation to be changed out easily and allows for the excitation voltage to the multiple devices to be centralized in one location. Electrical power is available in 5VDC, 12VDC, and 120VAC power sources inside of the main ECU. The patch panel wiring schematic is shown in Figure 37.

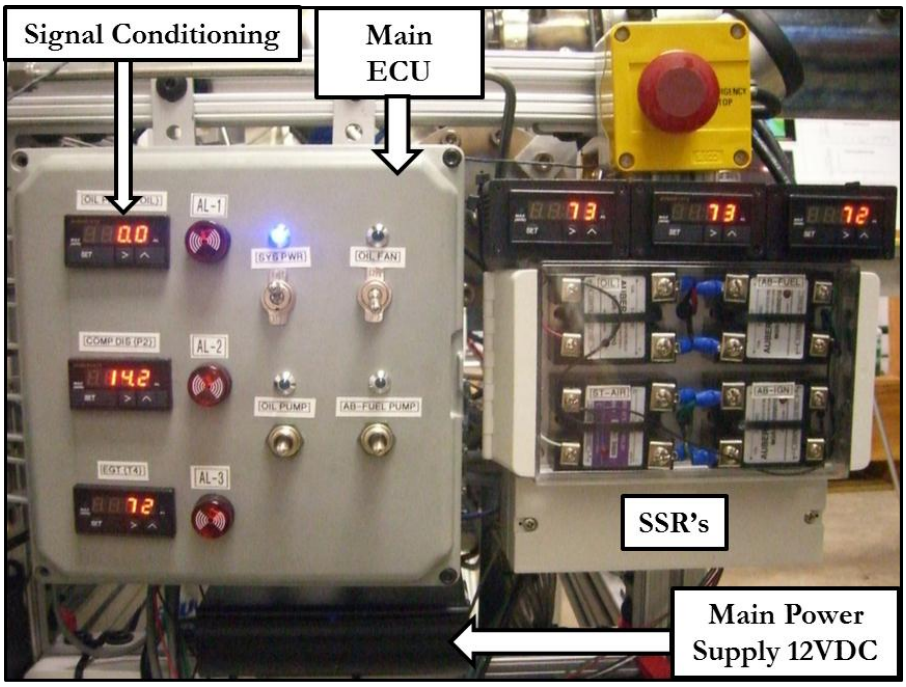

Figure 36. Main ECU and SSR's

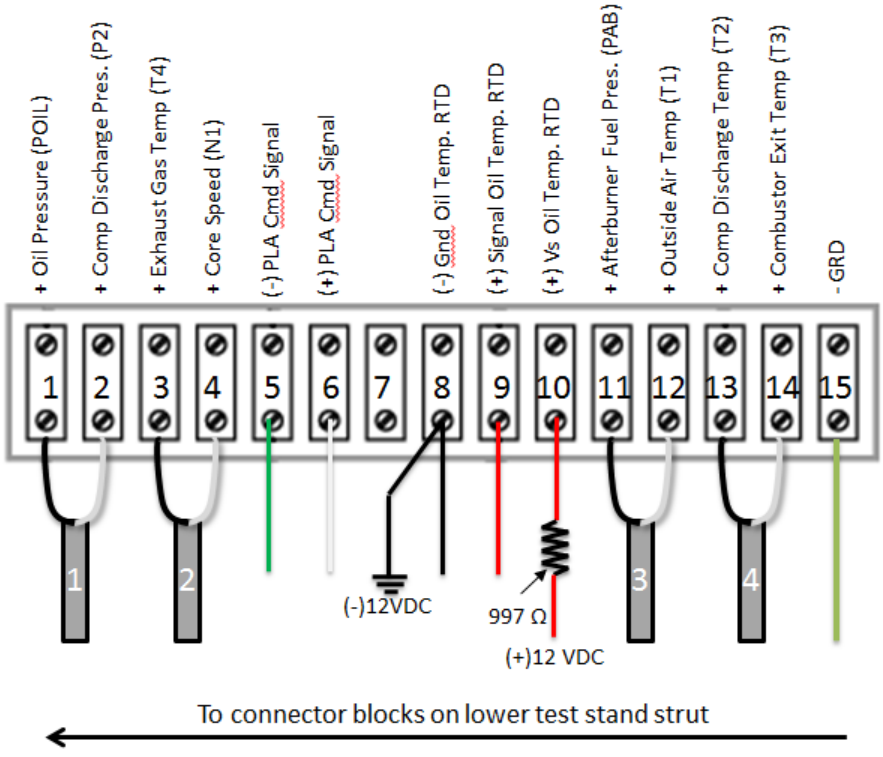

Figure 37. Patch panel wiring diagram inside main ECU

The connections made to the ECU are input through mil-spec type quick disconnects for making the engine as modular as possible, see Figure 38. This also makes swapping out instrumentation easy. The oil cooling fan is shown in the background of the figure. This cooling fan helps to not only remove heat from the oil flow, but also helps to pull cool air by the pumps and other engine support equipment, such as the power supply to aid in their cooling as well. The modular engine design was a main program objective and was incorporated throughout each step of the engine fabrication process.

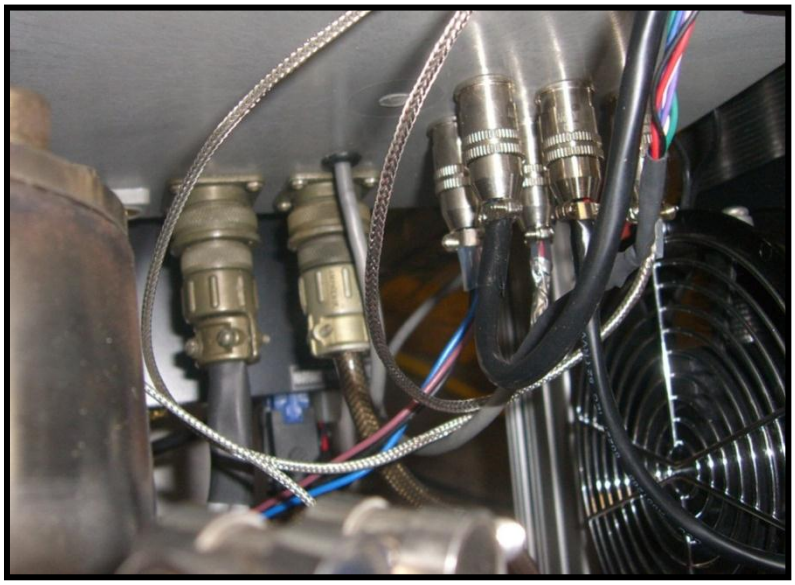

Figure 38. Back-view of ECU showing quick-disconnect type connections

Main Fuel Control Technique

The main fuel control for the combustor allows for the computer control of main engine combustor. The valve is a proportionally controlled brass solenoid valve that can be adjusted between 0 -100% of its rating with very minimal hysteresis and good repeatability required for the engine programed set-points, see the engineering drawing in Figure 39. The tank-fed propane gas is regulated through a pressure regulator down from ~120 psi to 80 psi upstream of the fuel control valve. It is important to keep this upstream pressure constant as the engine

throttle set points will vary with pressure deviation at the valve inlet. The propane tank is located in a separate area than the TECT and has a quick shut-off valve for emergencies that may arise from the control system locking up or not responding. When this valve is closed the engine will abruptly shut off, although damage to the bearings is likely to result if shutting down from a high power setting without a cool down cycle.

The main fuel valve is proportionally controlled through the NI-MyDAQ USB controller using a 0-10VDC analog voltage output controlled through the LabVIEW GUI. The NI-MyDAQ cards sole purpose is to provide control for the fuel control valve. The valve has an added Electronic Control Unit that converts the 0-10VDC analog voltage output from the DAQ to a Pulse Width Modulated (PWM) 300 Hz frequency to drive the valve position. The valve has the option to adjust up to a 3 second ramp rate to the commanded throttle set-points that has been programed and enabled for the TECT. This ramp rate will prevent the valve from moving too fast when snapping the engine from idle to max or vice versa, which could cause the main combustor to blow out from the fuel rich/lean environment, as well as give the potential to cause the engine to abort on high T4 (EGT). This ramp rate is only adjustable on the valve and not within the LabVIEW GUI. The main fuel control valve has a dedicated 1300mA 24DC power supply. A graph of the throttle commanded position vs. the engine speed is shown in Figure 40. Note that the valve is not used to its full capacity on the TECT, therefore the operator must be careful to not overspeed (excessive, *N*) the engine by using too much fuel. The main computer control has the option to put high and low limits on the valves operation to reduce this risk. The full technical data sheets for the proportional control valve and the electronic valve control unit are listed in Appendix E.

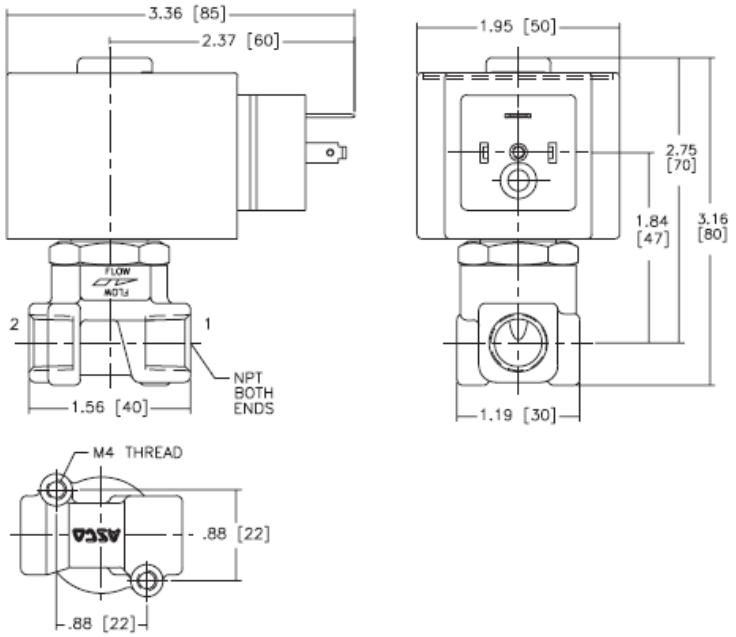

Figure 39. Main fuel control valve engineering drawing

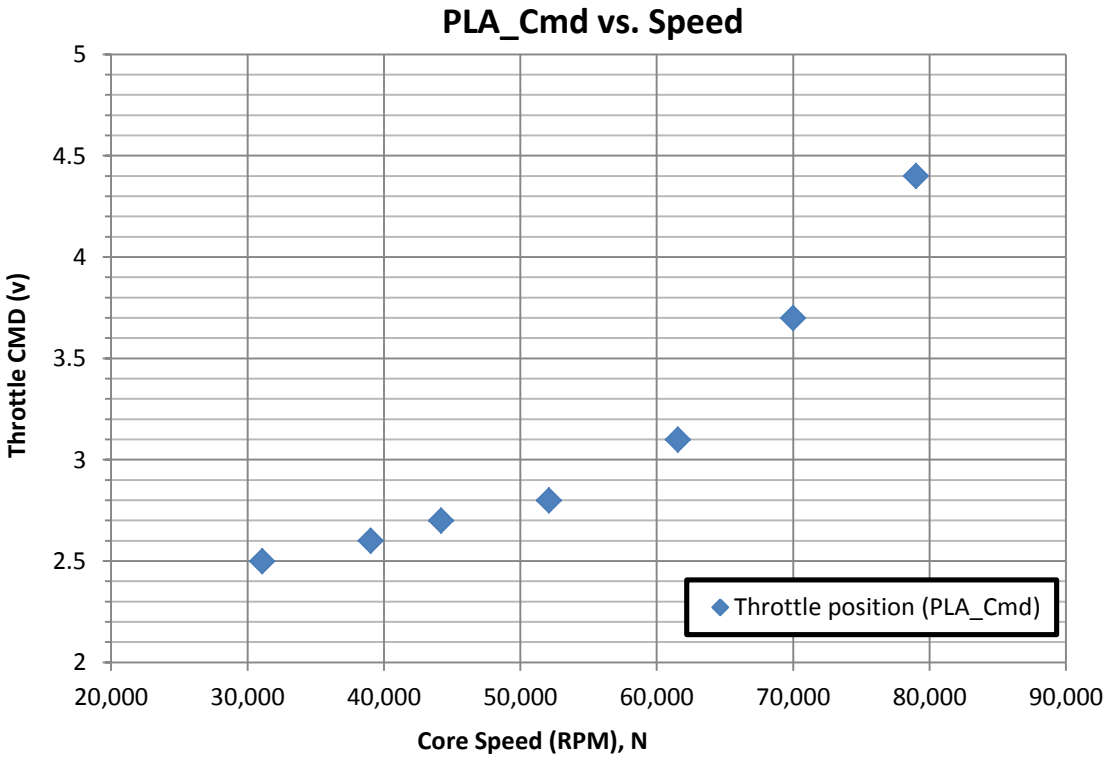

Figure 40. Graph of throttle command vs. core speed

Main Computer Control Graphical User Interface

The TECT has the capability to be controlled during operation by a computer when put into the computer controlled mode on the main ECU. The main control GUI is programmed using the National Instruments LabVIEW programming environment because of its adaptability. A trade study was undertaken to show the different options of three programming environments for control. The results of this study which involved software packages from National Instruments (LabVIEW), Mathworks (MatLab), and DataQ (WinDAQ) are shown in Table 9. The LabVIEW environment was chosen for use because of its inherent flexibility and adaptability for use as both a control system, as well as a data acquisition system. The LabVIEW graphical based programming is intuitive in nature.

Table 9. Control software trade study results

	Matlab Data Acquisition Toolbox	*NI LabVIEW*	*DataQ WinDaq*
Real time data display	x	x	x
Analog input	x	x	x
Digital output TTL		x	x
Playback capability		x	x
GUI Interface	x*	x	
closed loop control		x	x**
Calculated channels		x	x**
Analog triggers	x	x	x**
Real time meters/gauges		moderate	limited**
Analysis during recording			x
Required programming time	moderate	moderate	very short
Output to Excel	x	x	x
computing resources	moderate	high	low
Post analysis	very strong	moderate	moderate
Overall ease of use	low	moderate	high
Overall cost	moderate	high	low

*requires additional programming

**requires 3rd party software add-ons

The main GUI provides both the engine control as well as the data acquisition interfaces by communicating through the USB data acquisition devices. There are both manual and auto-control modes built into the GUI that will allow manual control of the pumps, valves, igniters, and relays from the control room. This type of remote control was crucial for the TECT build J1-H-02 for personnel safety to keep the engine away from test personnel. The main page of the LabVIEW GUI is shown in Figure 41. The GUI also has separate tabs to control visual and audible alarms as well as throttle set points. The built in alarms have the option to be in an Enabled or Disabled state with both high and low alarm limit set points on all input instrumentation as well as a warning set point before the limit is reached. The alarms when sensing a high or low value respond by changing the background color of the specific piece of instrumentation to yellow for a warning and then to red when the limit is broken. When the high or low alarm limits are broken an audible alarm will automatically sound to get the users attention.

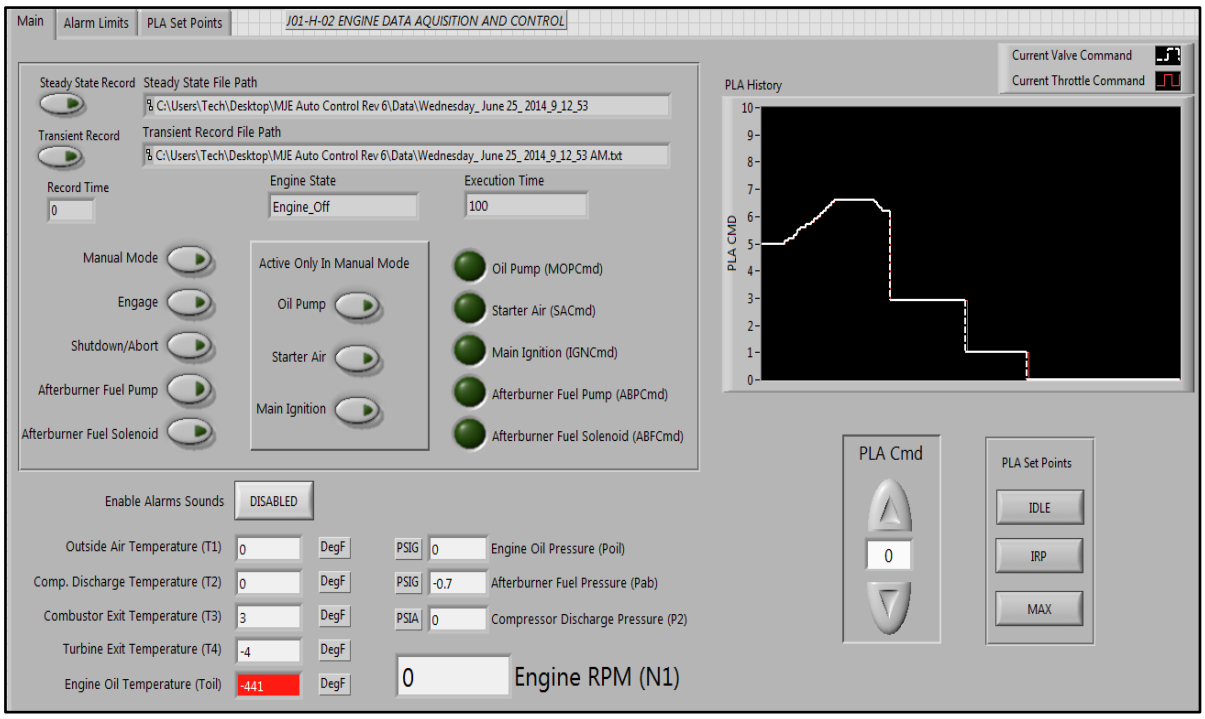

Figure 41. Main engine control front page

The MJE Auto Control is a LabVIEW program developed using a state machine architecture that utilizes data acquisition system information to control the startup, operation, and shutdown of the TECT. Depending on the state of the machine when the shutdown/abort signal is given determines the shutdown method. If the engine is spooled or running, the program will shut down the TECT by maintaining oil pressure and using starter air to continue to turn the engine until turbine exit temperature falls below “EGT Starter Air Cut Out” temperature. The shutdowns turn on the starter air to put the engine through a cool down cycle before coming to rotor rest. This prevents the engine oil from overheating and ‘coking’ in the center housing resulting in restricted oil flow over time and therefore cooling and lubrication of the bearings. Next, the program turns off starter air but maintains oil pressure until shaft rotation falls below “Oil Off Cut Out Speed” is reached. When the GUI is placed in to the ‘MJE Auto Control’ mode the machine states are determined from the feedback from the engine. While in the ‘manual’ mode the only machine state that is active is the initialization state. The different machine states of the engine and the computers actions while in those states are described as follows:

Machine States

Initialization: Initialization is the safe state for the device. It sets all digital outputs to a logic low level and the PLA Cmd to 0 (Hard CLOSED).

Wait for Oil Pressure: Wait for Oil Pressure engages the Oil Pump SSR and waits for the oil pressure to reach 10 psi before continuing.

Engine_Air_On: Engine_Air_On engages the Starter Air SSR and waits for a shaft rotation of 9000 rpm.

Main_Ignition: Main_Ignition engages the Ignition SSR, sets PLA Cmd to “Start Set Point” Value, and waits until Turbine Exit Temperature is greater than 600°F for 8 seconds. User input can be used to control PLA Cmd (1 (Soft Closed) to 10 (Full)

Engine Running: Engine Running disengages the Starter Air SSR and Ignition SSR. User input is required to control throttle position. This loop will automatically shut down the MJE if shaft rotation of 85,000 rpm is exceeded, turbine exit temperature of 1200°F is exceeded, or if oil pressure falls below 8 psi.

Engine_Shut_Down: Engine_Shut_Down engages the Starter Air SSR and waits for the Turbine Exit Temperature to fall below “EGT Starter Air Cut Out” temperature.

Engine_Air_Off: Engine_Air_Off disengages the Starter Air SSR.

Engine_Off: Engine_Off waits for shaft rotation to fall below “Oil Off Cut Out Speed” and then disengages the oil pump and stops the program.

If the GUI is put into the auto-control mode, the engine will operate without user input based on pre-programmed conditions. While in this mode, the engine’s automatic abort limits are activated and will automatically shut down the engine when predetermined operating conditions are met. These abort limits are easily adjusted when the engine is not operating. Without the use of the ‘auto control’ functions, the engine would be extremely difficult to operate with a single operator. This would be particularly difficult if the system under test required additional control, which is likely the case unless the system under test is for sensor development . The TECT engine has an automated start sequence where the engine will start itself according to the decision tree in Figure 42. Note that there are abort limits during this sequence. The air impingement starting system is shown in Figure 43. The air starting system is pneumatically actuated into the front of the compressor during starting and then automatically returns to its original position away from the inlet after the engine start is complete. This system is under the control of the ECU. A complete list of engine operation and procedures for the TECT is given in Appendix A.

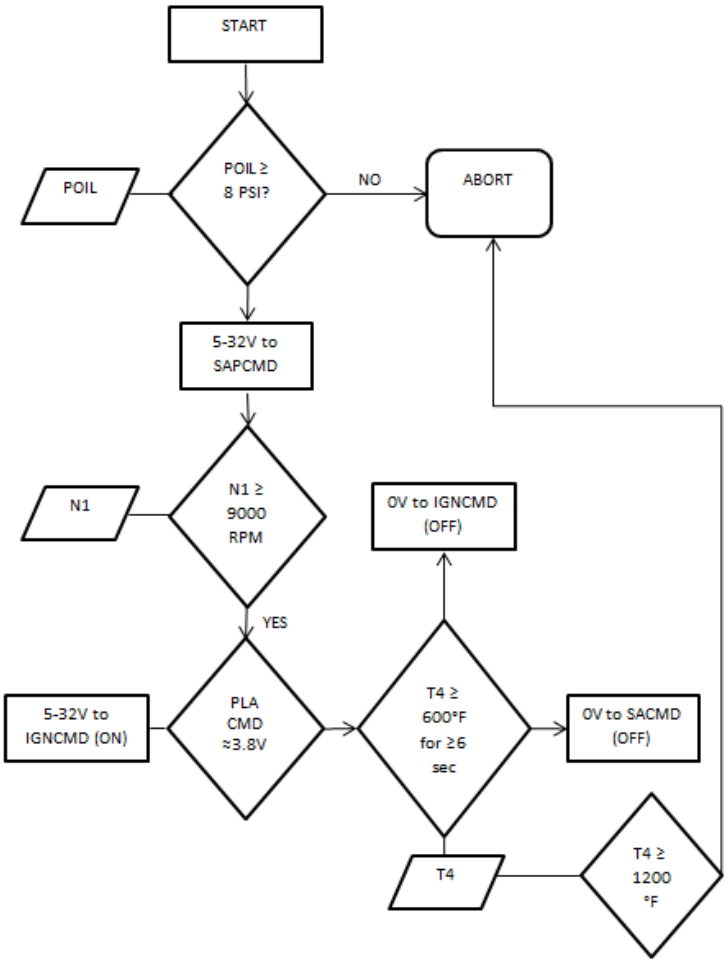

Figure 42. Engine automated start sequence decision tree

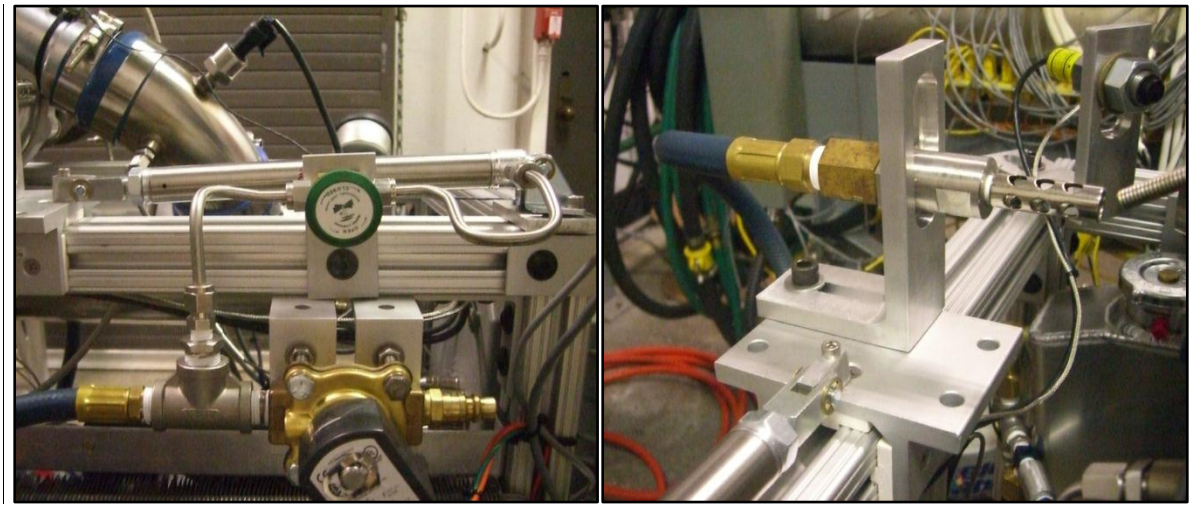

Figure 43. Air starter system

Completed TECT Engine

The completed TECT engine (J01-H-02) is shown in Figure 44. Note that the engine is built on the engine test stand with all of the support equipment, for easy transport. The only facility requirement to run the engine is a shop air source for the compressed air starting system.

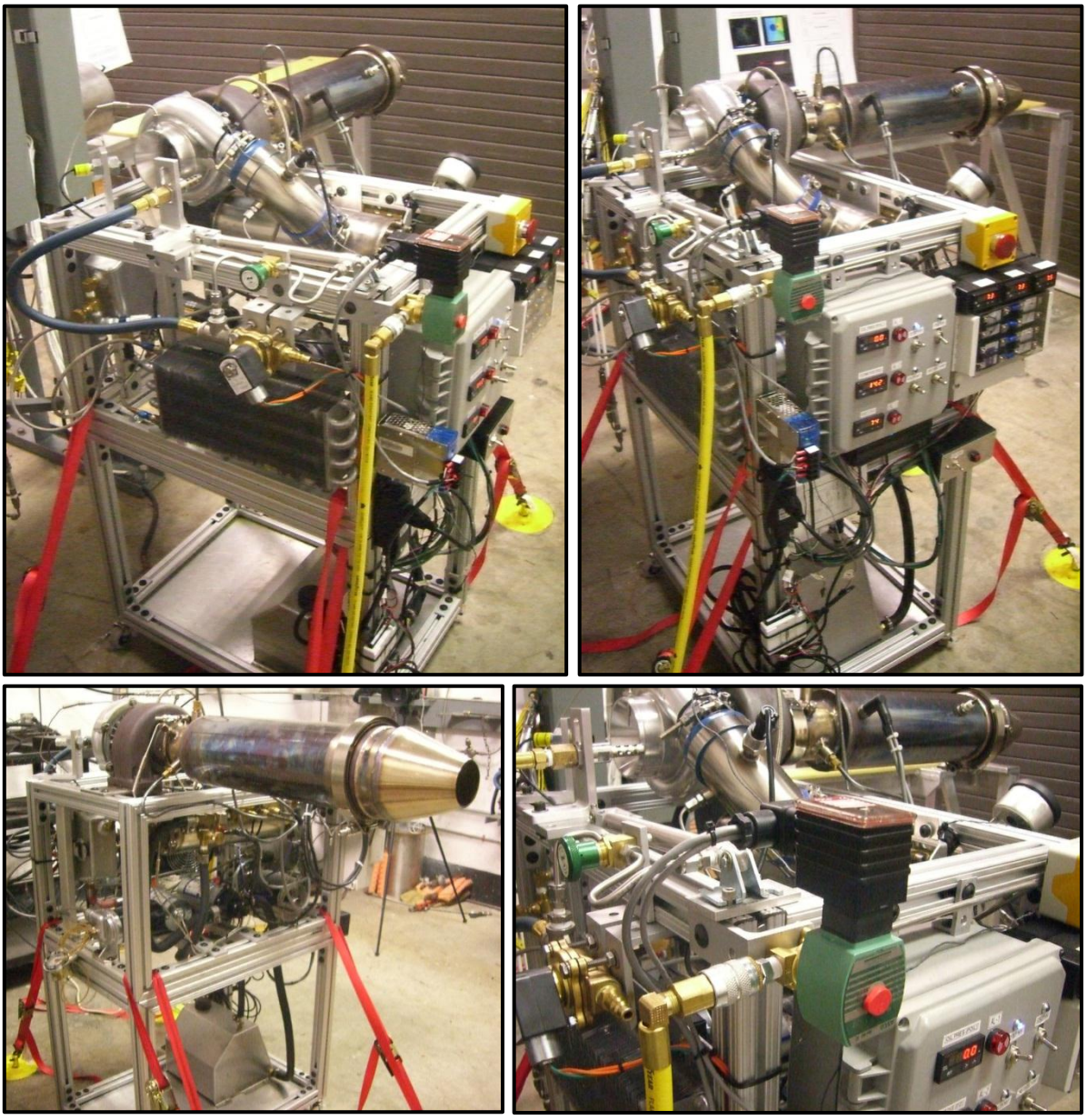

Figure 44. Views of the completed TECT engine

CHAPTER IV
EXPERIMENTAL ANALYSIS

Data Acquisition

The engine's data acquisition or DAQ for short, is handled through two National Instruments USB data acquisition cards (USB-6008 and USB-MyDAQ). These cards are USB powered and do not require any additional power sources to operate. Currently, 17 channels are used for both control and data acquisition functions (6 control/11 instrumentation) with additional channels available for added instrumentation and control. The TECT engine is designed with a basic set of performance and safety parameters that make up the 'core' instrumentation package. The complete instrumentation requirement sheet is shown in Figure 45. It is the design intent to keep this core set of instrumentation on the TECT at all times. When additional instrumentation is required, it can be acquired with a separate data system. This allows for the basic engine performance and health parameters to remain unchanged with different test objectives and allows for a historical set of data to track whether or not the engine is behaving differently with test objectives. It provides a baseline data set to trend change deviations.

The data rate is default programmed at 10 Hz acquisition for both steady state and transient data recording. The main control GUI has the capability to acquire steady state data points, which is a set of continuously acquired data from the engine for 10 seconds and then that data is averaged to give a single recorded value. This is useful for tracking engine performance while the engine is under steady operation and has reached a 'steady state' condition where engine performance is not changing with time. Another capability is to acquire data continually while recorded at the 10Hz sample rate. This is called the transient recording button. It is possible to run them both at the same time. There is a secondary high speed dynamic data acquisition system called CADMAAS. The CADMAAS data system is capable of acquiring dynamic data at up to 156 kHz per channel (24 channels available). This data system is separate from the main TECT

data system and acquires the high speed data required from the engine accelerometers. There are currently two accelerometers mounted on the engine to pick up the compressor engine order speeds, as well as on the combustor to pick up combustion harmonics/instabilities. These accelerometers provide insight into the dynamic phenomena of the TECT engine. The CADMAAS data system can be used for high response instrumentation such as microphones, accelerometers, close coupled pressure transducers, and strain gages.

DAQ	*Channel*	*Name*	*Description*	*Sensor*	*Type*	*Output*	*Units*	*Excitation*	*Sensor Range*	*Static Accuracy*
USB-6008	AI0	POIL	Main oil pressure	PT	AI	0-5v	psig	5.0±0.5 VDC	0.0 to 100 psi	1.5%FS
USB-6008	AI4	P2	Compressor discharge pressure	PT	AI	0-5v	psia	5.0±0.5 VDC	0.0 to 75 psi	1.5%FS
USB-6008	AI2	PAB	Afterburner fuel pressure	PT	AI	0-5v	psig	5.0±0.5 VDC	0.0 to 100 psi	1.5%FS
USB-6008	AI6	T1	Outside air temperature	RTD	AI	0-5v	°F			±1°F
USB-6008	AI3	T2	Compressor discharge temperature	K	AI	0-5v	°F		0-2000F	0.2%FS
USB-6008	AI7	T3	Combustor exit temperature	K	AI	0-5v	°F		0-2000F	0.2%FS
USB-6008	AI1	T4	Turbine exit temperature (EGT)	K	AI	0-5v	°F		0-2000F	0.2%FS
USB-6008	AI5	TOIL	Main oil temperature	RTD	AI	100ohm	°F		-199-500F	±1°F
USB-6008	PFI0	N1	Core speed	Optical Laser	AI	TTL pulse proportional to supply voltage	RPM	3-24VDC	1-250,000 RPM	-
MyDAQ	AO0	PLACMD	Power Lever Angle	Proportional Valve	AO	-	-	0-10VDC	-	-
USB-6008	0.0	MOPCMD	Commands oil pump ON/OFF	SSR	DO	-	-	3-32VDC	20A max	-
USB-6008	0.1	ABPCMD	Commands AB fuel pump ON/OFF	SSR	DO	-	-	3-32VDC	20A max	-
USB-6008	0.3	IGNCMD	Commands main ignition ON/OFF	SSR	DO	-	-	3-32VDC	20A max	-
USB-6008	0.2	SACMD	Commands starter air ON/OFF	SSR	DO	-	-	3-32VDC	20A max	-
USB-6008	0.4	ABFCMD	Commands AB fuel solenoid ON/OFF	SSR	DO	-	-	3-32VDC	10A max	-
CADMAAS	1	ZC1	Compressor Vibration Pick-up	Accelerometer	AI	volts	mils	9VDC	-	-
CADMAAS	2	ZC2	Combustor Vibration Pick-up	Accelerometer	AI	volts	mils	9VDC	-	-

Figure 45. Instrumentation requirements sheet

The TECT engines station nomenclature for the instrumentation locations is shown in Figure 46. This station numbering system is somewhat different than the international standard for gas turbines because the TECT is ground based without an inlet diffuser and therefore, the engine inlet face will be considered station 1 instead of the station 2 designation that is common amongst gas turbines.

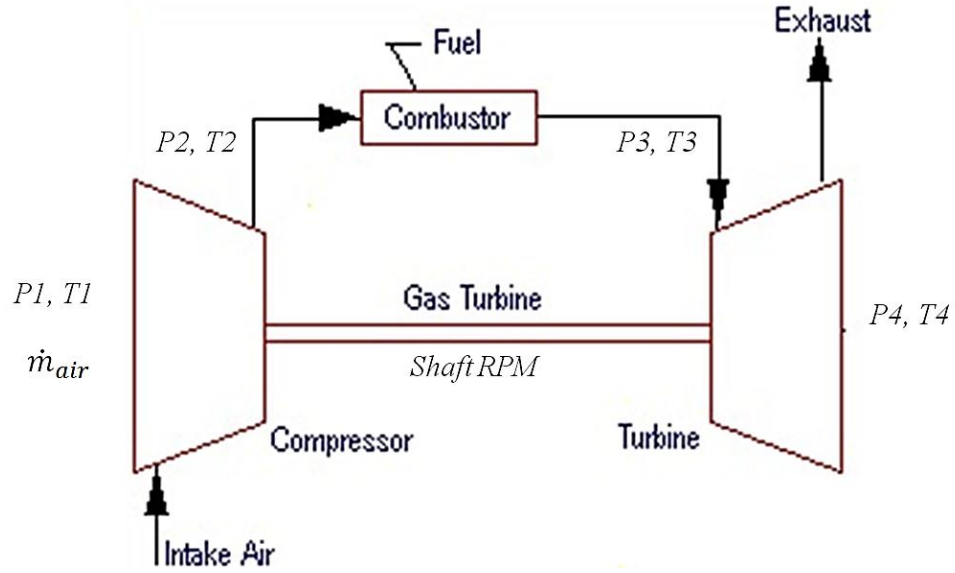

Figure 46. Instrumentation station nomenclature

Core Speed Measurement Technique

Several methods were explored for obtaining shaft speed. Initially, a magnet or encoder device was thought to be adequate but after some analysis the forces from the rotating unbalance caused by these devices would be excessive at such high rotational speeds and would ultimately most likely cause an engine failure from such high vibratory stresses. The best candidate was decided to be an optical laser sensor (*class 2*). Using the laser sensor allows the shaft RPM (*N*), to be determined extremely accurately and completely non-intrusive. The sensor can pick up contrast differences therefore, ¼ of the compressor nut was painted white while the remaining ¾ was painted black. The laser sends a single Transistor-Transistor-Logic (TTL) 5 VDC pulse when the white region becomes visible. The sensor is connected through a timer function on the National Instruments (USB-6008) card to

calculate the RPM's. The sensor is mounted at a 45 degree angle (max capability 60 degrees) to the normal of the compressor inlet to allow for air starting, see Figure 47. Also shown in the photo at top dead center is the compressor inlet temperature probe, *T1.* The sensor is mounted to a custom mount allowing the sensor to be moved in all 3-axis x, y, and z.

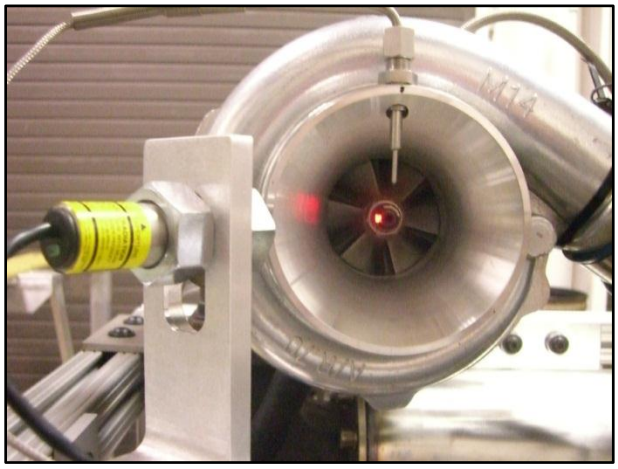

Figure 47. Core speed measurement technique, *N1*

The maximum RPM of the core will reach ~100,000 at max capability according to the supplied compressor map. The optical sensor is capable of sensing at max shaft speed and has been rated to 250,000 RPM by the manufacturer. The sensor receives its 12VDC excitation voltage supplied by the onboard main power supply.

Temperature Measurements

There are five temperature measurements that make up the core instrumentation set on the TECT. The parameter *T1, T2, T3,* and *T4* make up the performance temperature instrumentation while there is one engine health temperature, *TOIL,* for the engine oil temperature. The temperatures were taken using two different types of instruments. The lower temperature region at the compressor inlet *(T1)* and discharge *(T2),* as well as the oil temperature *(TOIL),* are measured using a resistance temperature detector (RTD) sensor. The RTD has very good accuracy +-1°F when compared to other types of temperature measuring devices but it is limited to relatively low temperatures (<500°F) and typically a slower response time. The other temperature measurements on the TECT engine, combustor exit temperature *(T3)* and turbine exit temperature *(T4),* require much higher temperatures and the thermal environment changes much quicker because they are both downstream of the combustor; therefore, they are out of the typical

range for a RTD type measurement. The K-type thermocouples were selected for use in this environment. The thermocouples are made with Inconel tips for high temperature applications up to 2,000°F. The *T3* thermocouple placement is shown in Figure 48. Note the turbine scroll is removed. The thermocouples need cold junction compensation to give accurate measurements. This signal conditioning is handled electronically inside of the instrument multimeter located within the main ECU. Each temperature measurement instrument is acquired into a multimeter display that has built-in lookup tables for engineering unit conversion for the thermocouple and RTD outputs. These values are displayed on the screen of the multimeter to give a real-time temperature display on the engine and then passes into the LabVIEW based data system.

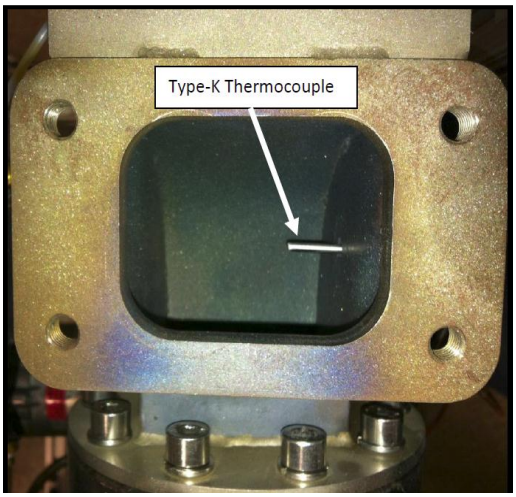

Figure 48. Thermocouple placement at combustor exit, *T3*

Pressure Measurements

The pressure measurements on the engine have 0-5 VDC outputs that are read into the USB DAQ cards then converted into engineering units via the calibration lookup. They require 5VDC excitation voltage which is provided from inside the main ECU. The *P2* measurement is an absolute (psia) pressure transducer that will not be required to measure pressures above 50 psia. This pressure measurement is crucial to get the compressor pressure ratio calculation. All of the TECT pressure measurements are static pressures and therefore a correction must be applied to calculate the total (stagnation pressure) for the *P2* measurement, see the *Data Corrections* section. A steady state data point is taken prior to each engine run to get ambient pressure from the *P2* measurement. This ambient pressure is then used for engine performance parameter corrections. The

other pressure measurements for oil pressure (*POIL)* and augmentor fuel manifold pressure (*PAB)* are both gauge pressure (psig) measurements rated up to 100 psig. The oil pressure is alarmed and display on the ECU so that it can be adjusted before the engine testing, while in the test-bay. The compressor discharge static pressure pickup location in shown in Figure 49.

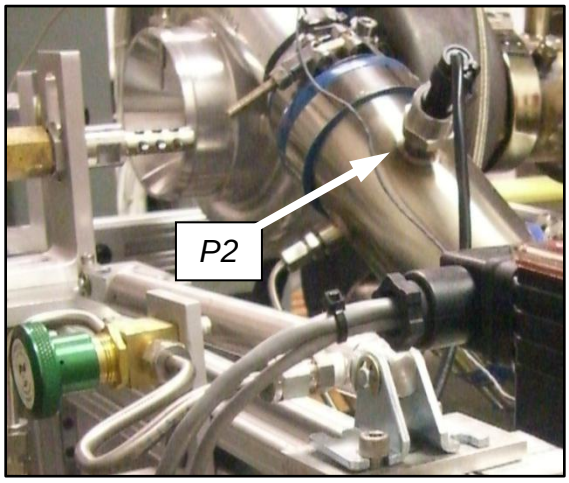

Figure 49. Compressor discharge pressure pickup location, *P2*

Centrifugal Compressor Analysis

The compressor to be analyzed has a 2 in. inducer inlet diameter and a 3 in. outlet diameter**.** The compressor is analyzed based on its geometric properties and inlet conditions and then compared to the actual steady state data taken during engine runs for comparison. The compressor analysis is based on properties listed in Table 10.

Table 10. Compressor analysis properties

Polytropic efficiency,	$e_c = 0.65/0.75$
Inducer inlet diameter,	$D_i = 2\ in$
Inducer outlet diameter,	$D_o = 3\ in$
Diffuser outlet velocity,	$v_3 = 300\ ft/s$
Total pressure at inlet face,	$P_{t1} = 14.6\ psia$
Total temperature at inlet face,	$T_{t1} = 518.7\ °R$
Slip Factor,	$\varepsilon = 0.9$

The polytropic efficiency, e_c was taken from the compressor map that was supplied by the manufacturer as shown in Figure 50. Note the max efficiency listed

in the center efficiency island is 75%, and this value was used for the current analysis. The analysis will also be performed with polytropic efficiency, e_c of 65% because of where the compressor may be operating within this efficiency island for some portion of the engine tests. For low compressor pressure ratio's the isentropic and polytropic efficiencies are very close, therefore for the current analysis considered interchangeable, see Figure 50 (Mattingly, 2006). The compressor map contains the compressor performance data. Note the stall or 'surge' line on the compressor map. Within this region the compressor enters a 'un-steady' region where the compressor cannot operate. One way to enter this region is maintain or increase the compressor pressure ratio, while not increasing mass flow rate through the engine. This can occur if the nozzle exit area is too small and becomes choked. This engine has a normal engine operating line. The difference between the stall line and the operating line is called the stall margin. It is important to have this stall margin to absorb any de-stabilizing inputs that may occur during engine operation, such as 'hard' augmentor light-offs caused by fuel pooling.

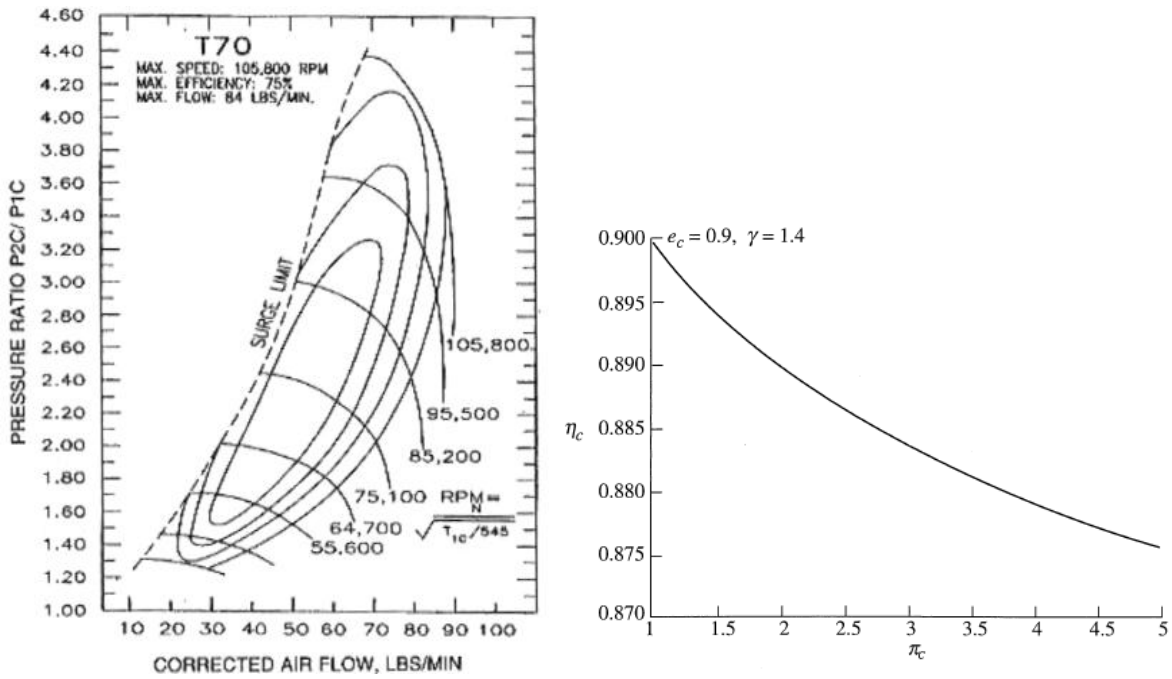

Figure 50. Centrifugal compressor map of current engine compressor and isentropic vs. CPR for constant polytropic efficiency

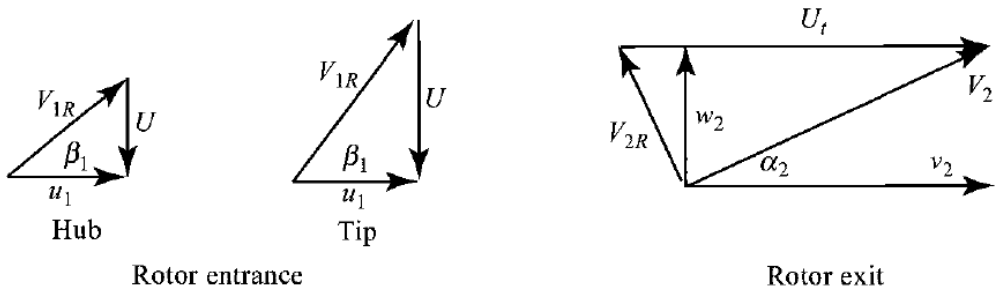

Figure 51. Velocity diagrams for radial vaned centrifugal compressor

Steady state data was taken for multiple engine runs at 40,000, 50,000, and 60,000 rpm. The following equations were used to predict compressor steady state performance. The velocity diagrams for the centrifugal compressor rotor/impeller are shown in Figure 51. The inlet flow is assumed uniform and the relative flow angle increases from hub to tip.

The impeller rotor velocity can be calculated using:

$$U_t{}^2 = \frac{g_c c_p T_{t1}}{\varepsilon}\left(\pi_c{}^{(\gamma-1)/(\gamma e_c)} - 1\right)$$

The impeller rotor velocity vector coming from the impeller is shown in Figure 52 below. Note that the velocity increases from hub to tip as the rotor imparts more kinetic energy into the flow as the radius increases.

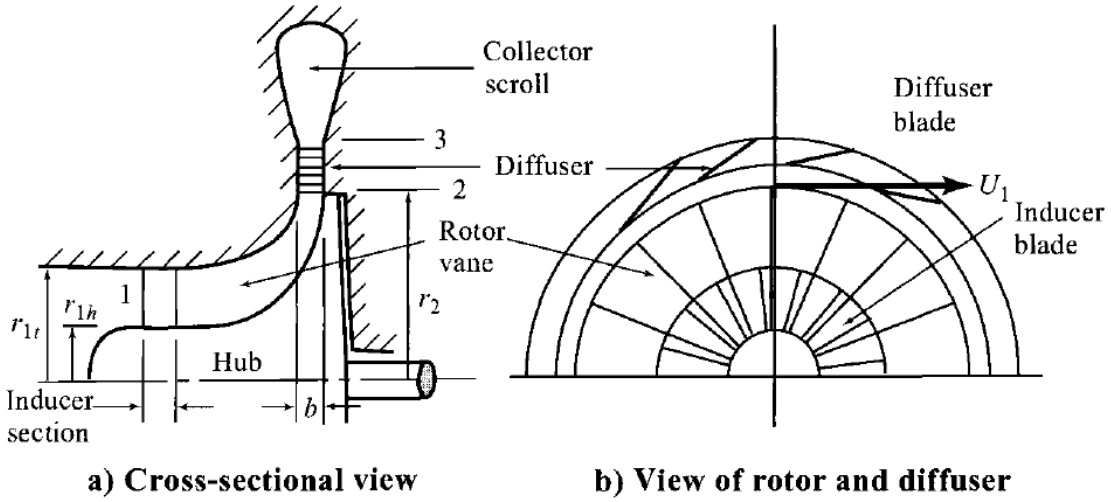

Figure 52. Station numbering and velocity vector for the rotor and diffuser

For the current analysis steady state rotational speeds are known, therefore the impeller rotor velocity U_t can simply be calculated from the relationship with the known inducer outlet diameter as:

$$U_t = \frac{N\pi d_2}{60}$$

The swirl velocity, v_2 can be assumed to be approximately 90% of the rotor velocity, U_t. The rotor velocity, U_t and the swirl velocity, v_2 are plotted over the speed range of the centrifugal compressor and are shown in Figure 53. The plot shows that at the upper end of the rotational speeds, the radial component of the velocity, w_2 which can be assumed as approximately equal to the inlet axial velocity, u_1 and the swirl velocity, v_2 are supersonic.

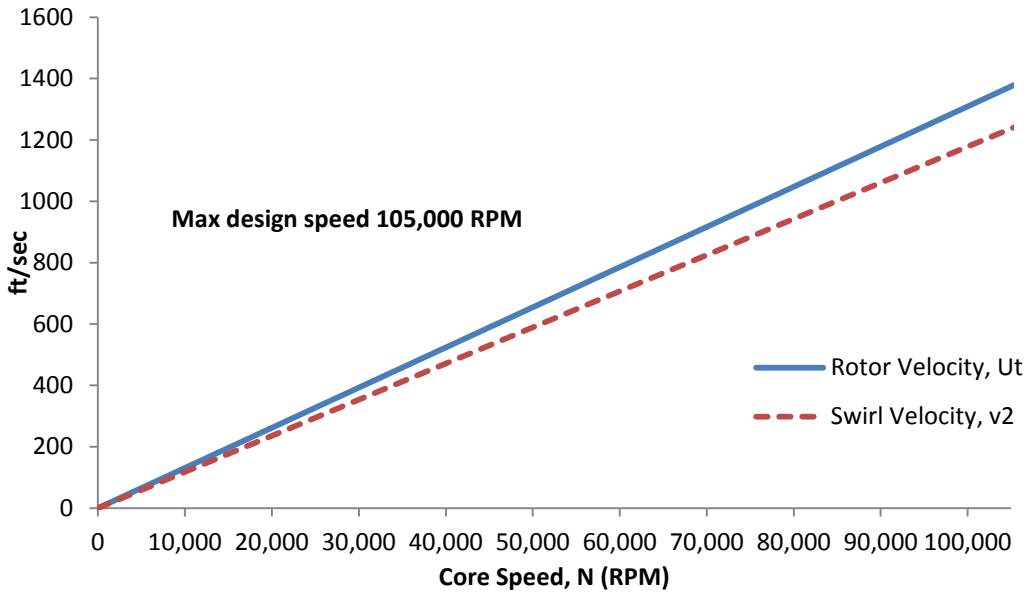

Figure 53. Graph showing rotor velocity and swirl velocity

Once the rotor velocity, U_t and the swirl velocity, v_2 are known, the Euler equation can be applied to a calorically perfectly gas, for a compressor with axial flow to give the compressor temperature rise:

$$T_{t2} - T_{t1} = \frac{v_2 U_T}{g_c c_p}$$

Using the definition of slip factor as the ratio of the exit swirl velocity, v_2 to the rotor velocity, U_t the compressor temperature rise can be expressed as

$$T_{t2} - T_{t1} = \frac{\varepsilon {U_t}^2}{g_c c_p}$$

Using the polytropic efficiency, e_c the compressor pressure ratio can be expressed as

$$\pi_c = \frac{P_{t2}}{P_{t1}} = \left(1 + \frac{\varepsilon {U_t}^2}{g_c c_p T_{t1}}\right)^{\gamma e_{c/(\gamma-1)}}$$

The results of the analysis are shown numerically for both a polytropic efficiency of 75% (Table 11) and then a polytropic efficiency of 65% (Table 12).

Table 11. Results of Compressor analysis, ec=0.75

Results of Compressor analysis, $e_c = 0.75$						
Core RPM, *N*	U_t (ft/s)	v_2 (ft/s)	M_2	ΔT (^{0}F)	M_3	π_c
20,000	261.8	235.6	0.21	8.6	0.27	1.04
30,000	392.7	353.4	0.32	19.4	0.26	1.1
40,000	523.6	471.24	0.42	34.5	0.26	1.18
50,000	654.5	589.05	0.53	53.8	0.26	1.3
60,000	785.4	706.9	0.63	77.5	0.25	1.44
70,000	916.3	824.7	0.74	105.5	0.25	1.63
80,000	1047.2	942.5	0.84	137.8	0.24	1.86
90,000	1178.1	1060.3	0.95	174.5	0.23	2.14
100,000	1309	1178.1	1.06	215.4	0.23	2.5

Table 12. Results of Compressor analysis, ec=0.65

Results of Compressor analysis, $e_c = 0.65$						
Core RPM, *N*	U_t (ft/s)	v_2 (ft/s)	M_2	ΔT (^{0}F)	M_3	π_c
20,000	261.8	235.6	0.21	8.6	0.27	1.038
30,000	392.7	353.4	0.32	19.4	0.26	1.087
40,000	523.6	471.24	0.42	34.5	0.26	1.157
50,000	654.5	589.05	0.53	53.8	0.26	1.25
60,000	785.4	706.9	0.63	77.5	0.25	1.37
70,000	916.3	824.7	0.74	105.5	0.25	1.52
80,000	1047.2	942.5	0.84	137.8	0.24	1.709
90,000	1178.1	1060.3	0.95	174.5	0.23	1.933
100,000	1309	1178.1	1.06	215.4	0.23	2.203

The analysis was performed over a range of compressor operating conditions all the way up through the max rotational speed of 100,000 RPM, the results are shown in Table 11 and Table 12. Note that at the maximum core speed the swirl velocity, v_2 is supersonic in the absolute frame. This is typical for centrifugal compressors, it is common to design for supersonic tip speeds in order to get the maximum pressure rise out of a single-stage. Although the absolute velocity is supersonic, the relative velocity is still subsonic and therefore, the total pressure losses are still low.

The steady state data points (SSDP) from the actual engine tests are recorded using the data acquisition software and corrected for total pressure using the swirl velocity Mach number M_2 (see Baseline Engine Performance section). The steady state data points were available for corrected engine speeds, *Nc* at 30k, 40k,

50k, 60k, 70k, and 80k rpm. The engine was tested to higher RPM's but the data was not used for comparison as the sensor would read erratically at these higher core speeds, resulting in skewed engine speed data passed the 80k point. The cause of this sensor behavior was due to higher engine vibrations causing the sensor to move its optical sight off of the compressor drive nut; this is what it used for its reference point for rotational speed. The steady state data points were recorded at 10 Hz for 10 seconds and then averaged. The results of the Steady State Data Points are shown in the Table 13 below.

Table 13. Results from SSDP vs. Predicted

Results from Engine Test, SSDP							
Core RPM, *Nc*	U_t (ft/s)	M_2	τ_C	π_c	% $\Delta\pi_c$, $\eta_c = 0.75$	% $\Delta\pi_c$, $\eta_c = 0.65$	% τ_C
30,000	392.7	0.32	1.02	1.14	3.5%	4.6%	1.6%
40,000	523.6	0.42	1.04	1.20	1.7%	3.6%	0.8%
50,000	654.5	0.53	1.08	1.32	1.5%	5.3%	2.1%
60,000	785.4	0.63	1.11	1.45	0.7%	5.5%	3.5%
70,000	916.3	0.73	1.14	1.59	2.5%	4.4%	5.4%
80,000	1047.2	0.84	1.18	1.82	2.2%	6.1%	7.5%

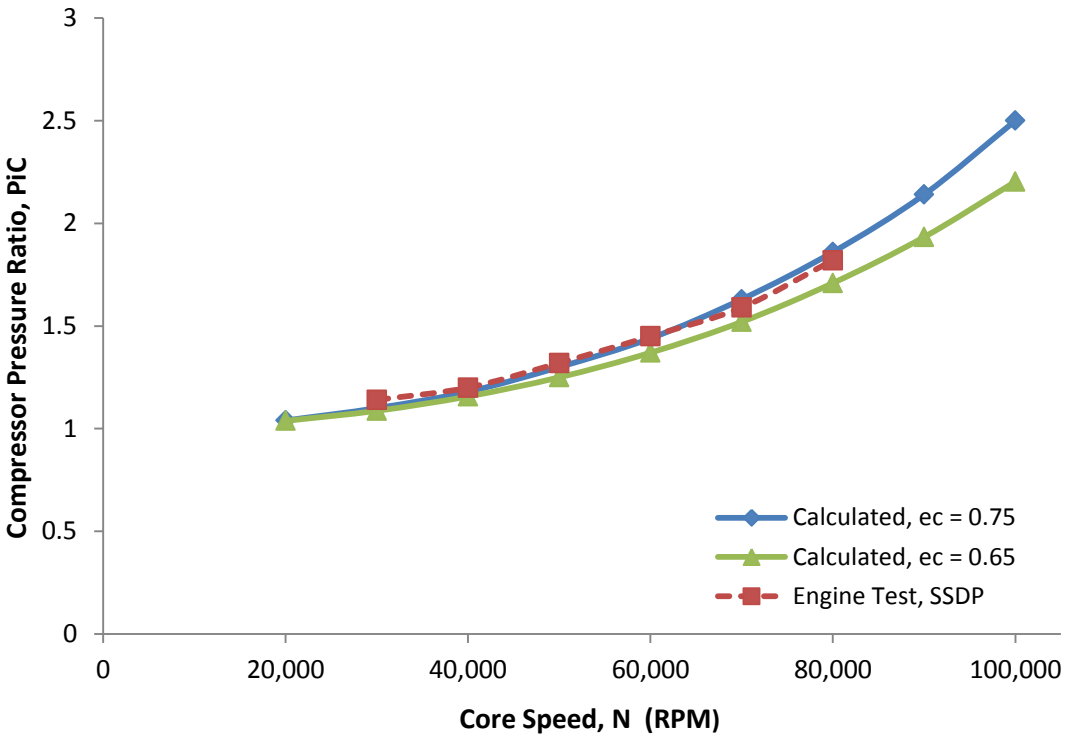

Figure 54. Graph showing results of compressor pressure ratio analysis vs. engine test

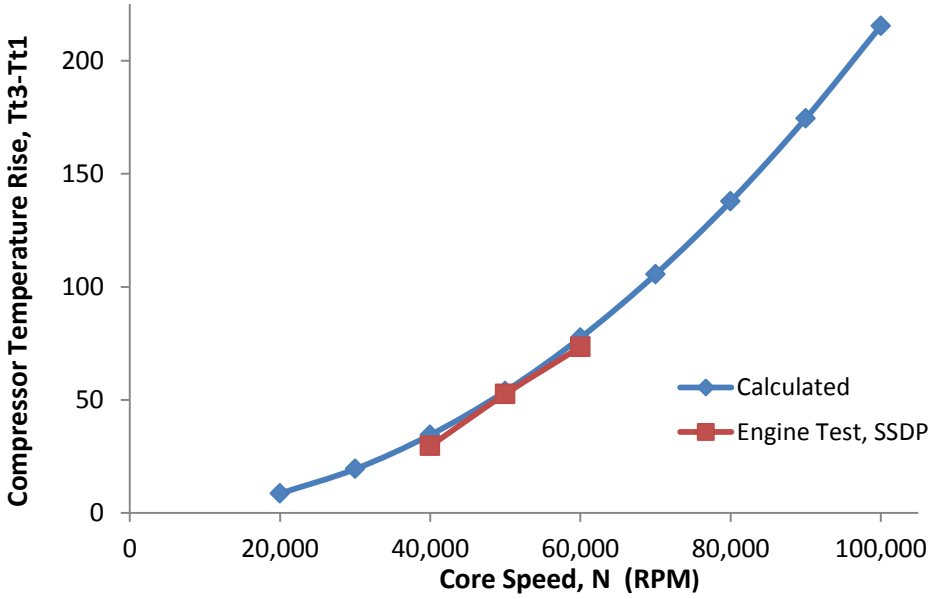

Figure 55. Graph showing results of compressor temperature rise analysis vs. engine test

The analysis was in good agreement with engine test, 0.7%-3.5% for π_c at polytropic efficiency of 75% and 3.6%-6.1% for a polytropic efficiency of 65%. The centrifugal compressor analysis matches well with engine test data, particularly at lower rotational speeds. Some source of error could be caused by multiple factors: static pressure pickup location, total pressure correction, sensor uncertainty, RTD heat soak, compressor efficiency assumption, as well as the assumptions listed in the basic assumptions for the analysis listed above. The analysis demonstrated provides a good first order approximation to actual compressor performance and is a great starting point for the designer when more elaborate computational tools are unavailable or not required for a quick analysis.

Baseline Engine Performance

The TECT engine demonstrates typical gas turbine characteristics that would be expected of full scale engines. It is for this reason the TECT project was developed. The engine was run at multiple throttle settings, with both transient and steady state data points taken. This section will document the baseline engine performance for the 'neutral' TECT engine without any additional hardware added. The baseline performance is important, as any change from this data must be attributed to the technology experiment or hardware degradation.

Data Corrections

All the engine data was corrected for temperature and pressure back to sea-level static (SLS). The pressure and temperature are made dimensionless by using the following relationships (Mattingly, 2006):

$$\delta_i \equiv \frac{P_{ti}}{P_{ref}}\text{, where } P_{ref} = 14.696\ psia \qquad \theta_i \equiv \frac{T_{ti}}{T_{ref}},\ where\ T_{ref} = 518.69°R$$

The corrected engine speed is a function of the upstream total temperature ratio using the relationship:

$$N_c \equiv \frac{N}{\sqrt{\theta_1}}$$

The engine speed N_c is corrected using the upstream temperature measurement *T1.* These dimensionless parameters are crucial to use when comparing multiple test parameters that may have been taken under different conditions. For example, if one set of test data is taken under ambient conditions on a cold day with low atmospheric pressure from weather front and then another test is taken on a much warmer day with a higher pressure, the engines performance will be shifted by the dissimilar conditions. This methodology of applying dimensionless corrections back to SLS, or another constant chosen condition, is standard practice within the gas turbine propulsion community. A list of common corrected gas turbine engine performance parameters is shown in Table 14. Although many of these performance parameters are applicable for use on the TECT, they are provided for reference and may be required for future potential TECT projects.

Table 14. Table of corrected performance parameters [19]

Parameter	Symbol	Corrected parameter
Total pressure	P_{ti}	$\delta_i = \frac{P_{ti}}{P_{\text{ref}}}$
Total temperature	T_{ti}	$\theta_i = \frac{T_{ti}}{T_{\text{ref}}}$
Rotational speed	$N = \text{RPM}$	$N_{ci} = \frac{N}{\sqrt{\theta_i}}$
Mass flow rate	$\dot{m}_i$	$\dot{m}_{ci} = \frac{\dot{m}_i\sqrt{\theta_i}}{\delta_i}$
Thrust	F	$F_c = \frac{F}{\delta_0}$
Thrust-specific fuel consumption	S	$S_c = \frac{S}{\sqrt{\theta_0}}$
Fuel mass flow rate	$\dot{m}_f$	$\dot{m}_{fc} = \frac{\dot{m}_f}{\delta_2\sqrt{\theta_2}}$

The TECT engine's instrumentation uses static temperature and pressure style pick-up probes and therefore must be corrected for total pressure. This correction factor is minimal, (<2% for pressure and <1% for temperature) but is applied as there is an effect on the performance parameters shown above. The total or stagnation temperature as it is commonly referred to, is defined as (Mattingly, 2006):

$$T_t = T\left(1 + \frac{\gamma - 1}{2} M^2\right)$$

and the total pressure is defined as:

$$P_t = P\left(1 + \frac{\gamma - 1}{2} M^2\right)^{\frac{\gamma}{\gamma - 1}}$$

Where γ is the ratio of specific heats. The Mach number is defined as:

$$M = \frac{V}{a} = \frac{V}{\sqrt{\gamma g_c R T}}$$

Where V is the absolute velocity, a is the local speed of sound, g_c is Newton's constant = 32.174, R is the universal gas constant = 53.35 and T is the local static temperature. Total pressure and temperature corrections are not applied to the station 1 instrumentation located at the compressor inlet. This assumption is made for the station 1 instrumentation because the engine is tested at SLS conditions with the inlet velocity assumed to be negligible. The station 2 instrumentation is corrected using the assumptions from the compressor analysis section, Table 10.

Introducing the compressor diffuser discharge pipe flow velocity $v_4 = 250\ ft/sec$ as the velocity of the flow after the diffuser has slowed it from $v_3 = 300\ ft/sec$. Therefore, the station 2 Mach number is defined as

$$M_2 = \frac{v_4}{\sqrt{\gamma g_c R T_2}}$$

This Mach number ($\sim \leq 0.160$) is used in the total temperature and pressure calculation to arrive at the corrected performance parameters such as the compressor pressure ratio:

$$\pi_c = \frac{P_{t2}}{P_{t1}}$$

As well as the compressor temperature ratio:

$$\tau_c = \frac{T_{t2}}{T_{t1}}$$

The turbine temperature ratio is defined as:

$$\tau_t = \frac{T_{t4}}{T_{t3}}$$

The station 3 total temperature, T_{t3} and station 4, T_{t4} are not corrected for stagnation properties. This is a reasonable assumption as the flow velocities in the combustor have dropped substantially from the compressor diffuser discharge, which has only a <1% effect even at the higher v_4 velocities. This flow velocity decrease is more apparent with the canned combustor design when compared to the more modern annular combustor that can have higher combustion flame velocities. The turbine casing/turbine nozzle is assumed to be adiabatic as the temperature pick up location for T_{t3} is located at the combustor exit plane and before the turbine casing/nozzle combination. This is a widely accepted practice in the gas turbine industry. The location of the radial inflow turbine makes it very difficult to instrument to give the 'true' inlet temperature and the added complexity does not justify the very small decrease in measurement uncertainty.

Engine Starting

Gas turbine engines require the use of a starting system to increase the engines core rotational (typically around 10% of rated core speed) speed before the fuel is introduced and ignited. The TECT engine uses an air-impingement starter, using ~100 psig compressed air to bring the engine up to ~9,000 RPM before the

engine sequence attempts to start. The starting characteristics for the TECT engine are shown in Figure 56, (Huenecke, 2005).

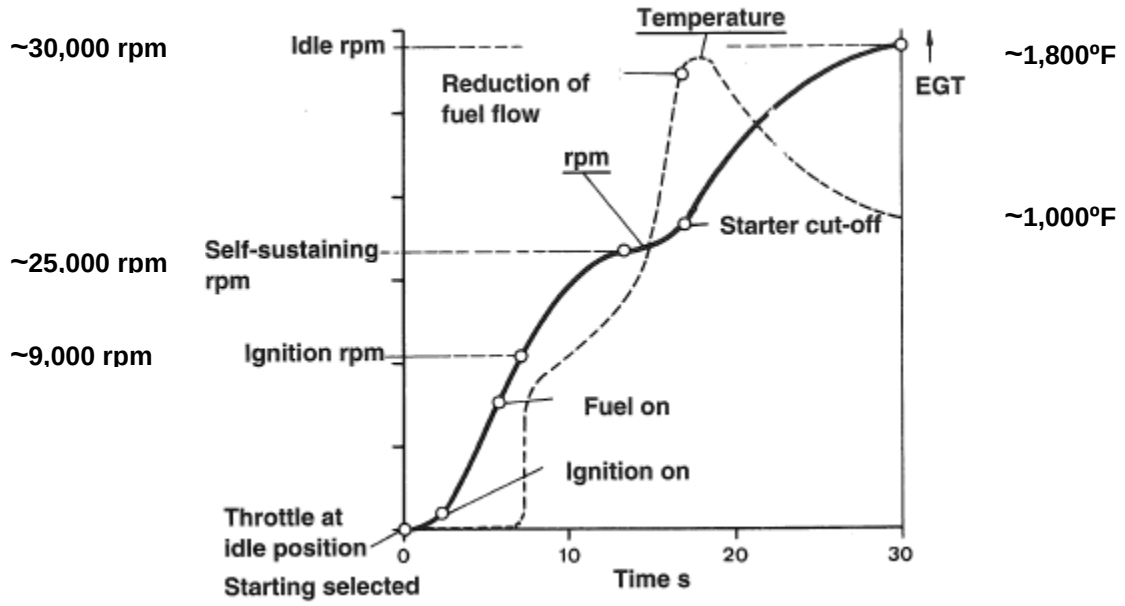

Figure 56. TECT starting behavior [12]

The raw data for a typical TECT start-up sequence is shown in Figure 57. The high combustor exit temperature, *T3* is a consequence of the mass flow rate through the engine. At the lower rotational core speeds, *N1* during the start-up, the engines combustion in not fully completing in the secondary combustion zone, but rather extending into the dilution region. This drives up the combustor exit temperature, as there is not adequate air for cooling in the dilution region. Once the engine makes enough power from the turbine to drive the compressor speed up, the mass flow rate of the engine increases to the point where the engine can sustain steady operation. This region is termed engine idle, and occurs ~30,000 RPM for the TECT engine. Once the engine comes to an idle condition, the high EGT's will come down to normal operating ranges. If the engine does not have adequate speed and ignition is attempted the engine will abruptly increase EGT, while not increasing core speed. This is termed a hung start and the TECT will automatically abort the start if the ECU senses this occurring.

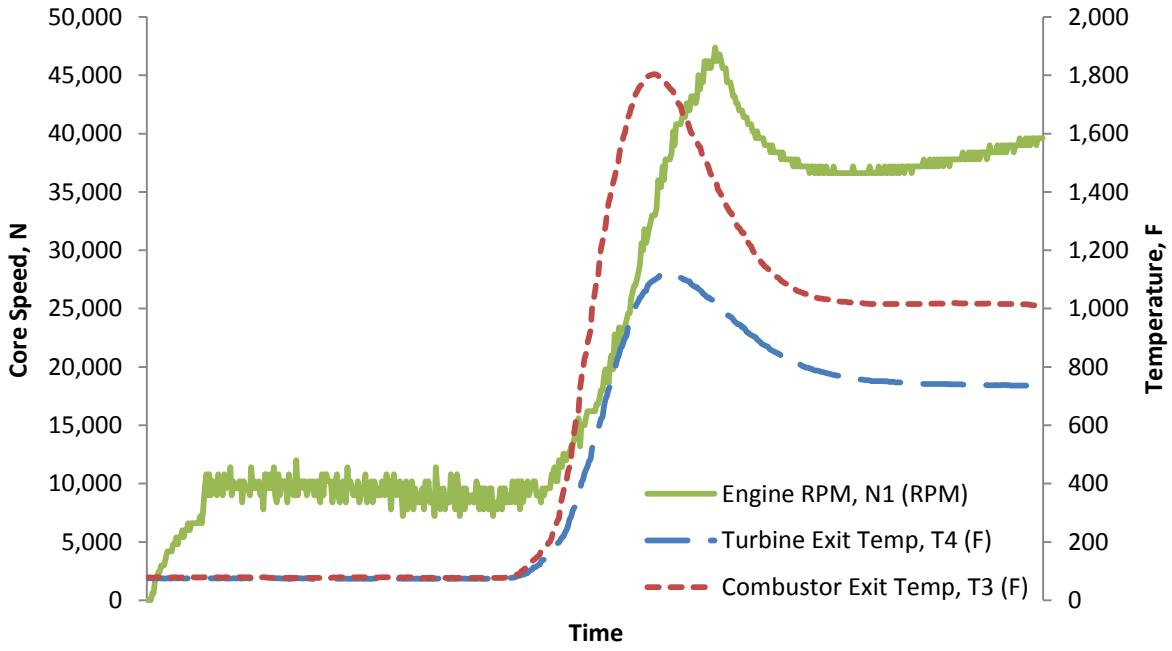

Figure 57. N1, T3, and T4 response for engine start sequence

Engine Vibration Response

The engine is instrumented with two high speed accelerometer measurements. One is mounted on the compressor housing, to pick up the compressor engine order speeds, as well as on the combustor, to pick up combustion harmonics/instabilities. Two different vibration G-responses are shown in Figure 58 for two different starting sequences. The plot on the left shows the typical vibration response for a ‘normal’ engine start. The plot on the right shows the response of a ‘low-speed’ engine start where the combustor has gone into a ‘un-steady’ mode and ‘pops.’ This ‘popping’ occurs repeatedly while the combustor ignites and then blows out. This is most likely a consequence of a combination of the low rotor speed during starting and a rich fuel/air ratio. The reduced core speed was a consequence of the engine oil temperature being lower than normal, causing the viscosity to increase. The combustion popping occurred at the same frequency

the igniter firing sequence, therefore the igniter was driving the re-lights, while the below normal speeds were causing the rich air/fuel ratio, leading to the blow outs. The ZMod plots of the vibration responses for the ‘’pop-start’ are shown in Figure 59. The color intensity (ZMod plot), consists of two graphical displays: an XY plot of spectral frequency vs. amplitude, and a color intensity display where the X-axis represents either time or shaft speed (RPM), the Y-axis represents frequency, and the amplitude is shown by its color. This type of start occurred during the fuel tuning for the start sequence and should be avoided for any future testing. This un-steady ‘popping’ is very hard on the engine components, as shown in the high levels of G-response. As a consequence of the un-steady ‘popping’, the engines hot section journal bearing and oil seal were required to be replaced from the high G-levels. These vibration measurements will be used to set high limits during ‘normal’ engine operation. Once the ‘normal’ levels are established they will be used as the baseline response. This will allow the operator early feedback if there is an outlier frequency response or higher than ‘normal’ magnitude from the vibration measurements that could expose an issue with the TECT and allow the operator or the ECU to shut-down the engine safely.

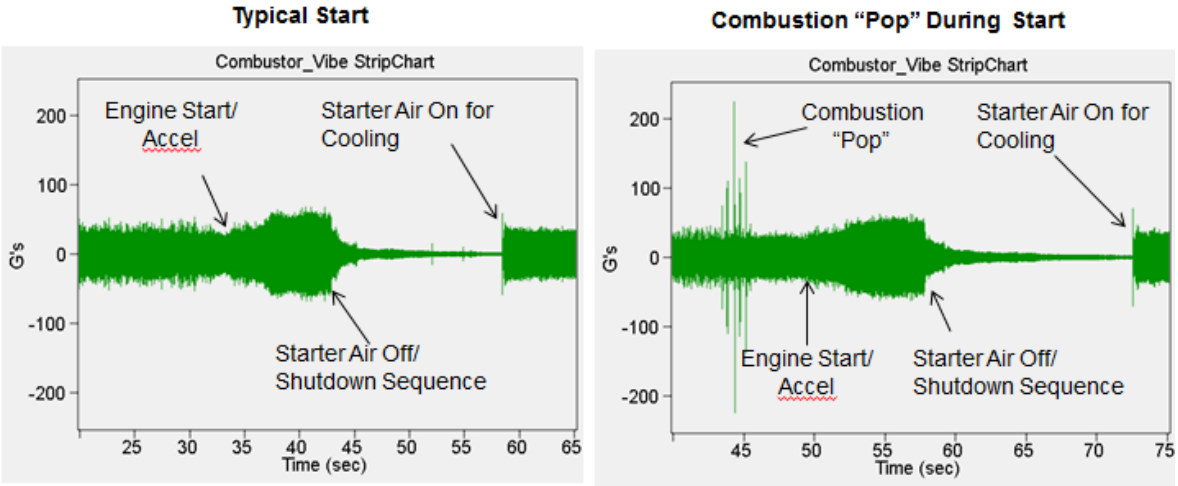

Figure 58. Vibration response during start, G's

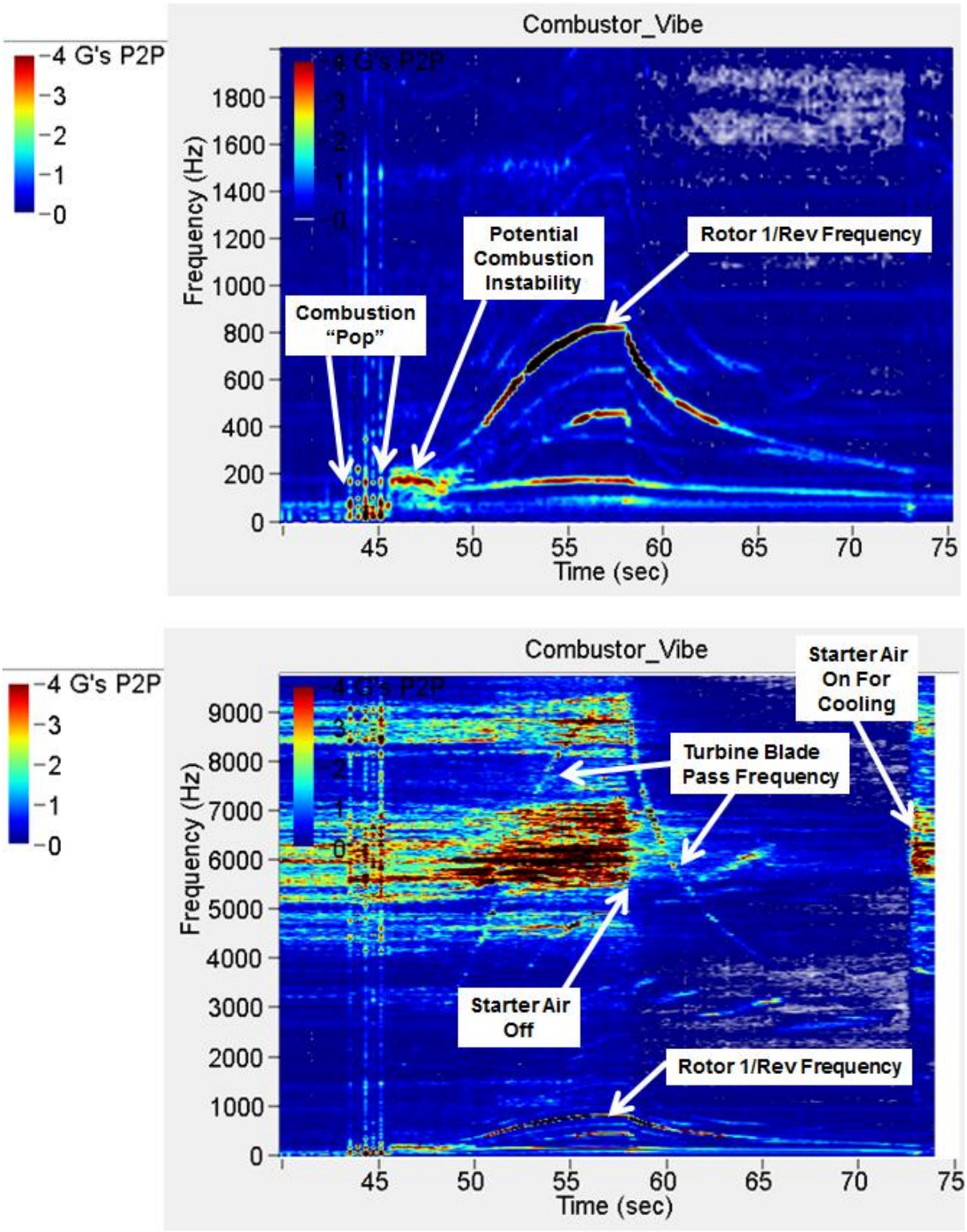

Figure 59. Engine vibration response (ZMod plots), frequency vs time

Engine Performance Characteristics

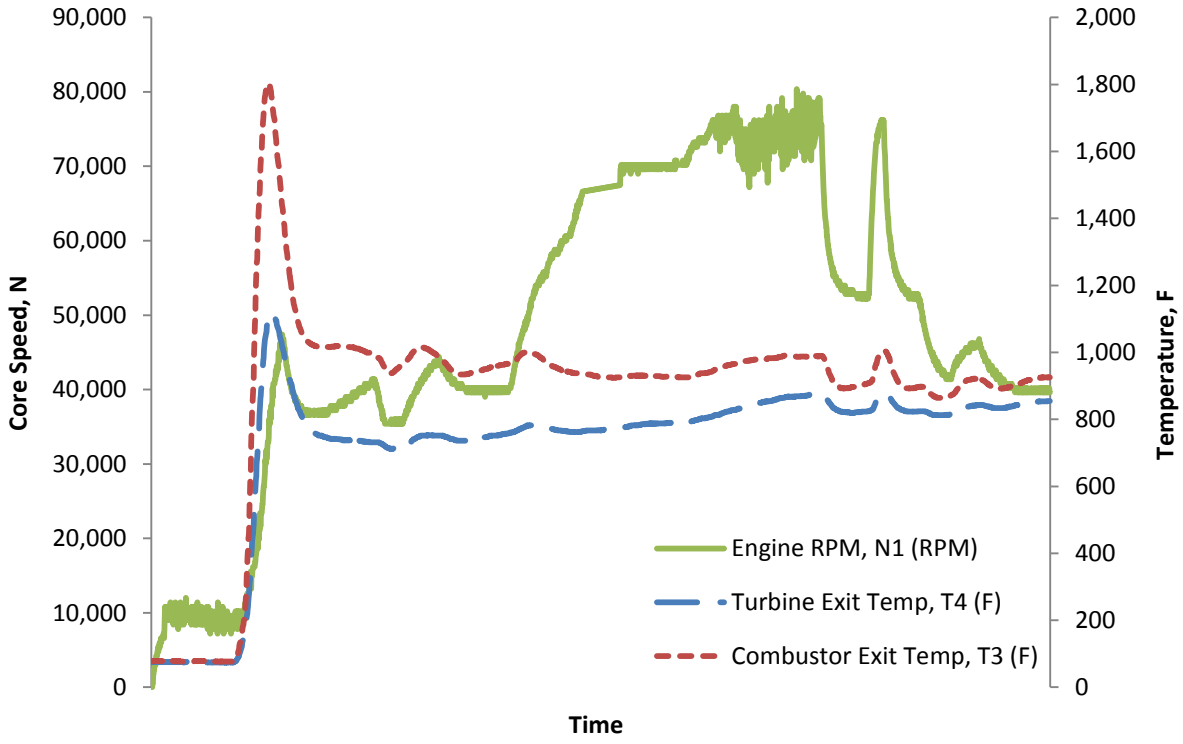

Figure 60. N1, T3, and T4 response for engine run to 80,000 RPM

The TECT was run up to 80,000 RPM's with the transient response shown in Figure 60. The engine start sequence is shown on the left where EGT's are the highest and then the throttle was taken to up to 80,000 RPM's. The engines core speed measurement started to become erratic above 76,000 RPM's during this run. This could be attributed to either the engine vibrations causing the reference point to enter in and out of the line of sight of the laser pick-up, or it could be caused by the data acquisition card timing function not having the required sample rate to keep up with the high rotational speeds. The TECT's data acquisition system outputs raw data files with both the instrumentation and control logic outputs as shown in Table 15. The '0' in the command column for the control parameters, indicates the component is set to OFF, while a '1' is being commanded to turn ON.

Table 15. TECT transient raw data output file

6/24/2014 8:49														
Engine Oil Pressure Poil (PSIg)	Turbine Exit Temperature T4 (F)	Afterburner Fuel Pressure, Pab (PSIg)	Air Temperature OAT (F)	Compressor Discharge Pressure P2 (PSIa)	Engine Oil Temperature Toil (F)	Compressor Discharge Temperature T2 (F)	Combustor Exit Temperature T3 (F)	Engine RPM, N1 (RPM)	Oil Pump Cmd	AB Fuel Pump Cmd	Starter Air Cmd	Main Ignition Cmd	AB Fuel Solenoid Cmd	Throttle Cmd (V)
20.91	820.90	0.53	77.53	23.31	72.12	126.88	959.10	76800	1	0	0	0	0	4.1
20.90	821.41	0.51	77.90	23.32	72.12	126.98	959.58	76800	1	0	0	0	0	4.1
20.89	822.43	0.54	77.25	23.32	71.65	127.07	959.51	76200	1	0	0	0	0	4.1
20.89	822.77	0.54	77.47	23.31	71.73	127.09	959.31	75000	1	0	0	0	0	4.1
20.90	823.11	0.53	77.09	23.31	71.57	127.06	960.87	76800	1	0	0	0	0	4.1
20.89	822.77	0.52	77.39	23.31	71.81	127.07	960.67	76200	1	0	0	0	0	4.1
20.89	822.94	0.53	77.66	23.31	71.97	127.13	961.21	75600	1	0	0	0	0	4.1
20.90	822.77	0.51	78.26	23.31	72.12	127.55	961.28	76800	1	0	0	0	0	4.1
20.89	823.28	0.54	78.51	23.31	71.57	127.98	961.01	76200	1	0	0	0	0	4.1
20.90	823.28	0.54	78.38	23.31	71.65	128.11	961.76	73800	1	0	0	0	0	4.1
20.89	823.62	0.53	77.89	23.31	71.81	128.19	962.23	76800	1	0	0	0	0	4.1
20.89	824.13	0.54	77.82	23.32	71.41	128.18	962.10	76800	1	0	0	0	0	4.1
20.90	823.62	0.54	78.25	23.33	72.20	128.17	962.64	76200	1	0	0	0	0	4.1
20.85	824.05	0.54	78.48	23.35	72.12	128.17	962.64	75600	1	0	0	0	0	4.1
20.84	823.96	0.54	78.52	23.37	72.20	128.16	962.57	76800	1	0	0	0	0	4.1
20.84	824.90	0.53	78.51	23.38	72.12	128.19	962.57	74400	1	0	0	0	0	4.1
20.83	824.98	0.54	78.51	23.37	71.89	128.17	963.05	76800	1	0	0	0	0	4.1
20.82	825.15	0.53	78.52	23.37	71.97	128.16	963.25	75000	1	0	0	0	0	4.1
20.82	826.52	0.51	78.55	23.36	71.89	128.19	963.32	76200	1	0	0	0	0	4.2
20.82	827.03	0.53	78.61	23.43	72.28	128.18	963.66	75000	1	0	0	0	0	4.2
20.82	827.54	0.55	78.54	23.47	72.28	128.45	964.34	76200	1	0	0	0	0	4.2
20.81	827.96	0.53	78.53	23.49	71.89	128.84	964.14	76200	1	0	0	0	0	4.2
20.82	828.13	0.56	78.96	23.59	72.12	128.84	964.14	77400	1	0	0	0	0	4.2
20.83	827.96	0.55	79.49	23.62	71.65	128.92	965.29	77400	1	0	0	0	0	4.2
20.84	827.71	0.55	79.72	23.62	71.97	128.90	965.50	76200	1	0	0	0	0	4.2
20.83	827.79	0.51	79.74	23.62	71.73	128.94	965.43	78000	1	0	0	0	0	4.2
20.75	828.13	0.56	79.77	23.62	71.73	128.90	965.91	76800	1	0	0	0	0	4.2

While the ECU is in the ‘computer control’ mode of operation, throttle set-points can be pre-programmed at desired conditions. These set-points are based on the throttle PLA commanded positions as a voltage output. These set-points allow the engine to be rapidly moved from one throttle setting to the next. These rapid movements are typically called, throttle ‘snaps,’ because of the prompt rate at which the engine is commanded to different power settings. The time for the engine speed to increase to a steady state speed after a throttle snap is critical information as this correlates to engine thrust for an aircraft application. That is very useful information for an aircraft take-off condition where the engines are being ‘snapped’ from ground idle to max power and the time to thrust determines the runway distance.

The TECT engine was tested performing throttle snaps from high power to ~50,000 RPM then back up to a high power set-point. For the tested throttle snap the time for the core speed to reach a steady state operating condition was 2.8 seconds after the throttle command was initiated, Figure 61. This is very fast compared to typical gas turbine engines. There are multiple reasons for this. The largest factor is the low inertia of the single-stage compressor. Another contributing factor is the component performance matching. The original design intent of the compressor/turbine matching was based on an automotive application where the turbine is driven by exhaust gases from an internal combustion engine. For the automotive application, the pressure rise from the compressor is called, ‘compressor lag,’ this lag time significantly effects vehicle performance because of the significantly increased amount throttle transients that automobiles operate under when compared to aircraft. To reduce this ‘lag’ time, the turbine is oversized for the compressor when compared to a gas turbine application; therefore, the compressor responds faster. The fuel control valve has an adjustable gain ramp that slows down the movement. These throttle snaps were performed with the ramp activated and therefore the engine response time could be decreased if required. The engines responses to the ‘throttle snap’ are shown in Figure 61-Figure 63. Note that the compressor pressure ratio is slower to react when compared to the core speed.

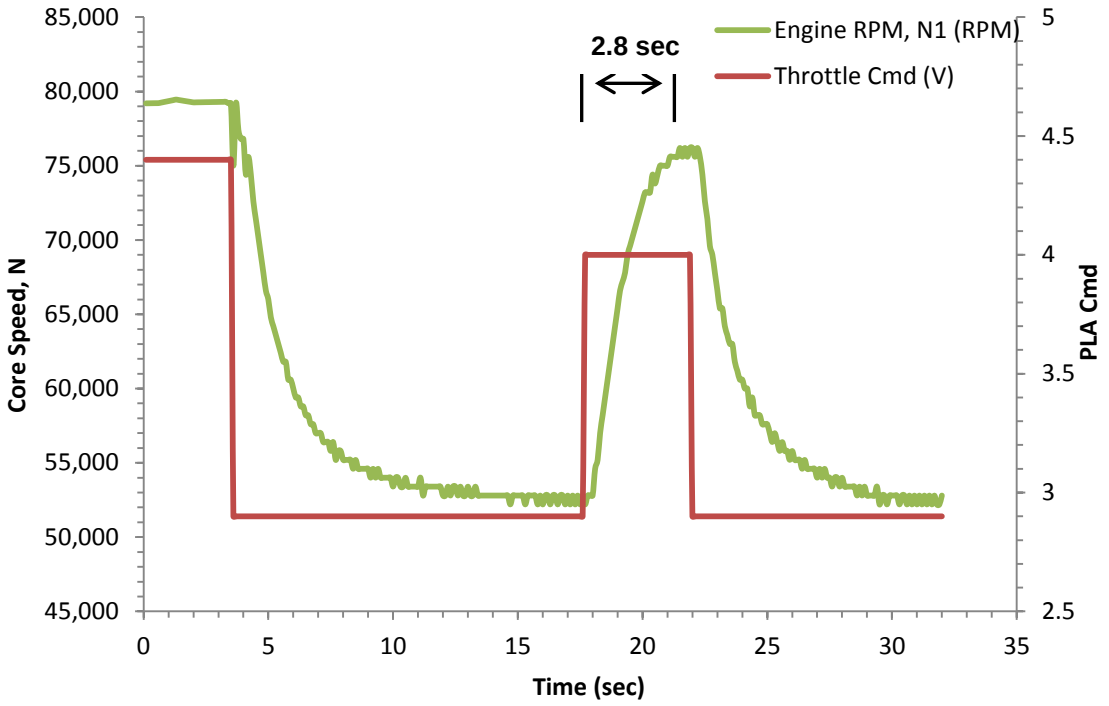

Figure 61. Engine speed response to throttle snaps

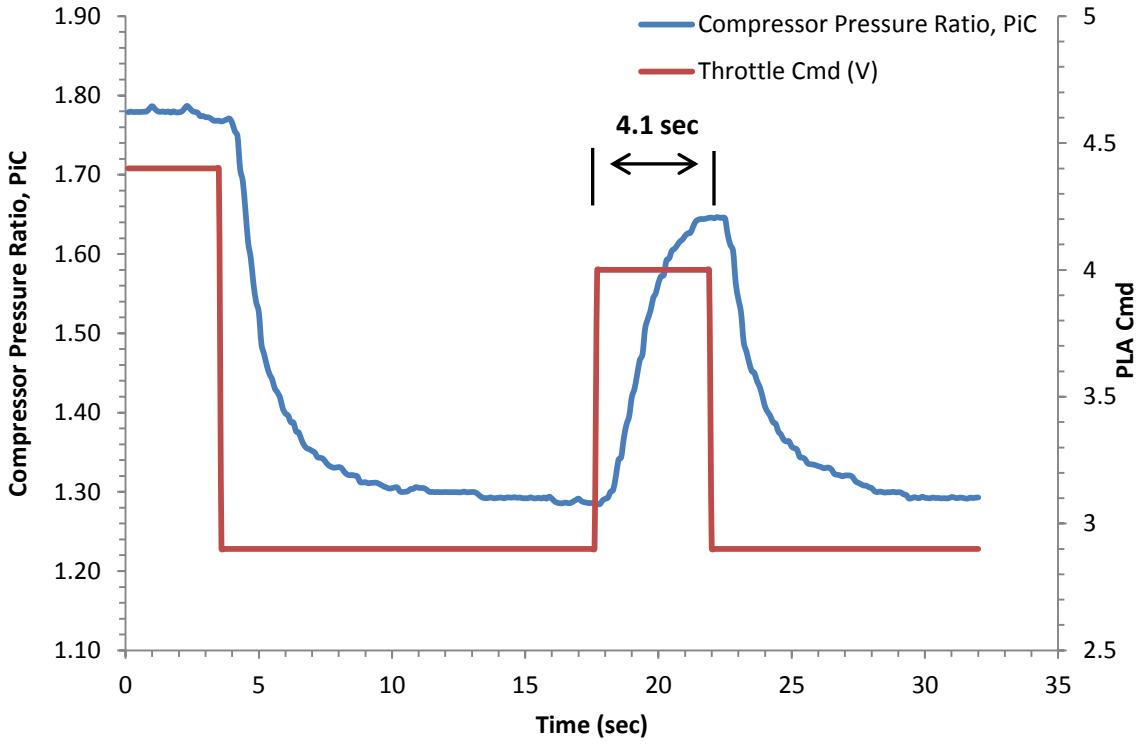

Figure 62. Engine compressor response to throttle snaps

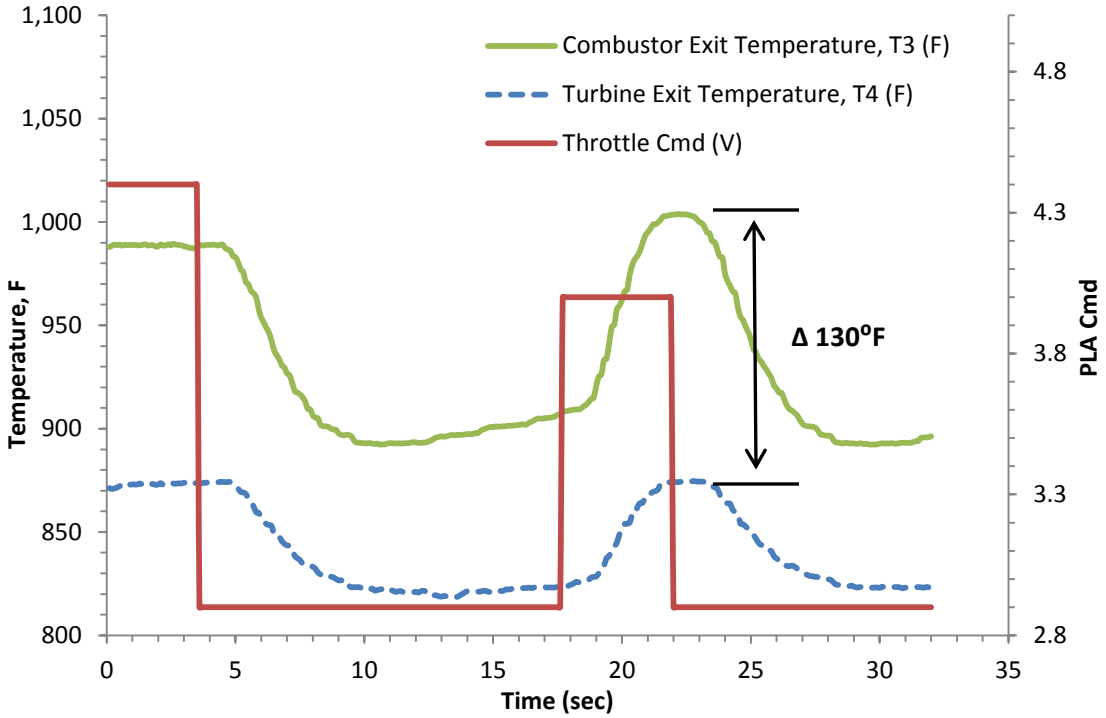

Figure 63. Engine temperature response to throttle snaps

The engines compressor temperature ratio along with the turbine temperature ratio is shown in Figure 64. This is typical gas turbine engine behavior and as should be expected, the compressor discharge temperature is increasing with increasing pressure. Not as obvious is the nearly constant turbine temperature ratio. This is an outcome of the nearly adiabatic turbine along with the nearly constant polytropic efficiencies that is typical of turbines. A constant turbine temperature ratio is a required assumption for the performance analysis (PERF software) that was ran in Ch.II.

The TECT engine was not tested in augmentor operation, as the control system still required increased development for the computer control. The engine has run under manual augmentor operation in the past with good results and the engine behaved as expected. This manual type of operation was not suitable for the TECT build as the safety concerns are very high. This control logic will be completed in the near future.

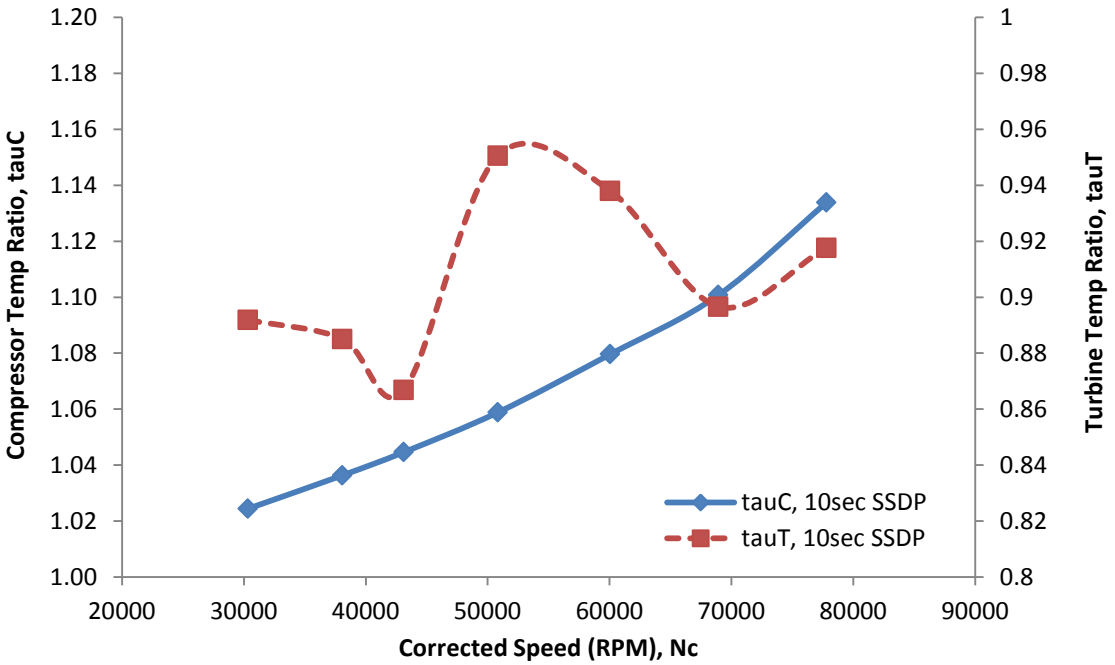

Figure 64. Compressor and Turbine temp ratio vs corrected core speed Nc from engine test

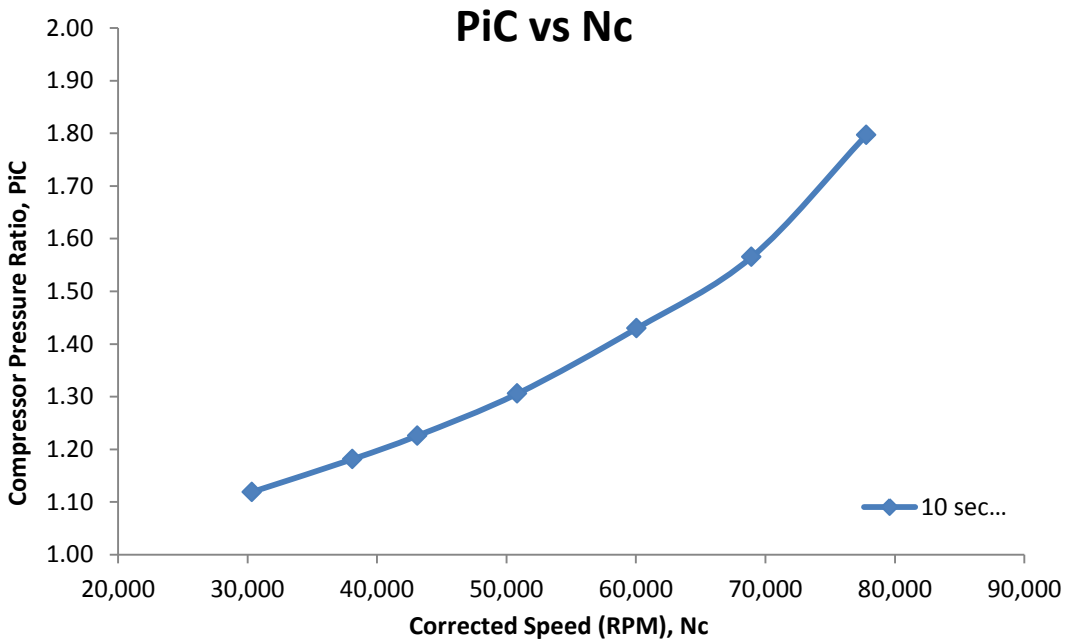

Figure 65. Compressor pressure ratio vs corrected core speed from engine test

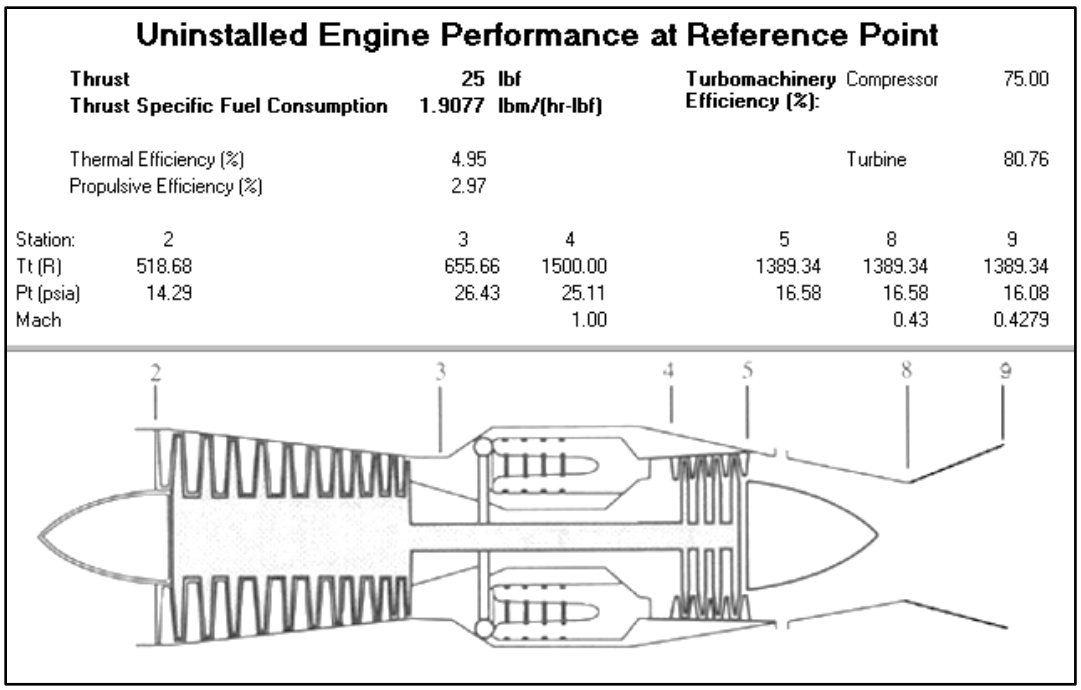

Figure 66. Engine performance analysis results for highest non-augmented test condition

The PERF performance analysis software that was used in Ch. II was run at the highest tested condition, see Figure 66. The higher compressor pressure ratios that were used for the previous analysis were not attainable at the lower tested core speeds <80,000RPM. Therefore, the engines performance was lower than expected and the TSFC was increased. The compressor pressure ratio does not increase linearly with speed as shown in Figure 65. Thus, a small increase in speed at the upper end of the compressor operating envelope results in a much higher increase in compressor pressure ratio, and therefore specific thrust. The engines combustor exit temperature was reduced when compared to the Ch. II performance analysis. The current case was run at 1450 °R vs. the 1660°R limit. The combustor exit temperature has a larger effect on performance when compared to the compressor pressure ratio if the mass flow rate through the engine is treated as a constant (40% decrease vs. 23% decrease for the TiT@1450°R and PiC@1.8). This is why gas turbine engines run their high pressure turbine inlet total temperatures beyond their material melting points, therefore they require active cooling.

CHAPTER V
CONCLUSIONS AND RECOMMENDATIONS

The Turbine Engine Component Testbed has met all project goal objectives for the J1-H-02 build. The TECT has proven to be an effective adaptable environment for turbine engine test projects. The TECT has promise as an applicable system to test new sensors or analytical techniques before full scale testing by allowing an intermediate Technology Readiness Level (TRL) at low-cost and quick schedule turnaround. The TECT was completed using a minor financial investment when matched to comparable capabilities.

A data acquisition and control system was developed and tested that allows for real-time engine feedback and control schemes. The engine has automatic starting and shutdown logic, as well as ABORT logic if the control system determines that this is required. The data and control system is easily adaptable to meet future test requirements. The TECT is a highly modular system that allows components to be changed out and modified easily. The components were analyzed for the proper failure modes, and performance was predicted using a combination of hand calculations and engine performance prediction software. The compressor performance was predicted using turbomachinery relationships and geometry, then compared with experimental data.

The TECT engine was tested across its intended operational envelope at sea-level static conditions, with the baseline performance data documented. The applied data reduction approaches were developed and presented. The TECT was tested for transient throttle operation, and the engine response documented.

It is recommended that the TECT be employed for its intended use as a technology demonstrator.

LIST OF REFERENCES

[1] 304/304L Data Bulletin." *AK Steel*. July 2007. Web. 25 Oct. 2010. <http://www.aksteel.com>.

[2] Boyce, Meherwan P. *Gas Turbine Engineering Handbook*. Houston, TX: Gulf Pub., 2002. Print.

[3] Budynas, Richard Gordon., and J. Keith. Nisbett. *Shigley's Mechanical Engineering Design*. Singapore: McGraw-Hill, 2008. Print.

[4] Cengel, Yunus A. Heat Transfer a Practical Approach. Boston (Mass.): McGraw-Hill, 2006. Print.

[5] Chen, Kevin K., Jonathan H. Tu, and Clarence W. Rowley. "Variants of Dynamic Mode Decomposition: Boundary Condition, Koopman, and Fourier Analyses." *Journal of Nonlinear Science* (2005).

[6] Church, Austin H. Centrifugal Pumps and Blowers. Huntington, NY: Krieger, 1972. Print.

[7] Cumpsty, Nicholas A. Jet Propulsion: a Simple Guide to the Aerodynamics and Thermodynamic Design and Performance of Jet Engines. Cambridge Univ., 2008. Print.

[8] Ebrahimi, Houshang B. *Overview of Gas Turbine Augmentor Design, Operation*. Proc. of 19th Annual Conference on Liquid Atomization and Spray Systems, Toronto. 2006. Print.

[9] Figliola, R. S., and Donald E. Beasley. Theory and Design for Mechanical Measurements. Hoboken, NJ: John Wiley, 2006. Print.

[10] Hartman, Joshua A., and Aaron Marshall. Gas Turbine Data Acquisition System Design. Rep.Wright State University, 2010.

[11] Hunecke, Klaus. "Combustion Chambers." *Jet Engines*. N.p.: Zenith, 2005. N.

[12] Hunecke, Klaus. Jet Engines: Fundamentals of Theory, Design and Operation. Osceola, WI: Motor International, 2005. Print.

[13] Jourdain, Guillaume. "Time-domain Modeling Of Screech-damping Liners In

Combustors And Afterburner." *ISABE* (2011): n. pag. Web. 1 Sept. 2013.

[14] Kerschen, Gaetan, Jean-claude Golinval, Alexander Vakakis, and Lawrence Bergman. "The Method of Proper Orthogonal Decomposition for Dynamical Characterization and Order Reduction of Mechanical Systems." Nonlinear Dynamics (2004):

[15] Khair, Magdi K. "Turbocharger Fundamentals." Turbocharger Fundamentals. N.p., n.d. Web. 03Apr. 2013. <http://www.dieselnet.com/tech/air_turbocharger.php>.

[16] Lieuwen, Timothy C., and Vigor Yang. *Combustion Instabilities in Gas Turbine Engines*. Reston: AIAA, 2005. Print.

[17] Lieuwen, Timothy C. "Static and Dynamic Combustion Stability." *The Gas Turbine Handbook*. N.p., n.d. Web. 30 Aug. 2013. <http://www.netl.doe.gov/technologies/coalpower/turbines/refshelf/handbook/TableofContents.html

[18] Kotecki, Damian. "Stainless Steel." *Lincoln Electric*. Web. 25 Oct. 2010. <http://www.lincolnelectric.com>.

[19] Mattingly, Jack D. Elements of Propulsion: Gas Turbines and Rockets. Reston, VA: AIAA, 2006. Print.

[20] Lister, Jonathan. "Augmentor Testing." Aerospace Testing Alliance. TN, Arnold Air Force Base. 2012

[21] "Stainless Steel Fasteners." SSINA: Specialty Steel Industry of North America. Web. 5Nov. 2010. <http://www.ssina.com>.

[22] Saravanamuttoo, HIH, and PV Strazincky. Gas Turbine Theory. 6th ed. London: Pearson Education, 2009. Print.

[23] United States of America. National Advisory Comittee for Aeronautics. Lewis Flight Propulsion Laboratory. *A Summary of Preliminary Investigations Into The Characteristicsof Combustion Screech In Ducted Burners*. Cleveland: n.p., 1954. Print.

APPENDICES

A. ENGINE OPERATION AND PROCEDURES

J1-H-02/TECT/MJE Operation procedures

Note: For the purpose of this operation document J1-H-02, TECT, and MJE are all synonymous

Startup Procedures

1 – Bay Door OPEN and Remove Plug from Turbine Exit

2 – Air Supply attached into Starter Air Control Solenoid and Compressor Cover Removed

3 – Oil Level Checked and Vent OPEN

4 – Air Supply Ball Valve OPEN

5 – Master Power Switch ON

6 – Oil Pump Switch AUTO

7 – AB Fuel Pump Switch AUTO (** If AB Required **)

8 – Oil Cooler Fan Switch ON

9 – Verify Propane Supply Attached

10 – Verify AB E-Stop OUT (** If AB Required **)

11 – Ignition Arm ON

12 – Hook USB into Control Computer

13 – Setup and Run MJE Auto Control Rev 9 (See MJE Auto Control Manual for Setup Details)

14 – Wait for “Initialization” Machine State and Verify SSR Lights Extinguished

15 – Propane Supply Tank ON and Regulated

16 – Power Strip Switch ON

17 – MJE Ready for Remote Operation using MJE AUTO Control Rev 9

Shutdown Procedures

1– Shutdown MJE using MJE Auto Control Rev 9 and Wait for .VI to Stop

2 – Propane Supply Tank OFF

3 – Power Strip Switch OFF

4 – Oil Cooler Fan Switch OFF

5 – AB Fuel Pump Switch OFF

6 – Oil Pump Switch OFF

7 – Master Power Switch OFF

8 – Air Supply Ball Valve CLOSED

9 - Air Supply removed from Starter Air Control Solenoid and Compressor Cover INSTALLED

10 – Propane Supply removed from Propane Control Valve

11 - Bay Door CLOSED and Turbine Exit Plug INSTALLED (** Exhaust Nozzle May Still Be Hot **)

MJE Auto Control

MJE Auto Control is a LabVIEW program developed using a state machine architecture that utilizes data acquisition system information to control the startup, operation, and shutdown of the MJE. Depending on the state of the machine when the shutdown/abort signal is given determines the shutdown method. If the engine is spooled or running, the program will shut down the MJE by maintaining oil pressure and using starter air to continue to turn the engine until turbine exit temperature falls below “EGT Starter Air Cut Out” temperature. Then the program turns off starter air but maintains oil pressure until shaft rotation falls below “Oil Off Cut Out Speed” is reached.

Machine States

Initialization: Initialization is the safe state for the device. It sets all digital outputs to a logic low level and the PLA Cmd to 0 (Hard CLOSED).

Wait for Oil Pressure: Wait for Oil Pressure engages the Oil Pump SSR and waits for the oil pressure to reach 10 psi before continuing.

Engine_Air_On: Engine_Air_On engages the Starter Air SSR and waits for a shaft rotation of 9000 rpm.

Main_Ignition: Main_Ignition engages the Ignition SSR, sets PLA Cmd to “Start Set Point” Value, and waits until Turbine Exit Temperature is greater than 600 F for 8 seconds. User input can be used to control PLA Cmd (1 (Soft Closed) to 10 (Full))

Engine Running: Engine Running disengages the Starter Air SSR and Ignition SSR. User input is required to control throttle position. This loop will automatically shut down the MJE if shaft rotation of 85,000 rpm is exceeded, turbine exit temperature of 1200 F is exceeded, or if oil pressure falls below 8 psi.

Engine_Shut_Down: Engine_Shut_Down engages the Starter Air SSR and waits for the Turbine Exit Temperature to fall below “EGT Starter Air Cut Out” temperature.

Engine_Air_Off: Engine_Air_Off disengages the Starter Air SSR.

Engine_Off: Engine_Off waits for shaft rotation to fall below “Oil Off Cut Out Speed” and then disengages the oil pump and stops the program.

Manual Mode: Manual Mode allows manual operation of the MJE using front panel buttons. **WARNING**: Manual Mode does not contain abort information if input limits are exceeded. The User is responsible for monitoring and shutting down the device.

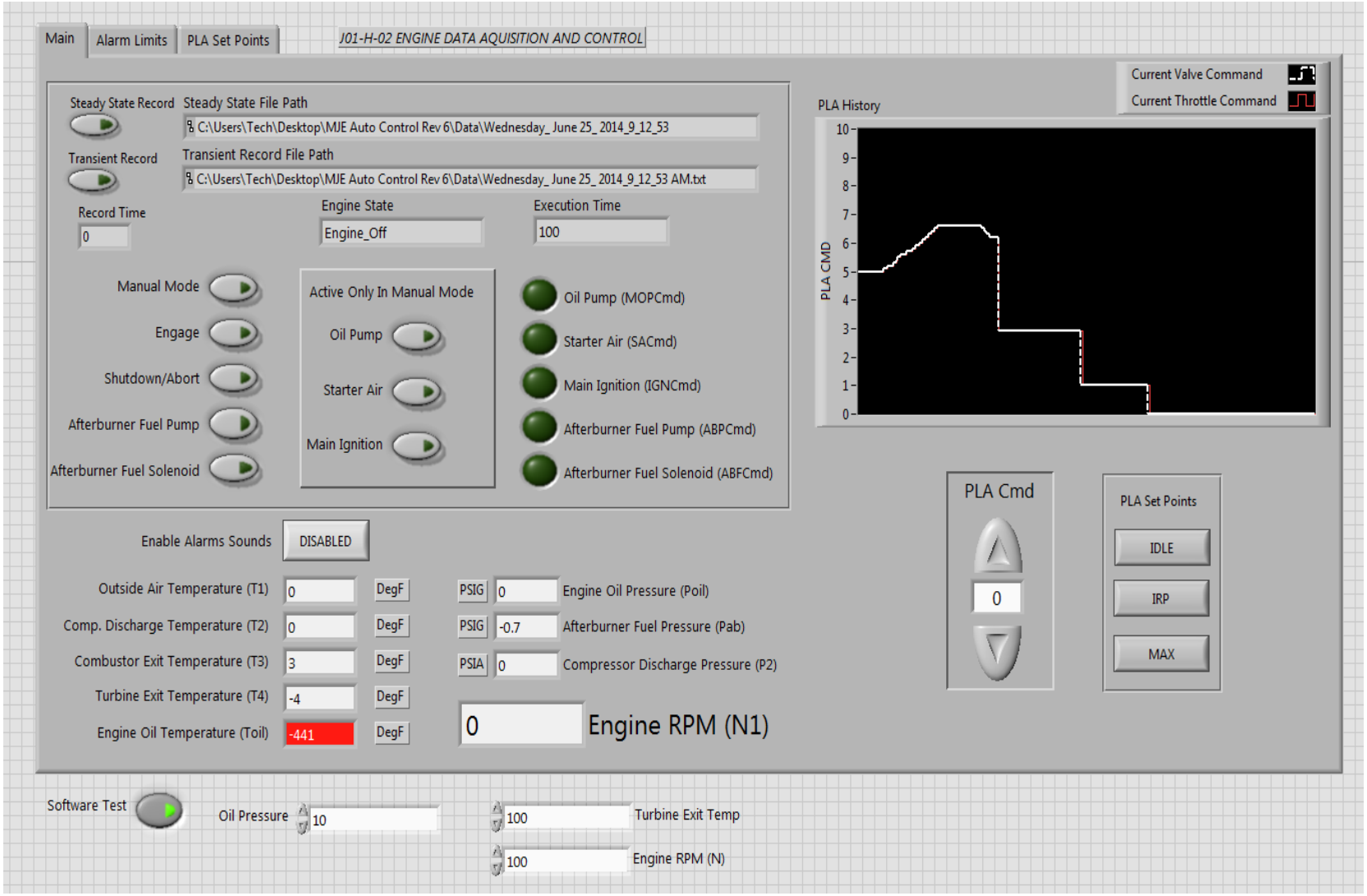

Figure 67. TECT engine data acquisition and control GUI

Description & Operation:

Run the VI

Data files are created automatically at startup. One data file records transient data for as long as the user has the “Transient Record” button depressed. The other file records steady state data at 10 second intervals each time the “Steady State Record” button is depressed. The files are located in the “Data” folder in the directory of the main LabView program. The files can be distinguished by the “_SteadyState” appended to the steady state data file. In any mode, when ready to collect data click the appropriate record button.

If the MJE is to be run in manual mode, click manual mode button and hit engage to enter Manual Mode

In manual mode, Oil Pump button, Starter Air button, and Main Ignition button become active. Afterburner Fuel Pump button, Afterburner Fuel Solenoid button and PLA Cmd are also active in manual mode and in Engine Running Mode. PLA Set Point buttons are also active so that if the user pushes the “IDLE” PLA set point, PLA Cmd will be set to “Idle Set Point” value.

If the MJE is to be run in auto mode, click engage to enter Wait for Oil Pressure mode

In Wait for Oil Pressure mode, the oil pump SSR is engaged. Once oil pressure rises to 10 psi, device will enter Engine_Air_On mode

In Engine_Air_On mode, air solenoid SSR is engaged. Once shaft rotation exceeds 7000 rpm, device will enter Main_Ignition mode

In Main_Ignition Mode, PLA Cmd is set to “Start Set Point” value, but is also active for user control (PLA Set Point buttons are also active). Once turbine exit temperature exceeds 600 F for 8 seconds, device will enter Engine Running mode

In Engine Running mode, the PLA Cmd can be manipulated to control the engine, and afterburner can be turned on.

From any mode, selecting Shutdown/Abort will start the shutdown process depending upon engine state. If engine is running or spooling, the device will enter Engine_Shutdown, Engine_Air_Off, and Engine_Off modes to safely shutdown the engine. When the MJE enters Engine_Shutdown and Engine_Off modes is controlled by “EGT Starter Air Cut Out” and “Oil Off Cut Out Speed” values.

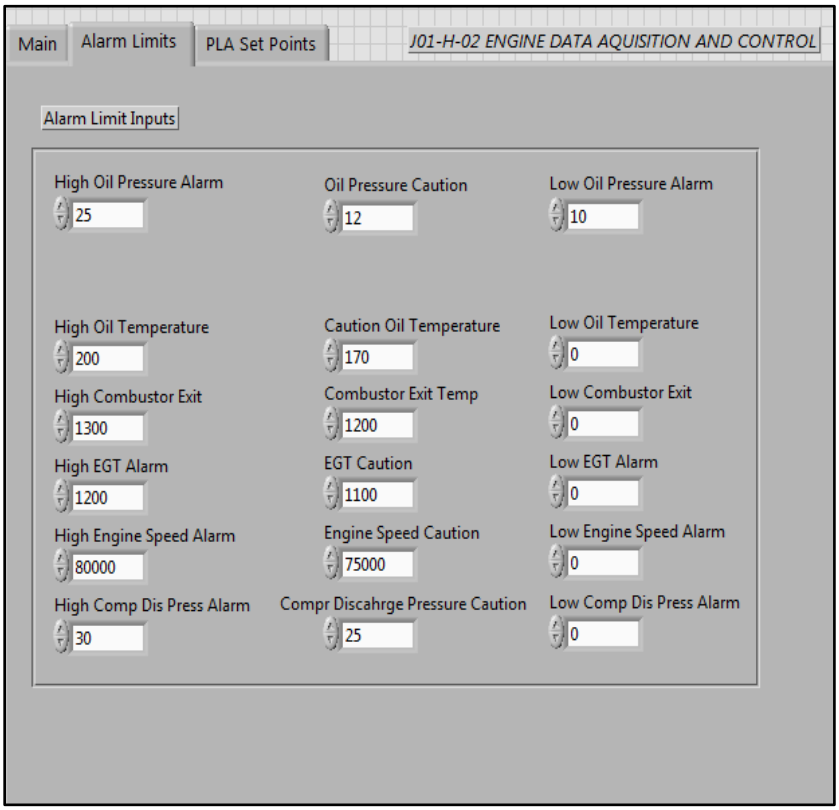

Figure 68. TECT alarm limit set points

In any mode, Alarm limits are utilized to alert the user if any parameters are out of specified limits. When alarm limits are exceeded, the corresponding front panel indicator will turn yellow if the caution limit has been exceeded and will turn red if the alarm limit has been exceeded. If alarm limits are exceeded and alarm sounds have been ENABLED on the front panel, an auditory alarm will sound.

The data packet indicators show the string of data being saved (if corresponding record buttons are depressed) to the data files.

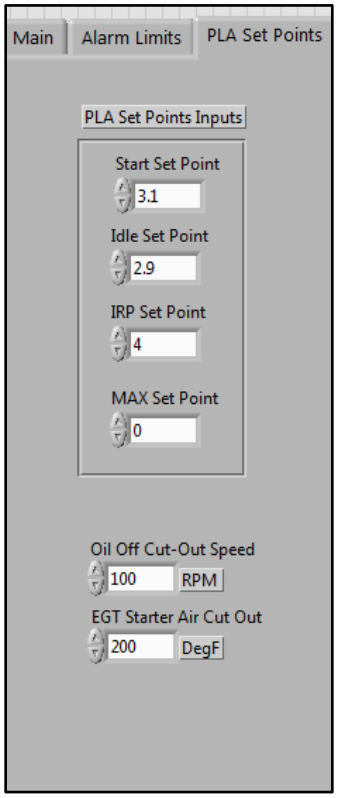

Figure 69. TECT engine PLA set points

The PLA Set Points tab contains the PLA Set Point parameters, and the “Oil Off Cut Out Speed” and “EGT Starter Air Cut Out” controls. PLA Set Point parameters determine the PLA Cmd for different engine power levels, and are active in Manual Mode and Engine_Running Mode.

“Oil Off Cut Out Speed” controls when the MJE shuts down. The control program will maintain oil pressure until the shaft rpm reaches this value.

“EGT Starter Air Cut Out” controls when the MJE transitions from Engine_Shut_Down mode to Engine_Air_Off Mode. The control program will maintain air flow to the engine until EGT temperature reaches this value.

**** The software test buttons located off of the tabbed display (shown in all of the data acquisition and control figures) are only utilized for testing and validation of control code when MJE is disconnected.**

B. MECHANISMS AND MODES OF COMBUSTION INSTABILITIES

APPENDIX B.
COMBUSTION INSTA.

C. COMBUSTOR DESIGN ANALYSIS MATLAB CODE

```
%MatLab code for mechanical design considerations of a gas turbine engine single canned
combustor
%All referenced equations can be found in Budynas, Richard Gordon., and J. Keith. Nisbett. Shigley's
Mechanical Engineering Design. 2008
%start code
clc
clear all
close all

%Thin walled pressure vessel analysis
Sy=23*10^3;       %304 SS Yield Strength @ 400F
Sut=72.0*10^3;    %304 SS Ult @400F
Ssy=0.577*Sy;     %Shear yield strength distortion-energy theory
p=65;             %Pressure inside combustor 'max'
di=5.00;          %Inside diameter (in)
t=0.060;          %thickness of material (in)
dr=3.5;           %Inner ring diameter (in)

sigmat=(p*di)/(2*t)    %Average tangential (hoop) stress (3-52)
sigmal=(p*di)/(4*t)    %Longitudinal stress (3-54)
sigmaA=(sigmat+sigmal)/2+sqrt(((sigmat-sigmal)/2)^2)   %Principle stress A (3-13)
sigmaB=(sigmat+sigmal)/2-sqrt(((sigmat-sigmal)/2)^2)   %Principle stress B (3-13)
```

```
sigmaVM=(1/sqrt(2))*((sigmaA-sigmaB)^2+(sigmaB)^2+(sigmaA)^2)^0.5   %Von Mises Stress (5-14)
VM=Sy/sigmaVM      %Factor of safety based on Von Mises
Tresca=Sy/sigmaA    %Factor of safety based on Tresca

%Weld Analysis
Aeff=pi*(di^2)/4; %Area of effective sealing diameter (in^2)
h=1/16; %Weld throat (in)
r=di/2;   %Radius of weld
A=1.414*pi*h*r  %Weld throat area (in^2)
V=Aeff*p       %Force on welds based on effective sealing diameter (lbf)
T1=V/A         %Primary shear in weld
Tall=min(0.30*Sut,0.40*Sy); %AISC code Table 9-4
N=Ssy/T1   %factor of safety against static weld

%Fatigue loading in weld
SeP=0.5*Sut;    %Endurance limit for steels (6-8)
Ssu=0.67*Sut;   %Torsional fatigue under fluctuating stresses (6-54)
ka=39.9*(Sut/1000)^-0.995;  %Surface Factor (6-19)
kb=1;       %Size factor (6-20)
kc=0.59;   %Loading Factor (6-26)
Sse=ka*kb*kc*SeP    %Marin Equation (6-18)
Kfs=2.0;     %Fatigue Stress-Concentration Factor Table 9-5
Ta=T1/2;    %Amplitude component for fluctuating stress
Tm=Ta;  %Midrange stress component for fluctuating stress
n=1/((Kfs*Ta)/Sse+(Kfs*Tm)/Ssu) %Factor of safety based on the Goodman failure criterion

%Bolt Analysis
d=0.315; %Nominal bolt diameter (in)
nb=10;    %# of bolts
ld=1/16;      %Length of useful unthreaded portion Table 8-7
lt=0.28125; %Length of useful threaded portion Table 8-7
```

```
l=3/8;     %Total grip
E=27.6*10^6;   %Youngs modulus SS 18-8 (psi) Table A-5
Sp=65*10^3;    %Proof strength of the bolts
Ad=0.0779;  %Nominal area of bolt (in^2)
At=0.0567;   %Tensile stess area (in^2) Table 8-1
Ap=pi*(3.5/2)^2;  %Effective sealing area (in^2)
P=(p*Ap)/nb;   %Load in bolt
kb=(Ad*At*E)/(ld*At+lt*Ad);    %Bolt stiffness
km=(0.5774*pi*E*d)/(2*log(5*((0.5774*l+0.5*d)/(0.5774*l+2.5*d))));  %Member stiffness 8-22
C=kb/(km+kb);  %Joint constant
Fi=0.75*At*Sp;  %Preload for non-permanent connection (8-30)
nlf=(Sp*At-Fi)/(C*P)   %Load factor (8-28)
no=Fi/(P*(1-C))  %Factor of safety against joint seperation (8-29)

%Fatigue bolt analysis
Se=18.6*10^3;  %Fully corrected endurance strength Table 8-17
Sut=100*10^3;  %Ultimate tensile strength for bolt
nf=(2*Se*(Sut*At-Fi))/(C*P*(Sut+Se)) %Factor of safety against fatigue for the goodman criterion
(8-45)
nfo=(2*Se*Sut*At)/(P*(Sut+Se))        %Factor of safety against fatigue joint seperation (8-46)
```

10 bolt design output 'English Units'

```
sigmat = 2.7083e+003
sigmal = 1.3542e+003
sigmaA = 2.7083e+003
sigmaB = 1.3542e+003
sigmaVM = 2.3455e+003
VM = 9.8061
Tresca = 8.4923
A = 0.6941
V = 1.2763e+003
```

T1 = 1.8388e+003

N = 7.2174

Sse = 1.2025e+004

n = 5.2348

nlf = 53.7312

no = 60.8979

nf = 53.1527

nfo =28.4382

5 bolt design output

sigmat = 2.7083e+003

sigmal = 1.3542e+003

sigmaA = 2.7083e+003

sigmaB = 1.3542e+003

sigmaVM = 2.3455e+003

VM = 9.8061

Tresca = 8.4923

A = 0.6941

V = 1.2763e+003

T1 = 1.8388e+003

N = 7.2174

Sse = 1.2025e+004

n = 5.2348

nlf = 26.8656

no = 30.4490

nf = 26.5764

nfo =14.2191

D. COMBUSTOR HEAT GENERATION ANSYS ANALYSIS

An electronics package filled with sensitive equipment is housed inside of a polyvinyl chloride (PVC) enclosure. This enclosure is in close proximity to a heat source because of space limitations. The heat source is a combustion chamber (combustor) for a small gas turbine engine that has a steady state temperature of 400˚C. This enclosure houses data acquisition equipment that has operating temperatures that cannot be exceeded because of maximum material temperature constraints. There is also a temperature constraint that will cause the data acquisition cards to thermally drift out calibration and report false values. Therefore it is crucial that this environment be kept below these manufactures suggested limits in order to obtain accurate data. The system is analyzed using the FEA software ANSYS. Maximum temperatures inside of the enclosure will be analyzed along with the appropriate temperature contours with the current set-up without any modifications for thermally insulting the enclosure.

Only the outer liner is under consideration for the current work as this is the only area transferring heat energy to the PVC enclosure. Temperatures inside of the combustor can reach 2000˚F (1093˚C), but since there is an air gap all the way around the combustor liner temperatures on the outer portion due not exceed 400 ˚C. The temperature vector plot is shown in Figure 70 below.

The FEA model was built in 2D to simplify the problem. This is a proper assumption as the model can be considered to be relatively symmetric and will reveal a conservative case for the true system. This approach saves time building the model as well as computational resources needed to converge on the solution of the model. The four-node bi-linear quadrilateral thermal solid element (PLANE55) was used. The model was broken up into 4 or 5 different areas with their own respective thermal conductivities depending on if an insulation or heat shield is used. The system is considered to have no heat generation outside of the combustor and assumed to be steady. Mesh sizes of course, medium, and fine were

all explored and meshed for element edge lengths of 1, 0.5, and 0.25 respectively. Mesh refinement was needed to converge to an accurate approximation.

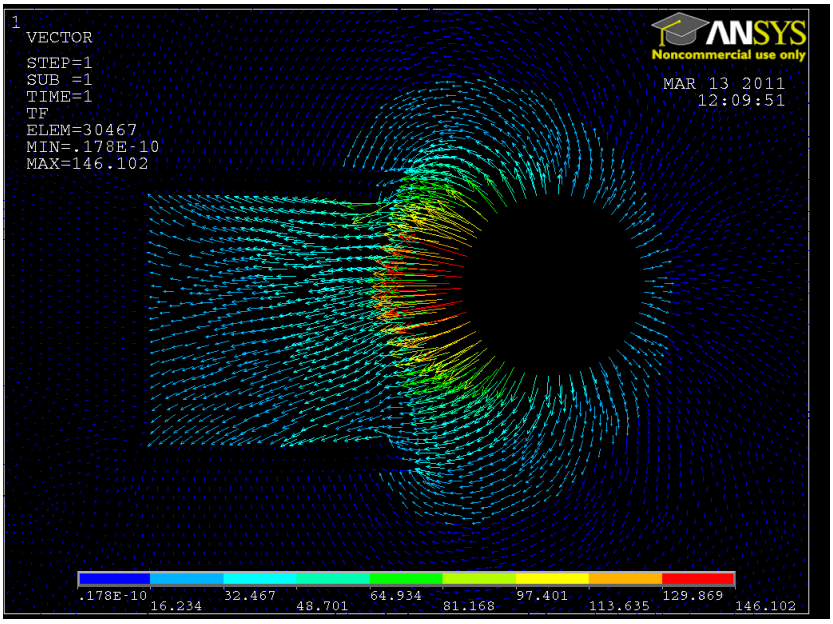

Figure 70. Temperature vector plot for the heat generation from the combustor

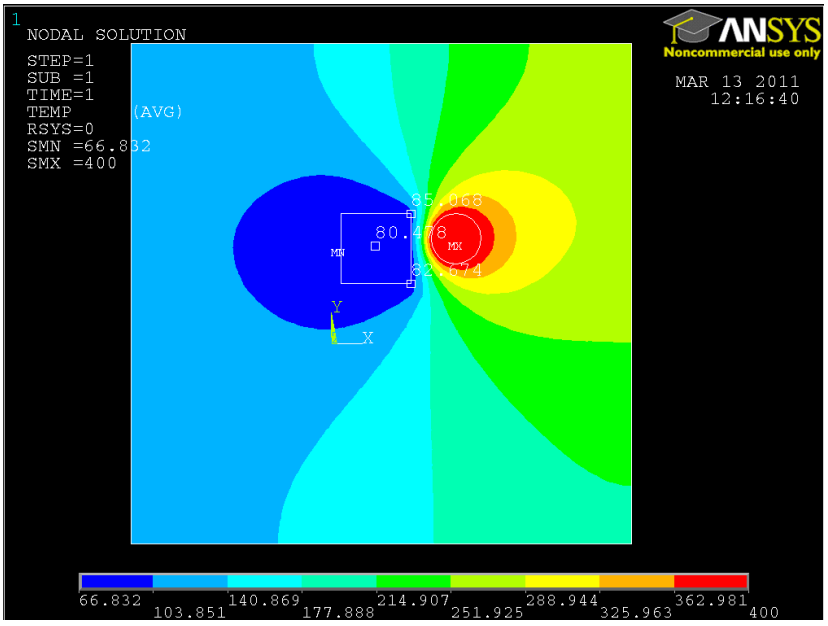

Figure 71. Temperature plot for the heat generation from the combustor medium mesh

E. TECHNICAL DATA SHEETS

Fuel/Oil Pumps

SHURflo®
First in Fluid Innovation™

PRODUCT DATA SHEET
MODEL: 8000-643-236

SPECIFICATIONS:

MODEL NUMBER: 8000-643-236
PUMP DESIGN: Positive Displacement 3 Chamber Diaphragm Pump
CAM: 3.0 Degree
MOTOR: Permanent Magnet, P/N 11-111-00
VOLTAGE: 12 VDC Nominal
PRESSURE SWITCH: Adjustable Shut-Off (Range 40-60 PSI)
Factory Set @ 60 PSI, Turn On 45 PSI ±5 PSI
LIQUID TEMPERATURE: 180 Degrees Fahrenheit (82 Degrees Centigrade) Max.
PRIME: Self-Priming Up To 11 Ft. Vertical,
PORTS: 3/8"-18 NPT Female
MATERIAL OF CONSTRUCTION:
PLASTICS- Nylon
VALVES- Buna-n
DIAPHRAGM- Geolast (Main), Buna-n (Switch)
FASTENERS- Zinc Plated Steel
NET WEIGHT: 4.1 Lbs (1.9 Kg)
DUTY CYCLE: Continuous (See Temperature Rise Chart)
TYPICAL APPLICATIONS: Agricultural Spraying

DIMENSIONS:

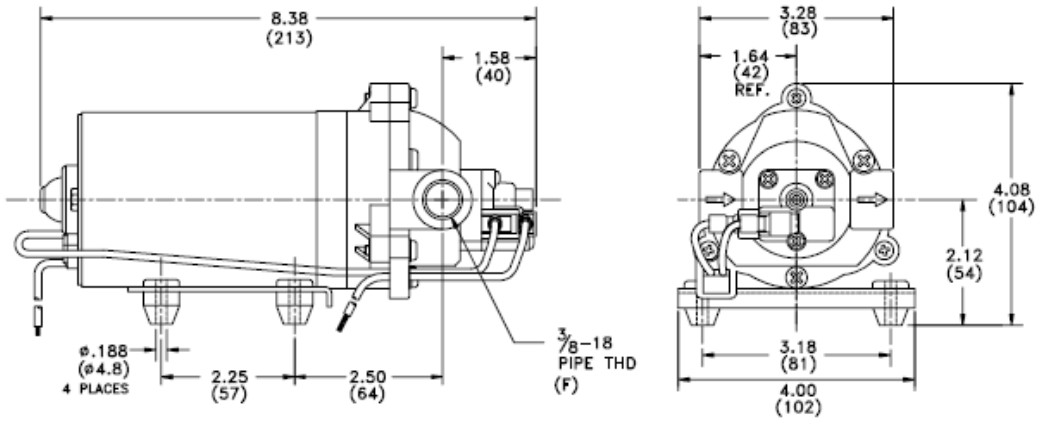

FILE # 8000-643-236 REVISED: 11/02 ISSUED: 9/20/90

MODEL: 8000-643-236

TEMPERATURE RISE

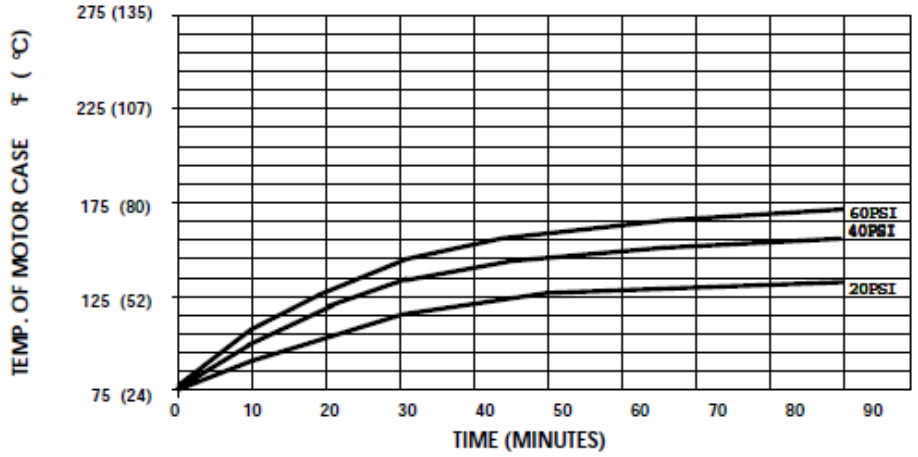

TYPICAL PERFORMANCE

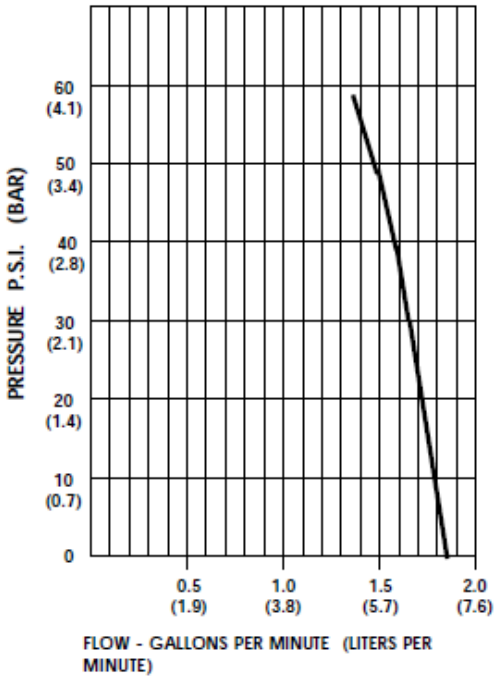

PRESSURE (PSI)	FLOW (GPM/LIT)	RPM MIN/MAX	CURRENT (AMPS)	VOLTAGE (VOLTS)
OPEN	1.8/6.8	2350/2420	2.7	12VDC
10	1.49/5.6	2280/2370	3.3	"
20	1.44/5.4	2235/2310	4.1	"
30	1.39/5.2	2175/2240	4.8	"
40	1.33/5.0	2120/2190	5.4	"
50	1.27/4.8	2075/2140	6.1	"
60	1.22/4.6	2035/2095	6.8	"

-SPECIFICATIONS SUBJECT TO CHANGE WITHOUT NOTICE.
-ALL DATA BASED ON TESTING WITH WATER AT AMBIENT TEMPERATURE.

Pressure Transducers

kulite

MINIATURE HIGH SENSITIVITY IS® PRESSURE TRANSDUCER

XCS-190 (M) SERIES

- High Output
- Silicon on Silicon Integrated Sensor **VIS®**
- High Natural Frequency

The XCS Series uses a diaphragm of advanced design which gives a substantially higher basic output allowing for high mV/psi sensitivities and improved signal to noise ratio.

OPTIONAL CONNECTOR VERSION

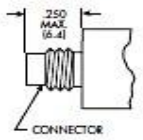

NOT AVAILABLE ON DIFFERENTIAL UNIT

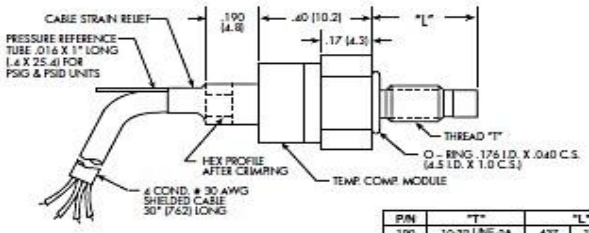

CONSULT FACTORY FOR SPECS. ON SEALED GAGE

P/N	"T"		"L"	
190	10-32 UNF-2A	.437	11.1 mm
190M	M5 x .8	.437	11.1 mm
190	10-32 UNF-2A	.760	19.3 mm
190M	M5 x .8	.760	19.3 mm

WIRING	
COLOR	DESIGNATION
RED	+ INPUT
BLACK	- INPUT
GREEN	+ OUTPUT
WHITE	- OUTPUT

INPUT Pressure Range	0.35 5	0.7 10	1.0 BAR 15 PSI
Operational Mode	Absolute, Gage, Sealed Gage, Differential		
Over Pressure	2 Times Rated Pressure With No Change In Calibration		
Burst Pressure	3 Times Rated Pressure		
Pressure Media	All Nonconductive, Noncorrosive Liquids or Gases		
Rated Electrical Excitation	10 VDC/AC		
Maximum Electrical Excitation	12 VDC/AC		
Input Impedance	1000 Ohms (Min.)		
OUTPUT Output Impedance	1000 Ohms (Nom.)		
Full Scale Output (FSO)	150 mV (Nom.) 50 mV (Nom.) for SG	150 mV (Nom.) 50 mV (Nom.) for SG	200 mV (Nom.) 100 mV (Nom.) for SG
Residual Unbalance	± 5 mV (Typ.)		
Combined Non-Linearity, Hysteresis and Repeatability	± 0.1% FSO BFSL (Typ.), ± 0.5% FSO (Max.)		
Resolution	Infinitesimal		
Natural Frequency (KHz) (Typ.)	150	175	200
Acceleration Sensitivity % FS/g Perpendicular Transverse	$1.5x10^{-3}$ $2.2x10^{-4}$	$1.0x10^{-3}$ $1.0x10^{-4}$	$7.0x10^{-4}$ $9.0x10^{-5}$
Insulation Resistance	100 Megohm Min. @ 50 VDC		
ENVIRONMENTAL Operating Temperature Range	-65°F to +350°F (-55°C to +175°C)		
Compensated Temperature Range	80°F to +180°F (25°C to +80°C) Any 100°F Range Within The Operating Range on Request		
Thermal Zero Shift	± 1% FS/100°F (Typ.)		
Thermal Sensitivity Shift	± 1% /100°F (Typ.)		
Steady Acceleration	10,000g. (Max.)		
Linear Vibration	10-20,000 Hz Sine, 100g. (Max.)		
PHYSICAL Electrical Connection	4 Conductor 30 AWG Shielded Cable 30" Long		
Weight	4 Grams (Nom.) Excluding Module and Leads		
Pressure Sensing Principle	Fully Active Four Arm Wheatstone Bridge Dielectrically Isolated Silicon on Silicon		
Mounting Torque	15 Inch-Pounds (Max.)		

Note: Custom pressure ranges, accuracies and mechanical configurations available. Dimensions are in inches. Dimensions in parenthesis are in millimeters.
Continuous development and refinement of our products may result in specification changes without notice - all dimensions nominal. (F)

KULITE SEMICONDUCTOR PRODUCTS, INC. • One Willow Tree Road • Leonia, New Jersey 07605 • Tel: 201 461-0900 • Fax: 201 461-0990 • http://www.kulite.com

Optical Laser Sensor

ROLS - Remote Optical Laser Sensor

SAFEGUARDS AND PRECAUTIONS:

WARNING – Class 2 laser product – This product emits a visible beam of laser light. Avoid exposure to the laser radiation. The use of optical viewing aids (binoculars, for example) may increase the ocular hazard.
CAUTION – The laser beam should not be intentionally aimed at people or animals.
CAUTION – Use of controls or adjustments or performance of procedures other than those specified herein may result in hazardous radiation exposure.

Read and follow all instructions in this instruction sheet carefully, and retain this sheet for future reference.
Do not use this instrument in any manner inconsistent with these operating instructions or under any conditions that exceed the environmental specifications stated.
This instrument is not user serviceable. For technical assistance, contact the sales organization from which you purchased the product.

DESCRIPTION:

The Remote Optical Laser Sensor has a visible red laser light source and green LED on-target indicator. The class 2 laser source acts as the aiming device during setup and can accurately measure speeds from 1-250,000 RPM from a distance of up to 25 feet with a maximum offset angle of 60 degrees from the rotating object. The sensor is housed in a threaded 303 stainless steel tube and supplied with a 90 degree mounting bracket, jam nuts and an eight foot shielded cable. ROLS-P comes with a 3.5mm (1/8") male stereo plug adapter. ROLS-W comes with 4 tinned wires.

SPECIFICATIONS:

Speed Range:	1-250,000 RPM
Illumination:	Visible Red Laser, Class 2
Laser Specifications:	**Classification:** Class 2 (per IEC 60825-1 Ed 1.2 2001-8)
	Complies with FDA performance standards for laser products except for deviations pursuant to Laser Notice No. 50, dated July 26, 2001.
	Maximum Laser Output: 1mW
	Pulse Duration: Continuous
	Laser Wavelength: 650 nm
	Beam Divergence: <1.5 mrad
	Beam Diameter: 4 x 7 mm typical at 2 meters
	Laser Diode Life: 8,000 operating hours MTBF (1 year warranty)
On-Target Indicator:	Green LED on wire end cap
Operating Range:	up to 25 feet [7.6 m] and 60 degrees offset from target
Power Requirement:	3.0 - 24 Vdc, 0.13W
Output:	Positive pulse when target present – Output Voltage=Supply Voltage Optional – Open Collector or TTL pulse, Negative pulse (Contact factory)
Operating Temp.:	14 °F to 158° F [-10 °C to 70° C]
Humidity:	Maximum relative humidity 80% for temperature up to 88 °F [31 °C] decreasing linearly to 50% relative humidity at 104 °F [40 °C]
Connection:	3.5 mm [1/8 inch] male stereo plug (ROLS-P) or Tinned wires (ROLS-W)
Cable Length:	8 feet [2.4 m]
Material:	303 Stainless Steel supplied with two M18 Jam Nuts and Mounting Bracket
Lens:	Acrylic Plastic
Dimensions:	Threaded Tube 3.12 in x 0.71 in diameter [M18 x 1.5 x 79.4 mm] long

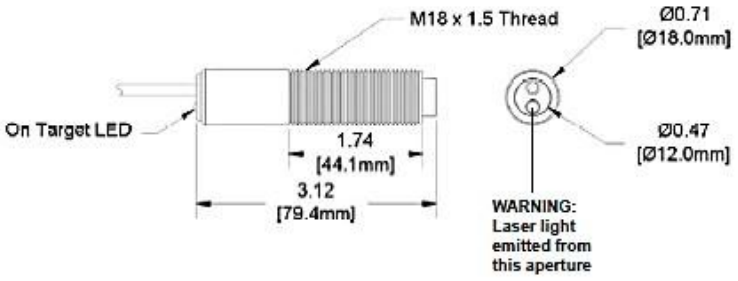

Signal Conditioning

AUBER INSTRUMENTS WWW.AUBERINS.COM

Instruction Manual

SYL-1812XA Thermometer/Pyrometer

A. Specifications

- ◆Power supply: DC12V (isolated)
- ◆Power consumption: <2W
- ◆Sampling rate: 4 samples/sec
- ◆Accuracy: 0.2% full scale ±1
- ◆Display range: -1999~9999
- ◆Relay contact rating: 3A @ 220VAC
- ◆Retransmit open-circuit voltage: 15V
- ◆Outside dimensions: 48×24×75mm
- ◆Mounting cutout dimension: 45×22mm
- ◆LED display: 0.28" red color
- ◆Working condition: 0~50℃, ≤85%RH

B. Front Panel

① Alarm and relay J1 indicator
② Up key
③ Shift key
④ Set key
⑤ Maximum and Minimum value indicator
⑥ Display window

1.AL on indicates alarm is on and J1 relay is pulled in (closed).

2.MAX(MIN) on when Display window shows the maximum value or the time of the Max. MAX(MIN) blinking when Display window shows the minimum value or the time of Min.

3. ">" shift key: In the parameter setting mode, press this key to select the digit to be changed. In the normal operation mode, press this key to change the display in the sequence as shown in the diagram below.

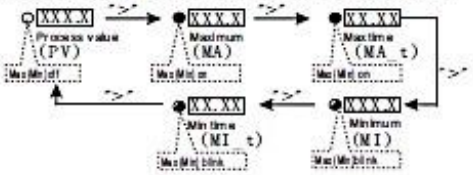

4."^" up key . In the parameter setting mode, press it to increase the displayed value. When displaying Max/Min, press and hold it for 3 seconds to clear the Max/Min stored. In normal function, this key has two functions, show operation time and change display brightness. Press and hold it down to show the operation time since on. Release the key to show the current temperature (process value). Each time the key is pressed, the display brightness will also be changed from bright to dim or from dim to bright.

C. Parameter Setting

1,Basic Parameter (Press ↵ then input code 0089 to enter)

a) Basic Parameters description

Symbol		Description	Setting range	Initial	Note
InPu	Inty	Input Type	See Table 1	P	
PuL	PuL	Input low limit	-1999~9999	0	4
PuH	PuH	Input high limit	-1999~9999	1000	4
dot	dot	Decimal point	0000~0.000	0.000	4
PSb	PSb	Zero offset	-1000~1000	0	1
PSbF	PSbF	Range coefficient	0.500~2.000	1.000	2
CorF	CorF	Temperature unit	C: °C F: °F	F	
FILt	FILt	Digital filter	0~3	0	3
End	End	Exit			

Note 1, for correcting the offset at zero: Display=measurement+PSb
Note 2, for correcting the error at Max: Display=measurement x PSbF
Note 3, Digital filter. 0=no filter. 1 weak, 2, medium, 3 strong.
Note 4, These parameters do not apply to temperature sensors.

【Table 1】 Input type options

Symbol	Input type	Range	Res.	Accy.	Impedance
t	TC, Type T	-200~400°C	1°C/F	0.3%	100K
r	TC, Type R	-50~1600°C	1°C/F	0.3%	100K
J	TC, Type J	-200~1200°C	1°C/F	0.2%	100K
WrE	TC, WRe3-WRe25	0~2300°C	1°C/F	0.2%	100K
b	TC, Type B	350~1800°C	1°C/F	0.3%	100K
S	TC, Type S	-50~1600°C	1°C/F	0.3%	100K
P	TC, Type K	-200~1300°C	1°C/F	0.2%	100K
E	TC, Type E	-200~900°C	1°C/F	0.2%	100K
Pt00	RTD, Pt100	-199.9~600.0°C	0.1°C/F	0.2%	(0.2mA)
Cu50	RTD, Cu50	-50.0~150.0°C	0.1°C/F	0.5%	(0.2mA)
375r	0-375Ω Pressure	Display range can be set in -1999~9999	16bit A/D	0.2%	(0.2mA)
75mV	0-75mV Current			0.1%	100K
30mV	0-30mV			0.1%	100K
5V	0-5 V			0.1%	100K
1-5V	1-5 V			0.1%	100K
10V	1-10V			0.1%	100K
10mA	0-10 mA			0.3%	150Ω
20mA	0-20 mA			0.2%	150Ω
4-20	4-20 mA			0.2%	150Ω

(TC, thermocouple sensor)

B)Basic Parameter setting (See【Fig3】)

2, Alarm Parameter (Press ↵ then input code 0001 to enter)

a) Alarm Parameters description

Symbol	Name	Description	Range	Initial	Note
AH1	AH1	J1 pull in Value	-1999~9999	900	4
AL1	AL1	J1 drop out value	-199~9999	800	
AH2	AH2	J2 pull in Value	-1999~9999	900	
AL2	AH2	J2 drop out Value	-1999~9999	800	
End	End	Exit			

2008. 03 P1/2

b) Alarm Parameter setting is similar to the Basic Parameters setting in Fig. 3 except access code is 0001 instead of 0089.

Note 4. Relay action setting (SYL-1812 does not contain J2 relay. Its setting (AH2, AL2) can be ignored).

1) Set AH 1=AL1, relay is disabled.

2) Set AH 1>AL1, relay is for high limit alarm. See Fig. 1

3) Set AH 1<AL1, relay is for low limit alarm. See Fig. 2.

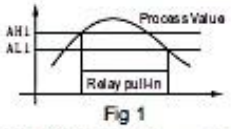

Fig 1

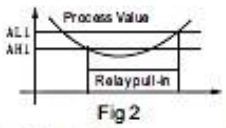

Fig 2

【Fig 3】 Basic Parameter setting flow chart:

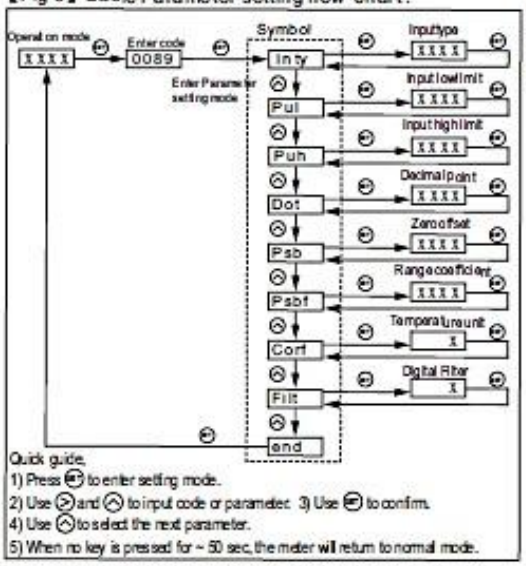

3. Peak Value (Press, then input code 0037 to enter)

a) Peak value description

Symbol	Name	Description	Range	Initial	Note
MA	MA	Maximum value	on/oFF	on	5
MA-t	MA-t	Time of maximum	on/oFF	oFF	
MI	MI	Minimum value	on/oFF	oFF	
MI-t	MI-t	Time of minimum	on/oFF	oFF	
End	End	End			

Note 5, Peak function is interlocked.

1) When MA is turned off, MA-t can't be set.

2) When MI is turned off, MI-t can't be set.

b) Peak Value setting is similar to the Basic Parameters setting in Fig. 3 except access code is 0037 instead of 0089.

c) Reset the peak value

The peak values is stored in the memory even the meter is powered off. To reset them, change display to show MA, MA-t, MI or MI-t. Then, press and hold "Λ" key for 3 seconds. The display will show "----", indicating the memory (for all four parameters) is reset. The meter will start to catch the new peak after 2 seconds.

4. Retransmit (Press, then input code 0036 to enter)

a) Retransmit parameters description

Symbol	Name	Description	Range	Initial	Note
obty	obty	Output type	0-20/4-20 mA	4-20	6
obL	obL	output low limit	-1999-9999	000.0	7
obH	obH	output High limit	-1999-9999	100.0	8
End	End	Exit			

b) Retransmit (analog output) parameter setting is similar to the Basic Parameters setting in Fig. 3 except access code is 0036 instead of 0089.

Note. 6, Output type selection. User can select either 0-20 mA or 4-20 mA.

Note 7. Output lower limit. The LED display value when output is at 0 mA or 4 mA. e.g. If you want 100 C to output 0 mA, set obL=100

Note 8, Output high limit. The LED display value when output is at 20 mA. e.g. If you want 1000 C to output 20 mA, set obH= 1000. This number will affect the resolution of the signal.

D. Terminal assignment

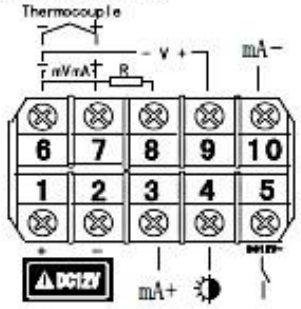

1) 1 and 2 are for power input

2) 2 and 5 are for alarm relay output. When alarm is turned on, 2 and 5 is connected. To drive a 12 V buzzard, connect one lead of the buzzard to the +12V. Connect the other lead to terminal 5.

3) 4 is for display brightness control. When connecting the illumination signal (+12 V) to it, the brightness with synchronized with headlight. If not connected, the brightness can still be controlled by "Λ" up key.

4) 6, 7, 8 and 9 are for different types of signal input. Use 6 and 7 for thermocouple input. Use 6,7 and 8 for RTD sensor input. Use 6 and 9 for pressure sensor.

5) 3 and 10 is for retransmit (analog output). To change the output from current to a voltage, install a 1% precision resistor between terminal 3 and 10. With a 250Ω Resistor, 1 ~ 5V, 0 ~ 5V output can be obtained. With 500Ω resistor, 2-10V or 0 ~ 10V output can be obtained.

E. Application examples

1) Exhaust Gas Temperature (EGT) measurement

The meter is preset for the EGT application. Wire the meter as the diagram below. It is ready to run.

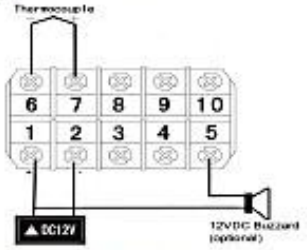

Auber Instruments

730 Culworth Manor, Alpharetta, GA 30022 USA www.auberins.com

Tel 770-569-8420 info@auberins.com

Data Acquisition Cards

NI USB-6008

12-Bit, 10 kS/s Low-Cost Multifunction DAQ

- 8 analog inputs (12-bit, 10 kS/s)
- 2 analog outputs (12-bit, 150 S/s); 12 digital I/O; 32-bit counter
- Bus-powered for high mobility; built-in signal connectivity
- OEM version available
- Compatible with LabVIEW, LabWindows™/CVI

Overview

The NI USB-6008 provides basic DAQ functionality for applications such as simple data logging, portable measurements, and academic lab experiments. It is affordable for student use but powerful enough for more sophisticated measurement applications. Use the USB-6008 with the included ready-to-run data logger software to begin taking basic measurements in minutes, or program it using NI LabVIEW or C and the included NI-DAQmx Base measurement services software for a custom measurement system.

To supplement simulation, measurement, and automation theory courses with practical experiments, NI developed a USB-6008 Student Kit that includes a copy of LabVIEW Student Edition. These kits are exclusively for students, giving them a powerful, low-cost, hands-on learning tool. Visit the NI academic products page for more details.

For faster sampling, more accurate measurements, calibration support, and higher channel counts, consider the NI USB-6210 and NI USB-6211 high-performance USB DAQ devices.

USB DAQ devices are compatible with the following versions (or later) of NI application software: LabVIEW 7.x, LabWindows/CVI 7.x, or Measurement Studio 7.x. USB DAQ modules are also compatible with Visual Studio .NET, C/C++, and Visual Basic 6.0.

Specifications

Specifications Documents

- Specifications (2)
- Data Sheet

Specifications Summary

General	
Product Name	USB-6008
Product Family	Multifunction Data Acquisition
Form Factor	USB
Part Number	779051-01
Operating System/Target	Linux , Mac OS , Pocket PC , Windows
DAQ Product Family	B Series
Measurement Type	Voltage
Isolation Type	None
RoHS Compliant	Yes
USB Power	Bus-Powered
Analog Input	
Channels	4 , 8
Single-Ended Channels	8
Differential Channels	4
Resolution	12 bits
Sample Rate	10 kS/s
Throughput (All Channels)	10 kS/s
Max Voltage	10 V
Maximum Voltage Range	-10 V , 10 V
Maximum Voltage Range Accuracy	138 mV
Minimum Voltage Range	-1 V , 1 V
Minimum Voltage Range Accuracy	37.5 mV
Number of Ranges	8

Simultaneous Sampling	No
On-Board Memory	512 B
Analog Output	
Channels	2
Resolution	12 bits
Max Voltage	5 V
Maximum Voltage Range	0 V , 5 V
Maximum Voltage Range Accuracy	7 mV
Minimum Voltage Range	0 V , 5 V
Minimum Voltage Range Accuracy	7 mV
Update Rate	150 S/s
Current Drive Single	5 mA
Current Drive All	10 mA
Digital I/O	
Bidirectional Channels	12
Input-Only Channels	0
Output-Only Channels	0
Timing	Software
Logic Levels	TTL
Input Current Flow	Sourcing , Sinking
Output Current Flow	Sinking , Sourcing
Programmable Input Filters	No
Supports Programmable Power-Up States?	No
Current Drive Single	8.5 mA
Current Drive All	102 mA
Watchdog Timer	No
Supports Handshaking I/O?	No
Supports Pattern I/O?	No

Maximum Input Range	0 V , 5 V
Maximum Output Range	0 V , 5 V
Counter/Timers	
Counters	1
Buffered Operations	No
Debouncing/Glitch Removal	No
GPS Synchronization	No
Maximum Range	0 V , 5 V
Max Source Frequency	5 MHz
Pulse Generation	No
Resolution	32 bits
Timebase Stability	50 ppm
Logic Levels	TTL
Physical Specifications	
Length	8.51 cm
Width	8.18 cm
Height	2.31 cm
I/O Connector	Screw terminals
Timing/Triggering/Synchronization	
Triggering	Digital
Synchronization Bus (RTSI)	No

Temperature Measurement

RTD Sensor Specifications:

This Air intake sensor features high accuracy and fast response time in the air because of its thin RTD sensor tip. When connected with Auber automobile multimeter gauges, it can provide less than one degree accuracy. The sensor comes with threaded adaptor and compression fitting. It allows a high pressure air tight seal and adjustable probe length that can be mounted on a broad range of vehicles. Four mounting options are offered, 1/8" NPT (most common), weld-in, 1/4" BSP, M8 x1 and M10x1. Please select the mounting type from the dropdown menu when ordering.

Specifications.

Sensor type, Pt100 RTD with three wires connection.

Cable length, 78" (2 meters)

Probe diameter. Tip 0.079" (2 mm), body 3/16" (0.187" or 4.8 mm)

Mounting adaptor: 1/8" NPT, weld-in, 1/4" BSPT, M10x1 and M8.

Max insertion depth: 1.35" (35 mm)

Compression fitting thread 3/8"-24

Maximum working temperature: 200 °C (400 °F)

Type K Thermocouple Specifications:

Product Description:

This EGT probe is the most durable type we offer. It is made of K type grounded thermocouple with a thin and sealed tip. The thin and sealed EGT probe design is widely used for aircraft application because its durability. It is also very popular in Europe. The tip of this probe is made of Inconel 600 alloy that provides the highest working temperature available for this type of sensor. The diameter of the probe is optimized to balance the requirement of mechanical stability and the response time.

This probe can also be used for air intake temperature measurement due to its small thermal mass.

Five types of mounting adaptor are offered. 1/8" NPT, Weld-in Stainless Steel (SS), M10x1, M8x1 or 1/4" BSP thread. Please make the selection at the "Mounting Type Option" box above.

Specification

K type thermocouple, grounded

Cable length, 78" (2 meters)

Probe diameter. 3.0 mm

Max insertion depth: 1.35" (35 mm)

Compression fitting thread 3/8"-24

Maximum working temperature: 1100C (2000F)

Augmentor Nozzles Technical Data

Table 16. Augmentor nozzles flow curve data

HAGO 416 SS AB Fuel Nozzles								
M5 nozzle rated flow @100 psi (gph)				5	Density of JP4 @60 degF(lbm/gal)	6.55	Total # of nozzles	3
Data	Pressure (psig)	Flow rate (gph)	flow rate (gpm)	flow rate curve fit (gph)	flow rate curve fit (gpm)	Total Flow Rate (gpm)	Total Flow Rate (gph)	Total Flow Rate (lbm/hr)
Extrapolated	5			1.12	0.01863	0.0559	3.354	21.97
Extrapolated	10			1.58	0.02635	0.0791	4.743	31.07
Extrapolated	20			2.24	0.03727	0.1118	6.708	43.94
Extrapolated	30			2.74	0.04564	0.1369	8.216	53.81
Empirical	40	3.16	0.05267	3.16	0.05270	0.1581	9.487	62.14
Empirical	60	3.87	0.06450	3.87	0.06455	0.1936	11.619	76.10
Empirical	80	4.47	0.07450	4.47	0.07454	0.2236	13.416	87.88
Empirical	100	5	0.08333	5.00	0.08333	0.2500	15.000	98.25
Empirical	200	7.07	0.11783	7.07	0.11785	0.3536	21.213	138.95
Empirical	300	8.66	0.14433	8.66	0.14434	0.4330	25.981	170.17
Empirical	500	11.18	0.18633	11.18	0.18634	0.5590	33.541	219.69

TECHNICAL DATA SHEET

Fine Atomizing Water Spray Nozzles — TYPE "M" & TYPE 'MW" MINI NOZZLES

Our unique Mini nozzles are the perfect solution where small size, accurate flow rates, very fine atomization and low cost are desired. Hago Mini nozzles are widely used in both professional and home green houses for plant and seedling misting, in industry for process cooling or humidifying and in agriculture for livestock cooling. In recent years they have been used in dry climates for home patio cooling.

TYPE "M" MINI NOZZLE FEATURES:

Applications:
- Misting, cooling, humidifying
- Spraying light oils, insecticides, and waxes

Materials:
- Brass
- 416 Stainless steel
- Nickel Silver (optional - see reverse)

Construction:
- Integral 120 mesh stainer
- Unique design allows easy cleaning and maintenance.
- Shipped with protective plastic cap
- Individual spray testing assures quality
- 1/8" male NPT

Spray Angles/Pattern:
- Standard spray angle is 80˚ @ 100 PSI water pressure.
- Spray pattern: Solid (full) cone

TYPE "MW" WIDE ANGLE MINI NOZZLE FEATURES:

"MW" designates "Wide Angle" and provides a very fine atomization in low volume flow rates with a wide spray angle and large coverage area..

Applications:
- Same as the "M" nozzle

Materials/Construction:
- Same as the "M" nozzle

Spray Angles/Pattern:
- Standard spray angle is 160˚ @ 100 PSI water pressure
- Spray pattern: Hollow cone

ORDERING INFORMATION:
Parts numbers on both nozzles represent the flow rate in gallons per hour (GPH) @ 100 PSI water pressure.
Examples:
M4 = 4.00 GPH @ 100 psi
MW5 = 5.00 GPH Wide Angle @ 100 psi

FLOW CHARTS, DROPLET SIZE INFORMATION AND CORROSION RESISTANCE CHART ON REVERSE SIDE

TYPE 'M'

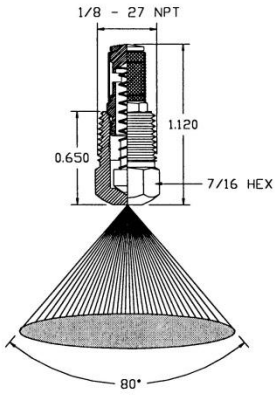

TYPE "MW"

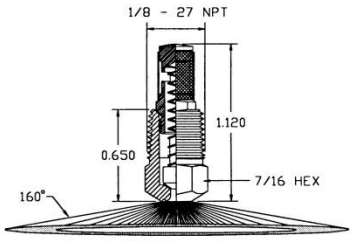

Hago Manufacturing Co., Inc.
1120 Globe Avenue Mountainside, NJ USA 07092
Tel 908.232.8687 • Fax 908.232.7246 • Sales 1.800.710.HAGO
E-Mail: sales@hagonozzles.com • www.hagonozzles.com

TYPE "M" & "MW" MINI NOZZLES

Flow rates at various operating pressures.
{gallons per hour (GPH)}

Nozzle size	40 psi	60 psi	80 psi	100 psi	200 psi	300 psi	500 psi
M1	0.63	0.77	0.89	1.00	1.41	1.73	2.24
M2	1.26	1.55	1.79	2.00	2.83	3.46	4.47
M3	1.90	2.32	2.68	3.00	4.24	5.20	6.71
M4	2.53	3.10	3.58	4.00	5.66	6.93	8.94
M5	3.16	3.87	4.47	5.00	7.07	8.66	11.18
M10	6.32	7.75	8.94	10.00	14.14	17.32	22.36
M15	9.49	11.62	13.42	15.00	21.21	25.98	33.54
MW5	3.16	3.87	4.47	5.00	7.07	8.66	11.18
MW7	4.43	5.42	6.26	7.00	9.90	12.12	15.65
MW11	6.96	8.52	9.84	11.00	15.56	19.05	24.60
MW15	9.49	11.62	13.42	15.00	21.21	25.98	33.54

Sauter Mean Diameter at various operating pressures.
microns (µm)

Nozzle size	40 psi	60 psi	80 psi	100 psi	200 psi	300 psi	500 psi
M1	39.4	34.1	30.3	28.4	22.6	20.7	17.4
M2	39.1	34.4	32.0	30.3	25.8	21.7	18.7
M3	39.5	35.9	34.8	32.4	25.5	22.4	18.3
M4	42.5	40.1	37.7	35.5	27.5	23.2	18.8
M5	45.2	38.8	35.5	33.7	29.3	24.6	19.3
M10	51.3	44.6	41.4	39.6	33.5	28.3	22.8
M15	65.7	61.5	58.4	55.0	38.6	31.9	23.9
MW5	50.4	46.7	44.1	41.7	29.7	24.0	17.4
MW7	54.7	54.9	51.0	48.3	33.1	28.7	20.3
MW11	64.9	63.1	55.3	55.8	47.4	38.4	28.3
MW15	76.4	65.3	60.2	55.8	50.0	40.8	29.3

Pressure vs. Flow
For general purposes, changes in flow rate due to changes in pressure can be estimated as being approximately equal to the square root of the pressure ratio. Therefore: Flow rate @ the desired pressure = RATED FLOW @ 100 PSI* $\sqrt{\frac{\text{DESIRED PRESSURE}}{100}}$

Or....$F_2 = F_R * \sqrt{\frac{P_2}{P_R}}$

Example: To determine the flow rate of a 2.00 gph nozzle @ 300 psi, multiply 2.00 time the square root of 300/100.....

OR 2.00* $\sqrt{\frac{300}{100}}$

The flow rate would be about 3.50 gph.

MATERIALS

Brass - Our "standard" material of construction. Supplied unless otherwise specified. Acceptable for most passive water applications.

Type 416 stainless steel - A high chrome grade of stainless steel that is rust resistant, but not absolutely rust proof. Good resistance to erosion at higher water pressures. Medium corrosion resistance. Works well; in water pressures. Medium corrosion resistance. Works well in water with high mineral content.

Nickel Silver - Our best grade of material. Nickel Silver is a trade name for a non-magnetic, nickel copper alloy that has become very popular due to its corrosion resistance which is comparable to Type 316 stainless steel. Reasonably priced due to its machinability.

HAGO PRECISION SPRAY NOZZLES
100% Tested 100% Guaranteed
100% Stainless Steel

Droplet sizes: Given in microns (µm)

Test Apparatus: MUNHALL PSA - 32 particle size analyzer which measures drops based on Fraunhofer's Diffraction Principle.

Verification: All tests are verified using a photomask test reticle which contains a known distribution of droplets per ASTM draft photomask / reticle method.

CHEMICAL	CONCENTRATION	TEMP (°F)	RATING
Acetic Acid	2.50%	70	A
Alcohols			A
Ammonia, Dry gas			B
Ammonium Chloride (solutions)		85	B
Bleach		70	B
Boric Acid		all	A
Chlorine, Dry gas		all	B
Chromic Acid	5%		
Citric Acid			A
Gasoline, Crude			A
Hydrochloric Acid	0.50%	70	A
Hydrochloric Acid	65%	70	A
Hydrofluoric Acid (anhydrous and solutions)	all	140/180	
Hydrogen peroxide		70	A
Lactic Acid	all	70	B
Mineral Oils			A
Saline (mist/gas)		all	A
Sodium Chloride	all	all	A
Sulfuric Acid	pure	70	B
Sulfuric Acid	3%	70	A
Water, Brine (extreme salt)			A

A=Very Good B=Good C=Fair D=Not Recommended

Posiflow® Proportional Solenoid Valves

Brass or Stainless Steel Bodies
1/4" to 1/2" NPT

2/2 SERIES 8202/8203 Proportional Valves

Features

- Flow rates adjustable between 0% and 100% of rating
- Flow rate can also be regulated by a range of electrical inputs (sensors, transmitters, PLC, etc.) via an ASCO Electronic Control Unit or similar circuit
- Suitable for use in air/gas, low vacuum service, as well as to precisely control flow of water

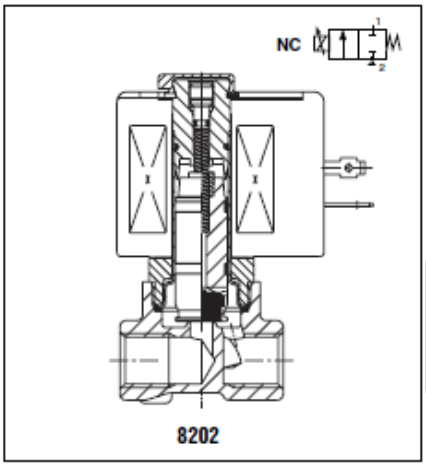

8202

Construction

Valve Parts In Contact with Fluids			
	8202		8203
Body	Brass	303 Stainless Steel	Brass
Seals and Disc/Diaphragm*	FKM		NBR
Core Tube	305 Stainless Steel		
Core and Plugnut	430F Stainless Steel		
Springs	302 Stainless Steel		
Rider Rings	PTFE		
Breaker Piece	Brass	303 Stainless Steel	Brass

Electrical

Standard voltage: 24 VDC
Coil: Molded Class F
Coil resistance: 25 Ohm at 68°F (20°C)
Operating current: 100 - 500 mA
Recommended PWM frequency: 300 Hz Air/Gas; 200 Hz Water/Light Oil
Hysteresis: <5% (<7.5% for 8203 Valves) ①
Repeatability: <3% (<1% for 1/8" NPT Valves) ①
Sensitivity: <2% (<1% for 1/8" NPT Valves) ①
① Based on ASCO Electronic Control Unit at constant differential pressure.

Solenoid Enclosures

Standard: RedHat II Class F coil with DIN connection (meets ISO 4400/DIN 43650A standards). For 22.6 watt solenoids.
Optional: For Class H coil, use prefix "SV" (for use with customer supplied electronics): General Purpose and Watertight, Types 1, 2, 3, 3S, and 4X on 22.6 watt solenoids.

Nominal Ambient Temp. Ranges

14°F to 104°F (-10°C to 40°C) for 22.6 watt solenoid.

Approvals (8202 1/4" to 3/8" only)

UL Recognized Component with DIN solenoid (prefix SD or SV).
UL Listed with threaded conduit (no prefix)
CSA certified.
Note: The Electronic Control Unit (sold separately) is only compatible with DIN connectors

SPECIAL SERVICE VALVES

ASCO®

Specifications (English units)

Pipe Size (Ins.)	Orifice Size (Ins.)	Cv Flow Factor	Operating Pressure Differential (psi) Min.	Max. Low Vacuum (Hg) ①	Max. Air/Gas/ Water/Oil	Max. Fluid Temp.°F	Catalog Number Air-Inert Gas	Catalog Number Water/Light Oil	UL ② Listing	Const. Ref.	Watt Rating/ Class of Coil Insulation ③
Brass Body											
1/4	3/64	.06	0	29	230	150	SD8202G001V	SD8202G051V	●	1	22.6/F
1/4	3/32	.14	0	29	115	150	SD8202G002V	SD8202G052V	●	1	22.6/F
1/4	1/8	.28	0	29	60	150	SD8202G003V	SD8202G053V	●	1	22.6/F
1/4	5/32	.50	0	29	35	150	SD8202G004V	SD8202G054V	●	1	22.6/F
1/4	7/32	.85	0	29	20	150	SD8202G006V	SD8202G056V	●	1	22.6/F
1/4	9/32	1.1	0	29	15	150	SD8202G007V	SD8202G057V	●	1	22.6/F
3/8	1/8	.28	0	29	60	150	SD8202G023V	SD8202G073V	●	2	22.6/F
3/8	5/32	.50	0	29	35	150	SD8202G024V	SD8202G074V	●	2	22.6/F
3/8	7/32	.85	0	29	20	150	SD8202G026V	SD8202G076V	●	2	22.6/F
3/8	9/32	1.1	0	29	15	150	SD8202G027V	SD8202G077V	●	2	22.6/F
Stainless Steel Body											
1/4	3/64	.06	0	29	230	150	SD8202G011V	SD8202G061V	●	3	22.6/F
1/4	3/32	.14	0	29	115	150	SD8202G012V	SD8202G062V	●	3	22.6/F
1/4	1/8	.28	0	29	60	150	SD8202G013V	SD8202G063V	●	3	22.6/F
1/4	5/32	.50	0	29	35	150	SD8202G014V	SD8202G064V	●	3	22.6/F
1/4	7/32	.85	0	29	20	150	SD8202G016V	SD8202G066V	●	3	22.6/F
1/4	9/32	1.1	0	29	15	150	SD8202G017V	SD8202G067V	●	3	22.6/F
3/8	1/8	.28	0	29	60	150	SD8202G033V	SD8202G083V	●	4	22.6/F
3/8	5/32	.50	0	29	35	150	SD8202G034V	SD8202G084V	●	4	22.6/F
3/8	7/32	.85	0	29	20	150	SD8202G036V	SD8202G086V	●	4	22.6/F
3/8	9/32	1.1	0	29	15	150	SD8202G037V	SD8202G087V	●	4	22.6/F

① Applicable to air-inert gas valves only.
② ● General Purpose valve. Refer to Engineering Section (Approvals) for more details.
③ Will vary with duty cycle (8.5 watts at 500 mA with ambient temp. – 104°F (40°C).

SPECIAL SERVICE VALVES

Pipe Size (Ins.)	Orifice Size (Ins.)	Cv Flow Factor	Operating Pressure Differential (psi) Min.	Max Water/ Light Oil	Max. Fluid Temp.°F	Catalog Number Water/Light Oil	UL ② Listing	Const. Ref.	Watt Rating/ Class of Coil Insulation ③
Brass Body									
3/8	1/2	2.4	5	150	150	SD8203G001	-	5	22.6/F
1/2	1/2	2.4	5	150	150	SD8203G002	-	5	22.6/F

Dimensions inches (mm)

Const. Ref. 1

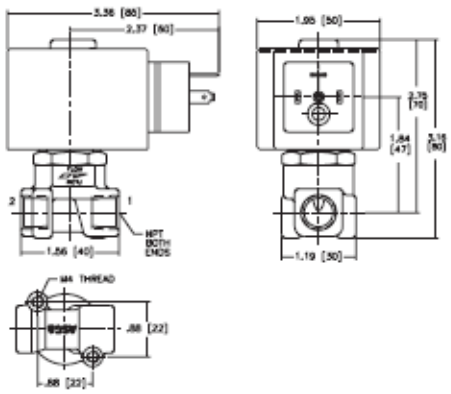

Const. Ref. 2

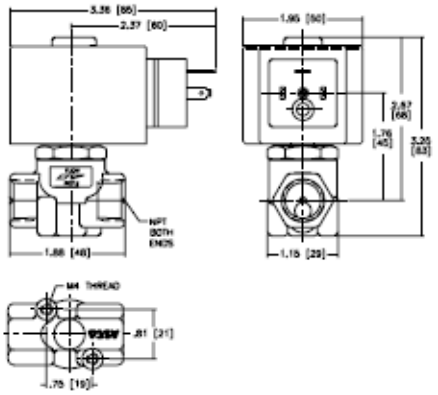

Const. Ref. 3

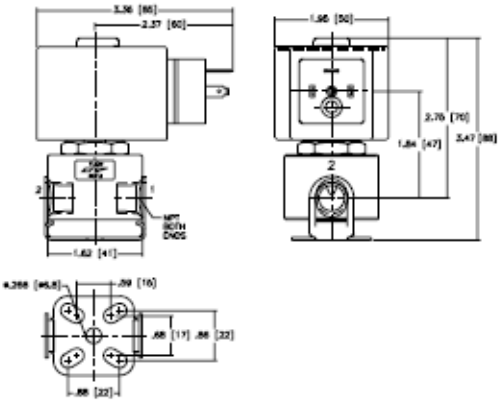

Const. Ref. 4

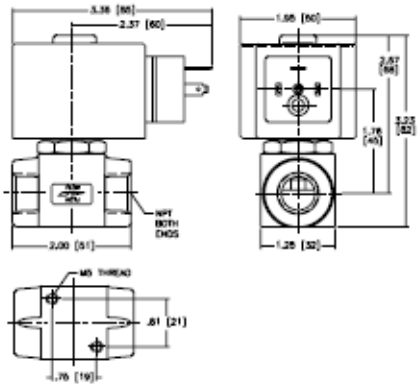

Const. Ref. 5

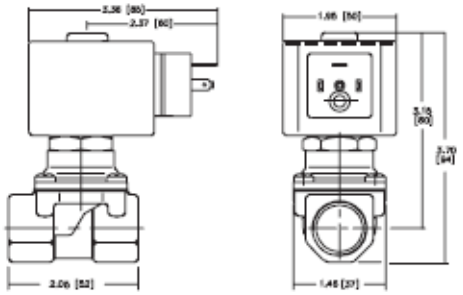

Electronic Control Unit
For Proportional Posiflow Solenoid Valves

SERIES 8908

Description

One unit, Catalog Number 8908A001, can be used for all 1/4" to 1/2" Posiflow valves with DIN solenoids.

To maintain a specific flow rate, current through the coil must be kept constant and substantially independent from changes in the coil winding resistance (caused by temperature variation). The Electronic Control Unit will accomplish this quite efficiently via pulse width modulation. Voltage to the coil is cut into rectangular pulses by rapidly switching it on and off. By varying the "on" time (pulse width) percentage to compensate for temperature variations, current through the coil is kept constant.

Electrical Characteristics

Nominal supply voltage:
24 VDC ± 10%,maximum ripple 10%

Maximum full-load current:
1100 mA (factory set at 500 mA)

Input control signal (selectable):
0-10 VDC or 0-20 mA or 4-20 mA

Switch-off current:
<2% of max. input control signal

Adjustable off-set:
15-50% of pulse width modulation voltage

Adjustable full-load:
30-100% of pulse width modulation voltage

Ramp time:
Manually activated via on/off switch; adjustable 0.1-3 seconds

Adjustable PWM frequency:
40-700 Hz

Power consumption:
0.8 watts

Construction

Housing Assembly	PA + FV
Cover	PA + FV
Screw	Zinc plated steel
Gasket	NBR
Connector Specification	ISO 4400/DIN 43650
Protection	IP 65 (Dust-tight Protection against water jets from any direction)

Dimensions inches (mm)

Catalog No.	A	B	C	D	E	F	G	H
8908A001	2.76 (70)	1.89 (48)	1.18 (30)	1.61 (41)	1.18 (30)	0.16 (4)	1.26 (32)	2.03 (51.5)

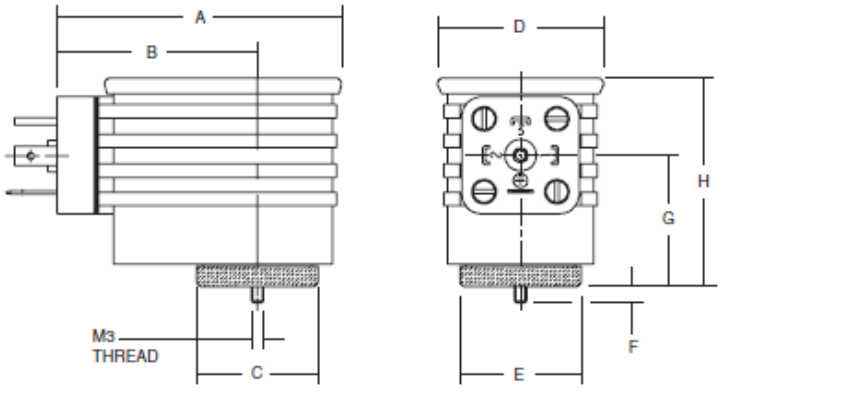

SPECIAL SERVICE VALVES

EMERSON
Industrial Automation

ASCO Valve, Inc.
1561 Columbia Highway
Aiken, SC 29801 USA
T (803) 641-9200
F (803) 641-9290
www.asconumatics.com

CERTIFICATE OF COMPLIANCE

Date JANUARY 22, 2014

Customer VALIN CORPORATION

Customer P.O. No. 1266725

Consignee _____

Consignee P.O. No. _____

ASCO Shop Order No. OB 249055

ASCO Work Order No. A100000

ASCO Part No. 8908A001 ELECTRONIC MODULE POSIFLOW **Quantity** 1

This is to certify that we have supplied the above item ordered and it was manufactured in accordance with ASCO Quality Control procedures, specifications and drawings on file.

ASCO®

Dated January 22, 2014

Cheryl L. Hensley

Authorized Signature
Cheryl L. Hensley
Quality Assurance Manager

ASCO numatics

Form Va QA 2725 (A) R3 – 7/2006

EMERSON
Industrial Automation

ASCO Valve, Inc.
1561 Columbia Highway
Aiken, SC 29801 USA
T (803) 641-9200
F (803) 641-9290
www.asconumatics.com

CERTIFICATE OF COMPLIANCE

Date APRIL 10, 2014

Customer VALIN CORPORATION

Customer P.O. No. 1266725

Consignee

Consignee P.O. No.

ASCO Shop Order No. OB 249055

ASCO Work Order No. A840270

ASCO Part No. MAP SUBMINATURE CONVERT **Quantity** 1

SD 8202G002 V 24/DC D

This is to certify that we have supplied the above item ordered and it was manufactured in accordance with ASCO Quality Control procedures, specifications and drawings on file.

ASCO®

Dated April 10, 2014

Cheryl L. Hensley

Authorized Signature
Cheryl L. Hensley
Quality Assurance Manager

ASCO numatics

Form Va QA 2725 (A) R3 – 7/2006

VITA

Joshua A. Hartman was born on March 28th 1987. He obtained his Bachelor of Science degree in Mechanical Engineering from Wright State University, Dayton, OH in 2011. During his studies at WSU he was awarded a Department of Defense SMART program scholarship to continue his education and start a career as an Aeropropulsion Engineer and Test Project Manager at the USAF's Arnold Engineering Development Center, Tullahoma, TN working in the Turbine Engine Ground Test Complex. He attended the University of Tennessee Space institute starting in 2011. He was awarded a Master's of Science degree in Mechanical Engineering from the University of Tennessee, Knoxville in August 2014.